THE UNIVERSITY OF
SYDNEY

A thesis submitted in fulfilment of the requirements for the degree of Master of Philosophy

Formulation of biologically-inspired silk-based drug carriers for pulmonary drug delivery targeted for lung cancer

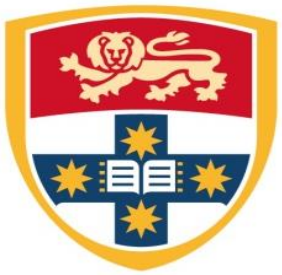

THE UNIVERSITY OF SYDNEY

Sally Yunsun Kim

Supervised by: Dr Wojciech Chrzanowski & Prof Hak-Kim Chan

2014

Faculty of Pharmacy

The University of Sydney

Originality Statement

The work described in this thesis was performed between March 2013 and April 2014 in the Faculty of Pharmacy at the University of Sydney, and partially at the Department of Biochemical Engineering at University College London as a visiting student for 12 weeks. I declare that this submission is my own work and none of this material has been previously submitted for award of any other degree at the University of Sydney or any other educational institution, except where due acknowledgement is made in the thesis. Any contribution made to the research by others, with whom I have worked, is also explicitly acknowledged in the thesis.

Sally Yunsun Kim

April 2014

Acknowledgements

Firstly I would like to thank my supervisors Dr Wojciech Chrzanowski and Professor Hak-Kim Chan, for providing their ongoing guidance, direction and support for this project.

I would like to acknowledge Professor Subhas C. Kundu and his team at the Department of Biotechnology, Indian Institute of Technology Kharagpur, for preparing silk materials and kindly supplying to us as needed. I also thank Dr Helen Agus at the School of Molecular Biology at the University of Sydney for guiding me through the antibacterial studies, and Associate Professor Anandwardhan Hardikar and the Islet-biology group for training and helping me through the basic cell culture techniques. I would like to thank Dr Ivan Wall for allowing me to visit and conduct experiments at the Regenerative Medicine Lab, Department of Biochemical Engineering at University College London for three and a half months.

I also acknowledge the facilities, and the scientific and technical assistance, of the Australian Microscopy & Microanalysis Research Facility at the Electron Microscope Unit, The University of Sydney.

And without my family, friends and colleagues, it would have not been possible to complete this thesis, so I would like to take this opportunity to thank them also.

Praise God!

Abstract

A novel controlled release delivery system has been formulated using natural silk proteins extracted from cocoons of silkworms. The benefits of using silk fibroin, the major protein in silk, has been widely established in many applications, however this is the first time to report silk fibroin as being formulated and tested for pulmonary drug delivery. Silk fibroin particles were formulated and engineered for efficient delivery to the airways via dry powder inhalers and demonstrated high aerosolisation performance through the measurement of *in vitro* lung deposition. Various drugs were incorporated into the silk particles, and ultimately silk particles were loaded with cisplatin to develop controlled-release drug delivery systems that target lung cancer. Human lung epithelial cell line was used to test cytocompatibility of silk particles and the cytotoxicity of silk-cisplatin particles with normal or cross-linked silk formulations. Positive results were obtained and contributed for the optimisation of silk-based controlled-release delivery systems for pulmonary drug delivery.

Table of Contents

Originality Statement 1
Acknowledgements 2
Abstract 3
Table of Contents 4
List of Tables and Figures 8
List of Abbreviations 11
I. Inroduction 12
1. Background 12
2. Silk as a biomaterial 13
2.1. Sources and types of silk used as biomaterials 13
2.2. Composition of silk from silkworms 15
2.3. Applications of silk fibroin 15
2.4. Potential antibactieral action of silk proteins 18
3. Rationale for uses of silk proteins as drug carriers 19
3.1. Biocompatibility 19
3.2. Biodegradability 20
3.3. Superiority of silk fibroin compared to other polymer biomaterials for drug delivery 22
3.4. Recent applications in drug delivery for the treatment of cancer 23
3.5. Drug encapsulation and release 24
4. Rationale for development of inhalation treatment for lung cancer 27
4.1. Epidemiology and trend in research funding 27
4.2. Advantages and challenges of pulmonary delivery 30
4.3. Anticancer drug delivered via inhalation 31
5. Summary 33
II. Research Proposal 35
1. Significance and aims of the project 35
2. Specific aims 37
3. Research plan 37
III. Materials and methods 38
1. Formulation of silk-based particles 38

1.1. Source of materials 38
1.2. Silk protein solution preparation 38
1.3. Incorporation of drug to silk solutions 38
1.4. Crosslinking of silk fibroin for controlled release of drug 39
1.5. Fabrication of particles from spray-drying 39
1.6. Fabrication of particles from spray-freeze-drying 39
2. Characterisation of silk-based particles for pulmonary delivery 41
2.1. Assessment of particle size and morphology 41
2.1.1. Particle size distribution by dynamic light scattering 41
2.1.2. Particle size and morphology 41
2.1.3. Three-dimensional analysis of surface topography 41
2.2. Determination of amorphous or crystalline structures 42
2.3. Stability of particles upon exposure to humidity 42
2.4. *In vitro* aerosolisation performance and lung deposition 42
3. Investigation for antibacterial action naturally exhibited by silk proteins 43
3.1. Preparation of silk samples 43
3.2. Antimicrobial susceptibility testing 43
3.2.1. Disc diffusion assay 43
3.2.2. Broth dilution assay 44
3.2.3. Determination of minimum bactericidal concentration 44
4. *In vitro* cytocompatibility of silk proteins and cytotoxicity of silk-cisplatin particles 45
4.1. Cell culture and maintenance 45
4.2. Preparation of samples for cell viability assays 46
4.2.1. Formulation of two dimensional (2D) silk scaffolds using silk solutions 46
4.2.2. Preparation of silk conditioned media using formulated particles 46
4.3. Cell viability and proliferation assays 47
4.3.1. AlamarBlue® cell viability assay 47
4.3.2. MTT cell viability assay 48
4.3.3. CCK-8 cell viability assay 48
4.4. Picogreen® DNA quantification assay 49
4.5. Changes in cell morphology 49
4.5.1. Phase images 50
4.5.2. Immunocytochemistry 50

4.6. Cell Metabolism 52
4.7. Cell Migration and Invasion 52
4.7.1. "Accelerated escape" 53
4.7.2. "Suppressed attraction" 53
4.8. Cell wound repopulation assay 54
4.9. Statistical analysis 54
IV. Results and discussion 55
1. Characterisation of silk-based particles 55
1.1. Assessment of particle size and morphology 55
1.1.1. Particle size analysis of spray dried silk-based particles 55
1.1.2. Particle size analysis of spray-freeze-dried particles 58
1.2. Morphology 60
1.2.1. The morphology of spray dried particles 60
(a) Silk fibroin formulations, with no drug incorporated 60
(b) Silk fibroin formulations, containing antibiotics 61
1.2.2. The morphology of spray-freeze-dried particles 61
(a) Silk fibroin formulations, with no drug incorporated 61
(b) Silk fibroin formulations containing cisplatin 63
(c) Silk fibroin cross-linked with genipin loaded with cisplatin 64
1.3. The effect of lyoprotectant on formulation of particles 65
1.4. Structure of particles and determination of crystallinity 68
1.5. Stability of particles upon exposure to humidity 70
2. Investigation for antibacterial effects exhibited in natural silk proteins 72
2.1. Screening for presence of antibacterial activities 72
2.2. Determination of minimum inhibitory concentration 72
2.3. Assessment of the antibacterial activity 73
2.4. Conclusion and future studies 73
3. Particle dispersibility and *in vitro* testing for deposition in the lungs 74
3.1. Dispersion of spray dried particles for *in vitro* lung deposition 74
3.2. Dispersion of spray-freeze-dried particles for *in vitro* lung deposition 74
4. *In vitro* cytotoxicity assays of silk-based particles 76
4.1. Introduction 76
4.2. Cell Viability Assays 77

4.3. Double strand DNA content (Picogreen® assay) 83
4.4. Changes in cell morphology with silk-based treatment 84
4.5. Cell Metabolism (YSI) 88
4.6. Cell migration and invasion 90
4.7. Wound repopulation assay 92
4.8. Conclusion and need for further studies 94
V. Conclusions and Future Work 96
References 98

List of Tables and Figures

Figure 1. Type of silk, species and families of silkworms for biomaterial use

Table 1. Comparison of silk proteins from the cocoons of mulberry silkworm *B.mori*

Figure 2. The physical and chemical structure of fibroin

Figure 3. Extraction of fibroin and sericin from the cocoons of *B.mori* silkworms

Figure 4. Drug release profile of methotrexate released from silk fibroin (SF), silk fibroin-albumin (in ratios of 1:1, 2:1, 1:2) or albumin (Alb) nanoparticles

Figure 5. Cancer death rates by site of cancer, age-adjusted per 100,000 males or females population in the US, 1930-2008

Figure 6. The comparison of research funding spent on specific cancers by NCRI, related to the percentage of total cancer deaths in the UK by tumour site

Figure 7. Percentage of site-specific research funding for cancers in 2002 and 2010

Figure 8. The process for formulation of silk-based particles for optimised formulation of silk-based cisplatin particles for pulmonary delivery

Table 2. A list of silk-based particles formulated for the purpose of this project

Figure 9. A schematic diagram of the experiment design for cell migration assays per transwell; (a) "accelerated escape" and (b) "suppressed attraction" assays

Table 3. Mean particle size (μm) of spray dried particles, as determined by laser diffraction analysis; shows mass median diameter (D(0.5)) for each formulation

Figure 10. SEM micrographs of spray dried silk particles of: (a)(b) BM fibroin and (c)(d) AM fibroin produced using 2% (w/v) silk solutions

Figure 11. SEM micrographs of spray dried BM sericin *(left)* and AM sericin *(right)*

Figure 12. Particle size distributions for spray-freeze-dried: (a) silk + mannitol + cisplatin, (b) silk + mannitol + cisplatin + genipin and (c) silk + trehalose formulations

Figure 13. AFM images showing topography of BM and AM silk fibroin particles; used scan rate 0.30 Hz and 0.4 Hz and scan size 600 nm and 1.5 μm, respectively

Figure 14. SEM micrographs portraying silk as carriers of drugs; (a) spray dried AM fibroin 0.5% + ciprofloxacin 0.1%, (b) spray dried AM fibroin 0.5% + gentamicin 0.1%, (c) spray dried BM fibroin 0.7% + ciprofloxacin 0.07%

Figure 15. Spray-freeze-dried BM fibroin with sucrose as a lyoprotectant; silk:sucrose ratio was 2:1

Figure 16. A three-dimensional AFM image of spray-freeze-dried BM fibroin formulated with sucrose as a lyoprotectant with silk:sugar ratio 2:1, scan rate 0.4 Hz and scan size 10.24 μm

Figure 17. SEM micrographs of BM fibroin 1% mannitol 0.75% cisplatin 0.2%

Figure 18. Spray freeze-dried silk-cisplatin particles with trehalose used as a lyoprotectant. Ratio of silk fibroin to cisplatin were 1:1, 5:1 and 10:1

Figure 19. SEM micrographs of formulations of silk cross-linked with genipin; BM fibroin 0.5% + mannitol 1% + cisplatin 0.05% + genipin 0.05%

Figure 20. The effect of trehalose concentration on morphology of BM fibroin / trehalose particles compared at concentrations of: (a) 0.1% / 0.1%, (b) 0.5% / 0.25%, (c) 0.5%/1%, (d)(e) 0.5% / 0.5%

Figure 21. Spray-freeze-dried AM fibroin particles with trehalose as a lyoprotectant – "melting" AM fibroin 1% trehalose 1% and AM fibroin 0.5% trehalose 0.5% cisplatin 0.1%

Figure 22. Spray-freeze-dried silk fibroin containing mannitol as lyoprotectant, loaded with cisplatin: (a)(b) BM fibroin 0.5% mannitol 0.5% cisplatin 0.1%, (c)(d) BM fibroin 0.5% mannitol 1% cisplatin 0.1%

Figure 23. X-ray diffractograms showing amorphous structures for spray-freeze-dried particles: (a) BM fibroin 1% + sucrose 0.5% and (b) BM fibroin 0.5% + trehalose 0.5%; with angular increments of 0.02˚ covering a 2θ range of 2 to 80˚

Figure 24. X-ray diffractogram showing crystalline structures for spray-freeze-dried BM fibroin 0.5% + mannitol 1%; with angular increments of 0.02˚ covering a 2θ range of 2 to 80˚

Figure 25. Moisture sorption isotherms for spray-freeze-dried BM fibroin with trehalose and spray-freeze-dried BM fibroin with mannitol

Figure 26. Disc diffusion assay of BM sericin on *S.aureus*-inoculated Mueller-Hinton agar plate

Figure 27. Cumulative mass fraction for spray dried BM fibroin particles, showing fine particle fraction (FPF) of particles less than 5 μm in diameter; tested *in vitro* at airflow 60L/min for 4 seconds using NGI

Figure 28. Cumulative mass fraction for spray-freeze-dried particles of BM fibroin 0.5% with trehalose 0.5%, showing fine particle fraction (FPF) of particles less than 5 μm in diameter; tested *in vitro* at airflow 60L/min for 4 seconds using an NGI

Figure 29. Results of alamarBlue® assay showing cell growth on two-dimensional silk scaffolds of two concentrations 0.1% and 1%

Figure 30. Results of MTT assay showing cell growth on 2D silk scaffolds of two concentrations 0.1% and 1%

Figure 31. Results of CCK-8 assay: Cell proliferation with media containing silk fibroin ± sugar (Man = mannitol) ± cisplatin (Cisp) ± genipin (Gen) measured on days 1, 3 and 7.

Figure 32. Comparison between formulations of silk fibroin + cisplatin 1mg/ml or 10mg/ml with high or low mannitol concentrations

Figure 33. Comparison between formulations of Silk + Cisp (silk + mannitol + cisplatin; 10:20:1) or Silk (cross-linked) + Cisp (silk + mannitol + cisplatin + genipin; 10:20:1:1) at 1mg/ml or 10 mg/ml concentrations

Figure 34. Quantification of DNA contents purified from A549 cells cultured in the presence of silk alone, silk + sucrose (2:1), silk + mannitol + cisplatin (10:20:1), silk + mannitol + cisplatin (10:20:1:1) formulations, or control (no treatment)

Figure 35. Similar morphology can be observed for (a) Control (b) Silk alone (c) Silk + sugar, at 24 hours and 48 hours of treatment

Figure 36. Similarities in morphology of control and silk-treated cells, stained F-actin (green), beta-catenin (red) and DAPI (blue)

Figure 37. Morphological differences of A549 cells after 24 and 48 hours of treatment with silk-based cisplatin particles, with different impacts for normal and cross-linked silk

Figure 38. The conditioned media with different formulations have varying effects on the average size of the cells

Figure 39. Immunofluorescence images after 48 hours of treatment with (a) normal media (control) (b) silk alone, (c) silk + sugar, (d) silk + mannitol + cisplatin 10:20:1 and (e) silk + mannitol + cisplatin + genipin 10:20:1:1. Stained with F-actin (green) and DAPI (green)

Figure 40. Cell metabolism: Increasing lactate levels and decreasing glucose levels detected in media as cells proliferate during incubation with silk ± cisplatin formulations

Figure 41. Average number of cells migrated over 8 hours from low serum media containing silk alone, silk + mannitol + cisplatin (Silk + Cisp) or silk+ mannitol + cisplatin + genipin (Silk (cross-linked) + Cisp) particles to high serum media ("Accelerated escape")

Figure 42. Average number of cells migrated over 8 hours from low serum media to high serum media containing particles ("Suppressed Attraction")

Figure 43. Wound repopulation assay showing closed "wounds" for cells treated with silk alone with or without sugar and unclosed wounds for cells treated with cisplatin

Figure 44. Phase images of cells treated with silk + mannitol + cisplatin + genipin (10:20:1:1) formulation after 48 hours of incubation, before and after washing with PBS

Figure 45. Percentage of wound closed after 24 hours incubation with silk alone, silk + sugar (2:1) formulation, silk + mannitol (Man) + cisplatin (Cisp) (10:20:1) and silk + mannitol (Man) + cisplatin (Cisp) + genipin (Gen) (10:20:1:1) formulations.

List of Abbreviations

2D or 3D	Two dimensional or Three dimensional
AM	*Antheraea mylitta (A.mylitta)*
AFM	Atomic force microscopy
ANOVA	Analysis of variance
BM	*Bombyx mori (B.mori)*
BSA	Bovine serum albumin
$CaCl_2$	Calcium chloride
CCK-8	Cell Counting Kit-8
DMEM	Dulbecco's Modified Eagle's Medium
dsDNA	Double-stranded DNA
DVS	Dynamic vapour sorption
E.coli	*Escherichia coli*
FPF	fine particle fraction
FBS	foetal bovine serum
MBC	minimum bactericidal concentration
MIC	minimum inhibitory concentration
MTT	Methyl thiazolyl tetrazolium
NCRI	National Cancer Research Institute
NGI	Next generation impactor
OD	optical density
PBS	phosphate buffered saline
PLGA	poly(lactic-*co*-glycolic acid)
P.aeruginosa	*Pseudomonas aeruginosa*
S.aureus	*Staphylococcus aureus*
SEM	Scanning electron microscopy
TE	Tris-ethylenediamine-tetraacetic acid
UV	ultra-violet

I. Inroduction

1. Background

Silk has been used for centuries as fabric as well as in cosmeceutics, and is recently attracting immense attention in biomedical applications (1). Silk has been used as surgical sutures for decades due to its biocompatibility and outstanding mechanical properties exemplified by toughness that is two to three times higher than synthetic fibres like Nylon or Kevlar (2). In addition to these qualities, silk is known for properties including controllable biodegradability, superior mechanical strength and stability, elasticity, biocompatibility and uncomplicated processing procedures (1). These properties make silk a superior material when compared to other polymers such as poly(lactic-*co*-glycolic acid) (PLGA), silicone and collagen for application as biomaterials. Importantly silk proteins break down into amino acids that can be absorbed by the body (3). The rate at which silk proteins break down can be controlled by altering the crystallinity of the structure by changing the temperature, pH or solvents used when producing drug delivery systems (3). The increased degree of crystallinity yields a slower release of the encapsulated drug, resulting in longer effect and less frequent dosing of the drug (1, 4).

Silk fibroin, the major protein in silk, has been widely established as a platform for controlled drug delivery of various drugs via formulations of microparticle, spheres, film, coating, and hydrogel (1, 4). For example, silk fibroin coating on liposomes loaded with emodin (a model drug) enhanced the delivery of emodin to breast cancer cells and the overall efficacy of the drug (5). Silk scaffolds have been used for tissue engineering and furthermore have been developed for three-dimensional (3D) disease models, leading to advances in cancer models and therefore, cancer therapy research (1, 6). It is expected that even more applications of silk as biomaterial will be discovered through the current research focus.

2. Silk as a biomaterial

2.1. Sources and types of silk used as biomaterials

Silk produced by silkworms and spiders are the main natural sources of silk researched for biomaterial applications (7). Currently, more silk-based biomaterials are being sourced from silkworms due to easy domestication as well as widely established processing and production (7). Nearly 1000 metric tons of silk per year are produced in the global textile industry and the yield of fibre from a single silkworm cocoon is 600 – 1500 m (8). On the other hand, the lack of large-scale production systems as well as the cannibalistic nature of spiders and the heterogeneous nature of spider silk are limitations of using spider silk as biomaterials (8-10). With advancement of research in recombinant proteins, spider silk is increasingly investigated in its engineered and recombinant forms for biomaterial applications such as controlled delivery of protein drugs (10).

Hofer *et. al.* have pointed out that silk proteins obtained naturally from silkworms may vary in quality due to the inherent differences within the various species of silkworm, each individual silkworm and the various degumming processes that each silkworm species possesses (10). They identified that these qualities amounted to difficulties in ensuring quality control of delivery systems that are formulated from natural sources of silk, and therefore introduced recombinant spider silk as a promising biomaterial for novel drug delivery systems (10, 11).

Recombinant spider silk protein, known as “spidroin”, can be potentially used as a form of drug delivery vehicle, yet very few controlled studies of the properties of spidroin exist (9). The superiority of specific recombinant spidroin protein over fibroin in the behaviours of the scaffolds for bone tissue regeneration was demonstrated recently by Moisenovich *et. al.*, and therefore suggested promising applications for recombinant spider silk proteins (12).

Silkworms belong to the families Bombycidae or Saturniidae and produce silk which are classified as "mulberry" or "non-mulberry" as illustrated in Figure 1 (13). Mulberry silk, produced by the commonly domesticated *Bombyx mori (B.mori)*, is the most widely researched type due to its finest quality of raw silk and the highest fiber production (13, 14). *Antheraea mylitta (A.mylitta)* is a wild silkworm, from one of three types of species belonging to Saturniidae family and it produces non-mulberry silk which is increasingly studied for potential use as a biomaterial due to its tensile strength and larger cocoon size compared to *B.mori* (13). Wild silkworm cocoons have higher tensile strength compared to domesticated silkworm cocoons as the need to protect themselves from environmental hazards has necessitated such natural quality (15). In the area of cardiac tissue engineering in particular where the heart is constantly contracting, fibroin from *A.mylitta* is preferred as it possesses more favourable mechanical properties including elasticity and tensile strength (16). For this project, silk fibroins from both species of silkworm were used as they were the most readily available and the most widely researched species for biomedical uses of silk.

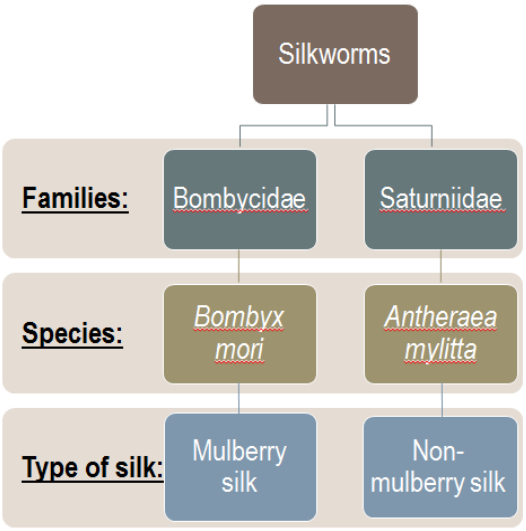

Figure 1. Types of silk, species and families of silkworms for biomaterial use

2.2. Composition of silk from silkworms

Both mulberry and non-mulberry silk consist of two biodegradable proteins, fibroin and sericin. Tao *et. al.* states that – silk proteins represent a unique family of biopolymers due to their structural and biological properties"(17). Fibroin is the major, structural protein proven to be biocompatible through many biomedical applications (18). This protein consists of a heavy chain (395 kDa) and a light chain (25 kDa) linked by a single disulfide bond and is formed with repeats of amino acid sequences consisting of glycine, alanine, and serine (19). Sericin constitutes about 20-30% of the total cocoon weight, and is less studied compared to fibroin despite its potential advantages (14). The comparison of fibroin and sericin from the most extensively studied *B.mori* silkworm are summarised in Table 1 below. Noting the extensive literature and study around fibroin, attempts to discover the potential of currently under-utilised sericin for novel biomaterial uses, especially with recent evidence indicating that sericin has natural antibacterial characteristics, are outlined in section 2 of Research Proposal (20).

2.3. Applications of silk fibroin

The scope of applications of silk as biomaterials has broadly expanded in the last few decades. Examples of their application include implants, coatings to control drug release, tissue engineering as well as vascular and nerve regeneration (1, 8, 21). Silk fibroin biomaterials have also been used for plastic and reconstructive surgery, in which slow biodegradation and good mechanical properties are critical (8).

Table 1. Comparison of silk proteins from the cocoons of mulberry silkworm *B.mori*

Protein	**Fibroin**	**Sericin**
Composition	Amino acids in a heavy chain and a light chain in a 1:1 ratio linked by disulfide bonds (22)	Polypeptide polymer consisting of 18 amino acids (23)
Type of protein	Structural protein	Glue-like protein
Proportion of cocoon	70%	20-30%
Structural properties	Hydrophobic; β-sheets and α-helices	Hydrophillic; remains in a partially unfolded state, with high proportion of random coil structure (23)
Molecular weight	26-370 kDa	24-250 kDa
Major properties	Biocompatible, biodegradable, crystallinity, mechanical properties, opportunity for chemical functionalization (24)	Antibacterial, UV-absorbing, high moisture absorbancy, antioxidant, antitumor, wound-healing (25)
Novel applications	Drug delivery, tissue engineering, implant coating, imaging and diagnostics (24)	Food, cosmetics, drug delivery, medical and pharmaceutical industries
Advantages for use in drug delivery	Aqueous processing, controllable biodegradation	Capable of carrying both hydrophilic and hydrophobic drugs (13)

Silk fibroin as a platform for controlled drug delivery has been widely established and is currently under further investigation for delivery of growth factors for tissue repair, as well as for applications to cancer therapy and treatment of epilepsy (1, 4). It was noted by Kundu *et. al.* that a more extensive understanding of the long term biocompatibility and biodegradability would lead to an ability to tailor silk-based biomaterials to meet tissue specific requirements (8).

The suitability of silk fibroin in drug delivery is attributed to its assembly and the ability to modify it. The structure of silk fibroin consists of alternating hydrophilic and hydrophobic blocks (Figure 2) (22). Functional groups including amines, alcohols, phenols, carboxyl groups, and thiols can be chemically modified or functionalized to improve interaction with other small molecules (1).

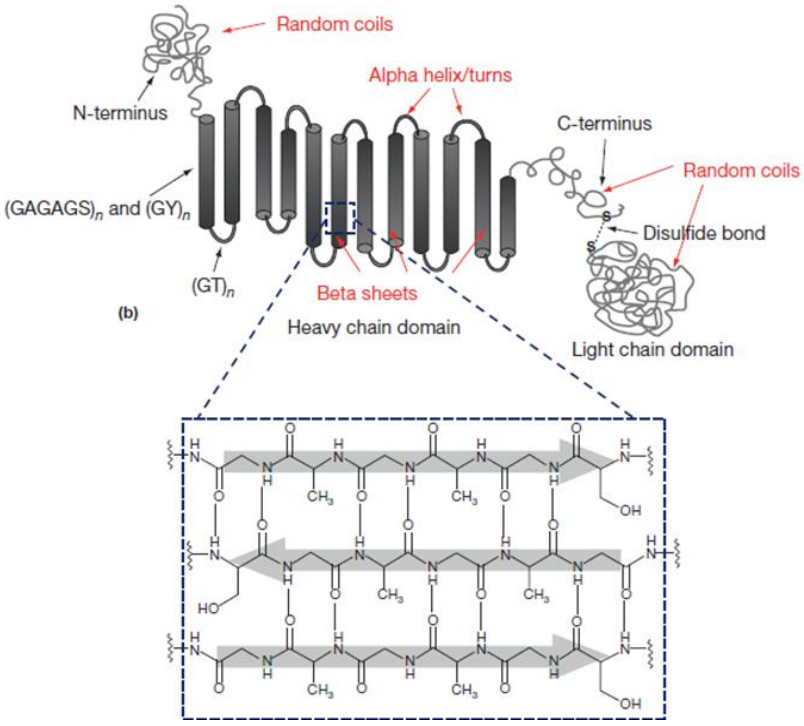

Figure 2. The physical and chemical structure of fibroin (22)

Functionalization is also beneficial as it promotes cell adhesion and spreading during delivery of the incorporated drug (1). Moreover, the structure of fibroin allows for hydrogen bonding or covalent attachment of proteins and compounds. It also offers a highly stabilising environment for a variety of incorporated molecules including proteins and bioactive molecules (18).

Silk fibroin functionalised by chemical modification of the potentially reactive side groups, has shown possible application in microfluidics, optics and photonics or electronic devices/biosensors (17). Recently Zhang *et. al.* demonstrated that functionalised silk fibroin films can provide stabilisation of vaccines and antibiotics, in order to potentially eliminate the need for refrigeration while transporting vaccines to developing countries (21).

Despite very broad use of silk in biomedical applications (and beyond), its potential as a drug delivery carriers for the drug delivery to the lungs has not been investigated and silk-based delivery systems are yet to be developed into an inhalable form. Therefore, this project will strive to develop novel, biologically-inspired silk-based inhalable drug delivery systems that target the lungs. It is desired that such drug delivery systems will work synergistically with the already established treatment regimens for lung cancer.

2.4. Potential antibactieral action of silk proteins

Silk cocoons are designed to protect silkworms from their surroundings including environmental stresses and physical attacks (15). Their functions include defence from predators, thermal regulation and the antibacterial function for the survival of the silkworm contained inside the cocoon (15). Researchers have been investigating silk materials in the light of their above-mentioned natural functions.

The antibacterial action exhibited naturally by silk proteins was investigated by Senakoon *et. al.* in 2009 and the zone of inhibition and minimum inhibitory concentration of sericin in *Escherichia coli (E.coli)* and *Staphylococcus aureus (S.aureus)* were documented (20). The results showed significantly reduced growths of both *E.coli* and *S.aureus* in the presence of sericin and thus it was concluded that sericin has antibacterial attributes against both Gram positive and Gram negative bacteria (20). Further studies however were required in this area because the above result was derived from experiments using only one particular species of silkworm; eri silkworm (*Samia ricini*). This will be investigated in this project for potential application of silk-based carriers for delivery of antibiotics.

3. Rationale for uses of silk proteins as drug carriers

3.1. Biocompatibility

Biocompatibilities of both fibroin and sericin are now well established (19, 26). Silk fibroin based formulations are valuable not only due to their non-toxic and non-antigenic nature, but also their stability during storage as well as *in vivo* (19). Wang *et. al.* has investigated the effects of silk fibroin coatings on PLGA and alginate microspheres for protein delivery. Silk coatings made beneficial changes to the surface properties of the PLGA and alginate microspheres and improved the biocompatibility of the particles when compared with the same tests undertaken with uncoated microspheres used as control (27). Additionally, their investigation observed that silk fibroin coatings prevented PLGA microspheres from aggregation and decomposition and therefore maintained their spherical shapes for two weeks as well as providing stabilisation from degradation (27). Furthermore, the ability to control coating thickness and crystalline content, together with the observed controlled protein drug

release, leads to silk fibroin acting as an effective diffusion barrier (27). The findings from this study can be used to broaden the scope of applications of silk fibroin.

A recent study by Qu *et. al.* demonstrated the behaviour of cells on the surface of silk fibroin microspheres and tight cell attachment indicated that silk fibroin is biocompatible (28). Qu *et. al.* also investigated the effect of cell growth depending on the size of the microspheres, and found that the smaller the silk fibroin particles, higher the cell proliferation due to larger specific surface area and higher number of pores compared to larger particles. Cell proliferation rate is accelerated with larger surface area provided by smaller sized spheres (28).

A cell viability assay conducted by Kundu *et. al.* demonstrated that the number of viable cells growing on silk fibroin microspheres rapidly increased on days 3 and 5 (19). By day 7, there was a large difference between silk fibroin microspheres with control group, due to the silk fibroin microspheres providing more space for cell growth and proliferation (19).

3.2. Biodegradability

The degradation behaviour of silk is important to understand when investigating it as therapeutic drug carriers. The degradation rate of silk biomaterials should be optimised to match the functional needs, for example, in the application of tissue engineering, the degradation rate of the scaffold should match the rate of tissue growth (3). For the application in tissue engineering, understanding of degradation is vital and it leads to successful control of cellular metabolism and differentiation (29). The process of biodegradation is one of the critical factors for success of a biomaterial in clinical applications (29). The degradation behaviour of sericin is not as well established and remains to be investigated in detail, however there are numerous studies evaluating the degradation of fibroin.

Being a natural polymer, fibroin degrades into amino acids glycine, alanine and serine, which are easily absorbed *in vivo.* Cao and Wang conducted *in vitro* studies to show that these amino acids resulting from the degradation of fibroin were taken up by the cells for further metabolism (3). This highlights the previously mentioned superiority of silk fibroin to one of the most commonly studied biodegradable polymers, PLGA, which degrades *via* hydrolysis into acidic products resulting in a low pH environment which in turn imposes detrimental effects on the incorporated drug (30).

Silk fibroin sheets were shown to degrade by 70% in 15 days when exposed to protease XIV (3). Fibroin is water soluble in its random coil and helical conformation, whereas it is water insoluble in its crystalline β-sheet conformation that may be induced by the use of organic solvents, increased temperature and altered pH level (31). In contrast to earlier studies where the rate of degradation was mostly associated with the molecular weight, structure and the level of crystallinity, Rajkhowa *et. al.* demonstrated that reduced crystallinity as well as high surface area and porous morphology increases the degradation of silk particles (3, 29).

In the case of porous silk particles, the mechanism of degradation is believed to be through hydrolysis by protease XIV contributing to pore surfaces fracturing into finer particles (29). This mechanism explains the increase in degradation rate, compared to the previously understood degradation by surface erosion mechanism alone. The mass loss of 60%, compared to 23% in a 12-day period, together with the observed reduction of particle size towards the end of the degradation tests, supported their conclusion (29).

Determining the exact biodegradation behaviour of silk is challenging due to other influencing factors such as a protease inhibitor in the silk gland embedded in the cocoons of *B.mori*, produced by silkworm itself, as well as gamma radiation causing reduction in the

tensile strength of fibroin fibers and thus increasing the rate of biodegradation of silk fibroin (3).

3.3. Superiority of silk fibroin compared to other polymer biomaterials for drug delivery

Although PLGA is the most extensively studied synthetic polymer for use as a drug carrier system, suitability for delivery of protein drugs is challenging due to the requirement of organic solvents for processing and reduction of pH caused by polymer degradation (32). In contrast, silk fibroin can be processed in an aqueous environment and is capable of being degraded into amino acids that are well absorbed by the body (32).

In the application for drug delivery it is significant that silk, unlike other polymer biomaterials, can be processed in aqueous systems in mild conditions of temperature, pressure and neutral pH, without the need of harsh manufacturing conditions that may potentially damage the incorporated drug (8, 24, 30). The process of extraction of fibroin and sericin from the cocoons of *B.mori* silkworms is shown in Figure 3. Silk fibroin can be prepared into various morphologies such as films, hydrogels, microspheres, sponges and nanofibres to suit different applications (18, 32). Chitosan and gelatin particles as drug carriers for protein delivery were also faced with limitations due to organic solvents being required as crosslinking agents to prevent the burst release of the encapsulated drug (32).

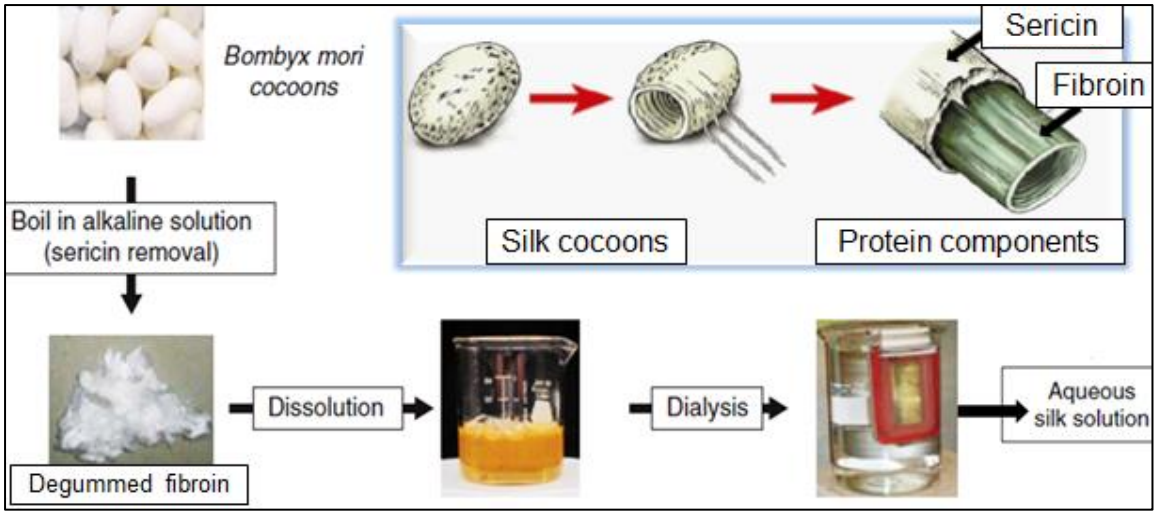

Figure 3. Extraction of fibroin and sericin from the cocoons of *B.mori* silkworms (24, 33).

3.4. Recent applications in drug delivery for the treatment of cancer

By using carriers, specific sites of cancer can be targeted and also the slow release formulations allow lowering of the required dose, therefore the common toxicity and side effects of anticancer drugs can be also reduced.

Silk films loaded with doxorubicin were evaluated for *in vivo* performance in primary breast cancer in mice and they provided reduced tumour growth and reduced metastatic spread (34). Silk fibroin and sericin can be prepared into nanoparticles or microparticles. The advantages of using nanoparticles as carriers of drugs include sustained drug release, reduced drug toxicity, as well as lesser frequency of dose administration (35). This is of great benefit to cancer treatment over the traditional intravenous chemotherapy, as the drug-loaded nanoparticles reach and stay in the target tissue and release the drug gradually to act on the growing cancer cell (31). Similarly, this thesis aims to provide an insight into improving local delivery of anticancer drug to the lungs via silk-based microparticles for better outcomes, including longer action of the delivered drug whilst having less systemic side effects.

3.5. Drug encapsulation and release

Loading and release of various drugs carried by silk fibroin particles have been studied *in vitro* and have demonstrated successful cellular acceptance of both the particles and the encapsulated drugs (36). High encapsulation efficiency was seen in drugs with high molecular weight, hydrophobic affinities and release rates were directly related to surface charge (36). A recent study of the *in vitro* release behaviour of encapsulated drugs found that the silk particles that are positively charged released the drug in a more prolonged fashion (37).

Crosslinking increases the surface hydrophobicity and thus leads to slow-release mechanisms; however it has been shown that the silk particle uptake and release of water-soluble drugs is mostly dependent on silk particle formation rather than crosslinking (38).

The rates of drug release are dependent on diffusion of drug through the silk, degradation of the silk fibroin carrier, or both (4). By manipulating the secondary structure of silk fibroin particles, the physicochemical properties may be manipulated in order to achieve controlled delivery to desired sites (7). Diffusion can be controlled by engineering morphology of silk fibroin carrier particles including their geometry, number and thickness of coating and porosity (24). The degradation of silk fibroin *in vivo*, and thus the release of its encapsulated drug can be controlled by using organic solvents, different silk concentrations, porosities, or altering crystallinity *via* regulation of β-sheet content during processing (22).

Silk fibroin has organised crystalline β-sheet conformations that stabilise its structure *via* physical crosslinks (21). Furthermore, the control of β-sheet content by altering the conditions during processing allows alteration in the level of crystallinity and thus allowing for the control of the release properties of the incorporated drug(s) (22). This structure explains the outstanding mechanical properties of silk fibroin to withstand load and

compression which are superior to other studied polymer biomaterials such as silicone, PLGA and collagen (1).

Recently Kundu reported an *in vitro* drug release study on tumour cells using silk fibroin-albumin nanoparticles as carriers to deliver methotrexate (39). The results of their study proved that methotrexate without any carrier was released almost completely within the first two days, and when silk fibroin was used, the release rate was significantly slower (Figure 4). The albumin blended together with silk into nanocarriers had resulted in the methotrexate being released gradually with very little burst release.

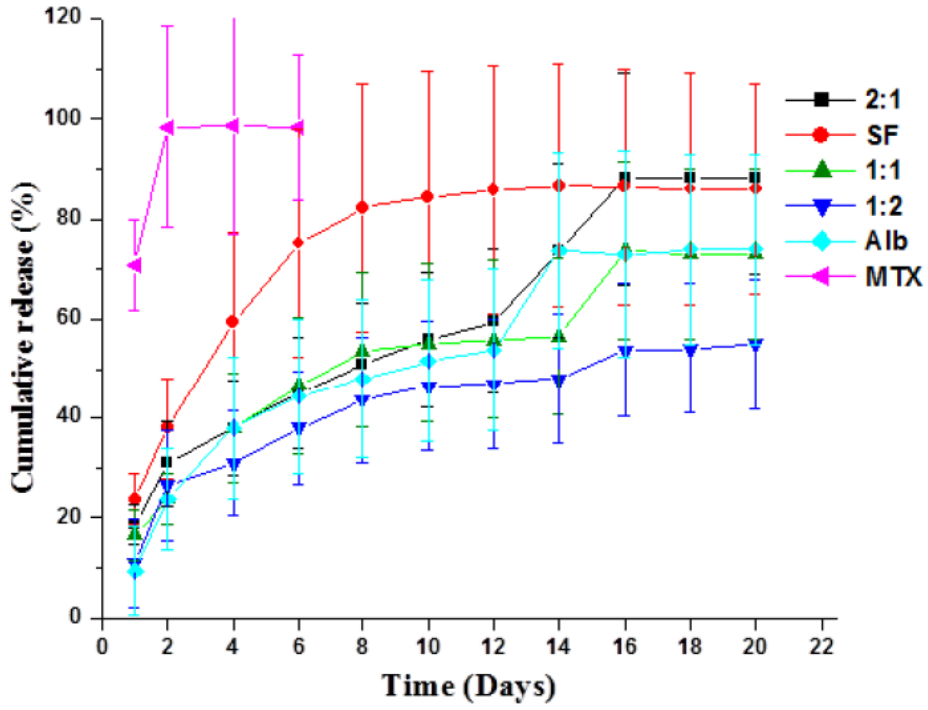

Figure 4. Drug release profile of methotrexate (MTX) released from silk fibroin (SF), silk fibroin-albumin (in ratios of 1:1, 2:1, 1:2) or albumin (Alb) nanoparticles into phosphate buffer solution at 37˚C (39). The results were evaluated by mean ± standard deviation for n = 3. This data was reproduced with permission from the authors of the article.

In this study, the nanoparticles were prepared in three different ratios of silk fibroin and albumin blends 2:1, 1:1 and 1:2 (v/v). Blending the two components together led to strong electrostatic interactions between the carboxyl groups of hydrophobic silk fibroin and the amino groups of hydrophilic albumin, and therefore successfully prevented leakage and improved encapsulation, drug retention and release rate (39). The initial burst release was avoided which therefore indicated the potential lowering of the incidence of side effects and toxicity of methotrexate (39). This study demonstrated that silk formulations can be modified into combinations with other proteins (e.g. albumin) and promoted silk nanoparticles as superior carriers of drug with controllable drug release characteristics.

The release mechanisms of a drug from porous silk fibroin microspheres were found to be outwards drug diffusion due to the swelling of the silk fibroin matrix, as well as the degradation and erosion of the silk fibroin matrix (40). The *in vitro* release behaviours of methylene blue (a model drug) from various silk fibroin microspheres formulated using water-in-oil emulsification-diffusion method were investigated by Imsombut *et. al.* for developing controlled drug delivery applications (40). The higher the ratio of methylene blue to silk fibroin, the higher was the burst release rate, since the drug concentration gradient was a major factor in the first 12 hours of drug release via swelling of the silk fibroin matrix (40). Therefore the optimisations of concentration of drug in the formulation, as well as controlling the degradation rate of silk fibroin, are critical for successful applications of silk fibroin as drug delivery systems.

4. Rationale for development of inhalation treatment for lung cancer

4.1. Epidemiology and trend in research funding

Scientific research related to the treatment of lung cancer has failed to significantly improve prognosis in the last several decades (41). The 5-year survival rate has not improved over the last 30 years, and lung cancer still causes more deaths than colon, breast and prostate cancers combined (42, 43). Similar data was presented graphically by the American Cancer Society which showed a significantly higher rate of cancer deaths caused by lung and bronchus cancer compared to other sites of cancer (Figure 5) (44). The highest rate of death caused by lung and bronchus cancer was reached in the early 1990s for males and late 1990s for females. Despite the rate decreasing, it still remains higher than other sites of cancer.

Each year, between 1.3 and 1.5 million people are newly diagnosed with lung cancer worldwide and the number of new diagnoses is expected to continue increasing with the epidemic of tobacco use (43). Data from the National Cancer Institute's Surveillance, Epidemiology, and End Results (SEER) study from 2003 to 2009 shows that the percentage of survival from lung and bronchus cancer in the United States is 16.6% (45). The 5-year relative survival rate, although diagnosed during the localised stage, is as low as 53.3% (45).

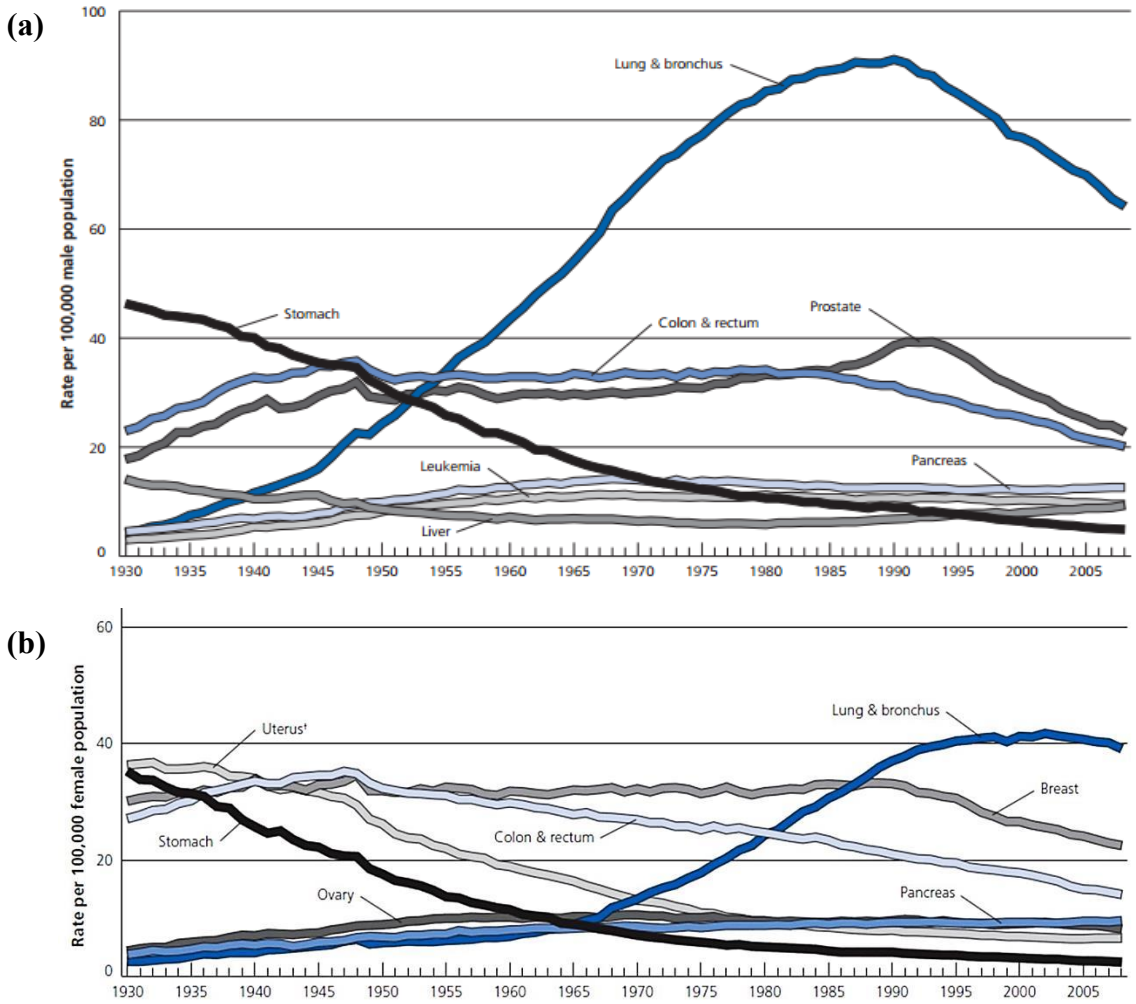

Figure 5. Cancer death rates by site of cancer, age-adjusted per 100,000 (a) male population or (b) female population in the US from 1930 to 2008 (44). Reproduced with permission from the American Cancer Society, *Cancer Facts & Figures 2014*

A review of research funding for "hard-to-treat" cancers by the UK National Cancer Research Institute (NCRI) in 2002 found that research funding spent for lung cancer did not reflect the fact that it was one of the most common and hard-to-treat cancers (46). The percentage of research funding spent by the NCRI for lung cancer was found to be lower than other cancers despite lung cancer having the highest percentage of total cancer deaths (Figure 6) (47). Since then, there has been an increase in the awareness of the need for lung cancer research and the site-specific cancer research funding for lung cancer has increased from £3.5 million in 2002 to over £11 million in 2010 (Figure 7) (46).

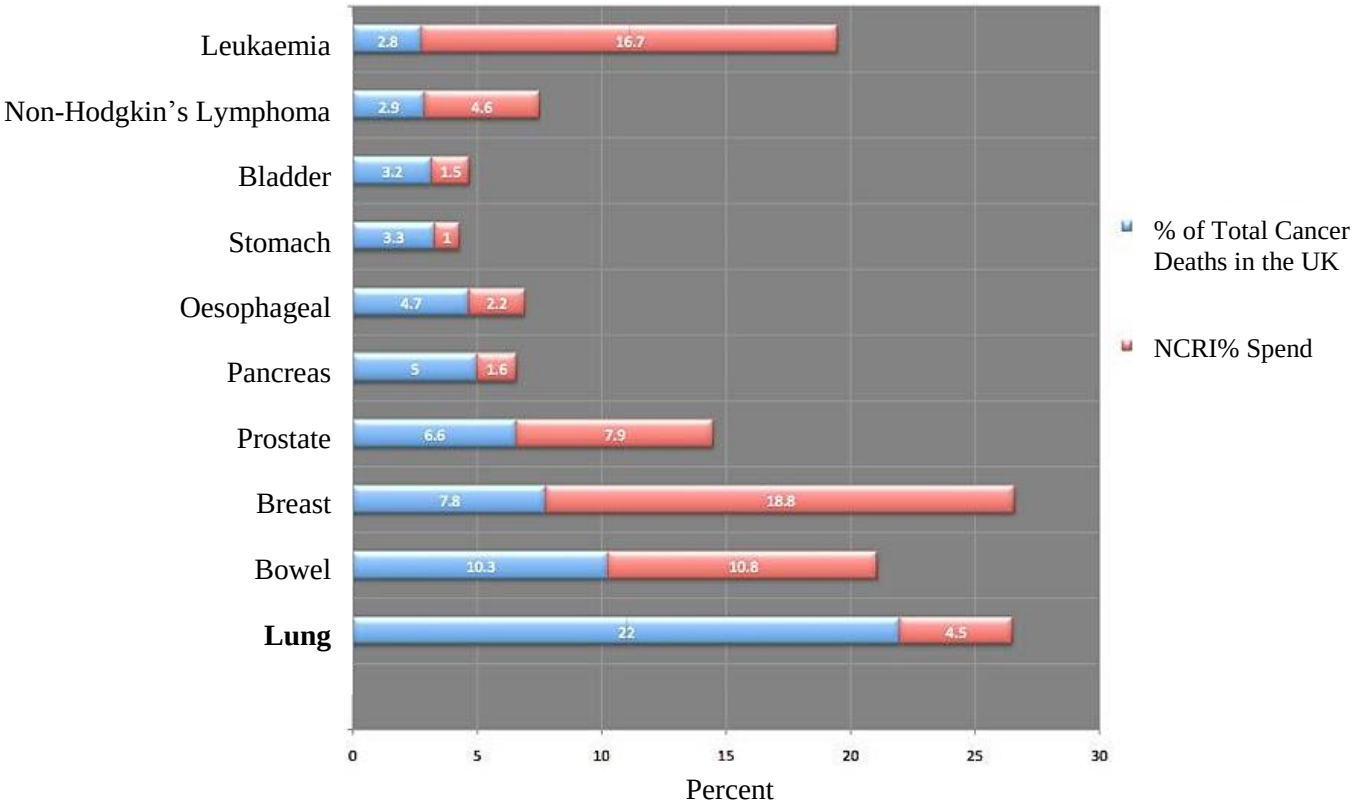

Figure 6. The percentage of total cancer deaths in the UK by tumour site *(shown in blue)* and the site-specific cancer research funding spent by NCRI *(shown in red)* (47). Reproduced with permission from the Pancreatic Cancer Society, UK

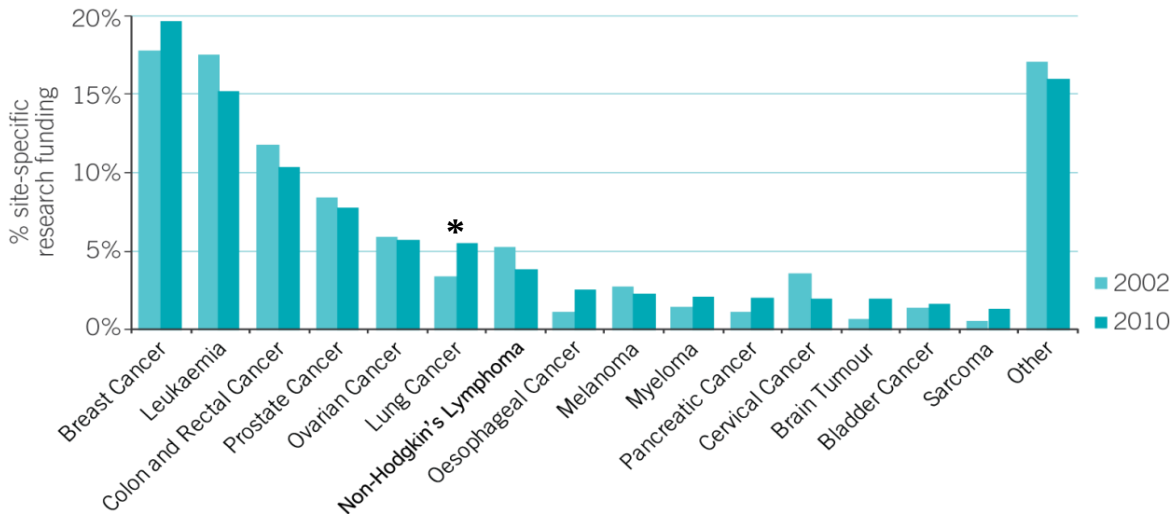

Figure 7. Percentage of site-specific research funding for cancers in 2002 and 2010 (46). * shows the significant increase in research funding for lung cancer. Reproduced with permission from National Cancer Research Institute, UK

4.2. Advantages and challenges of pulmonary delivery

Targeted delivery of drugs to the lungs for the treatment of chronic lung infections, lung cancers, tuberculosis and other respiratory conditions has been emerging as an innovative area of research in the last decade (48, 49). Potential advantages of targeted delivery include the reduction of dosage and side effects of the drug compared to systemic drug delivery (49). While the majority of commercially available inhalation products are for local treatment of lung diseases, a number of inhalation products designed to treat systemic diseases are undergoing clinical development (50). The lung is an attractive target for drug delivery due to the avoidance of first-pass metabolism, the large surface area and the rapid onset of action leading to enhanced absorption of drugs (49, 51, 52). Also, the limited proteolytic activities in the lungs reduce the metabolism and clearance rate which allows for longer action of the drug (49).

Further research is needed to understand the physicochemical properties of particles delivered to the lungs (49). Developments in drug carriers designed to enhance aerosolisation efficiency and lung deposition of the drug found major challenges in formulation (53). These challenges include fabricating particles with adequate aerodynamic properties, drug release, appropriate biodegradation and avoidance of particle uptake by macrophages that prevent drugs from reaching the site of action (53).

Recently, polymeric particles in the application of drug delivery to the lungs has been widely researched due to their biocompatibility, surface modification capability and controlled-release properties (52). More specifically, biodegradable polymers are recognised as promising excipients for sustained release formulations (54). There have been developments to the formulation of polymeric particles from biodegradable polymers, such as polylactic acid carrying cisplatin for targeted drug delivery (55). These polymeric particles

demonstrated the advantages of longer circulation half-lives and drug accumulation at the tumour sites (55, 56). However, further long term biodegradability and toxicity studies are required in order to avoid harmful accumulation of polymeric particles in the lungs (52).

The importance of long term studies was seen in the case of novel drug delivery systems for doxorubicin for the potential treatment of lung cancer. In 2008, polysorbate-80-coated nanoparticles loaded with doxorubicin were formulated and the *in vitro* studies demonstrated more effective cytotoxicity compared to free doxorubicin (48). The results showed that the doxorubicin-loaded nanoparticles were more readily internalised *via* endocytosis compared to free doxorubicin entering cells by passive diffusion mechanisms (48). This study was concluded with a promising outcome for the development of inhalable nanoparticles loaded with anticancer drugs. A study by Al-Hallak *et. al.* in 2010, found that the polysorbate-80-coating caused pulmonary toxicity and decreased tolerance in both *in vitro* and *in vivo* studies (48, 57). In 2011, Roa *et. al.* developed carrier particles consisting of sodium carbonate and lactose monohydrate in two different forms – effervescent and non-effervescent – to deliver doxorubicin *in vivo* to mouse models (58). The results showed that inhalable effervescent nanoparticle powder was an effective delivery vehicle with a significantly longer survival time compared to the intravenous administration of the same drug dose (58). This case of doxorubicin delivery for lung cancer highlighted the need for long term studies in developing novel drug delivery systems.

4.3. Anticancer drug delivered via inhalation

Novel routes for the administration of cancer therapies have been investigated for decades (59). Among the novel routes, pulmonary drug delivery for treatment for lung cancer has

been widely researched in the last two decades due to many obvious advantages including reduction of dosage required and therefore reduced systemic side effects (59).

Cisplatin is a platinum-based first-line chemotherapy drug for lung cancer currently delivered intravenously (56). The conventional cisplatin formulation delivered intravenously is widely distributed into body fluids and tissues and rapidly bind to tissue and plasma proteins, leading to low bioavailability to the target organ (60). The majority of the drug fails to reach the target site in the lungs and instead, highest concentrations are found in the kidneys and is excreted from the body predominantly via renal excretion (60). Thus there are common systemic side effects such as nephrotoxicity, ototoxicity, mucositis and mylosuppression often leading to life-threatening septicaemia (60, 61). Furthermore, the cytotoxic effect of cisplatin in currently marketed formulations is short lasting and requires frequent dosing to maintain the concentration of the drug within the therapeutic window (60). This increases the costs to healthcare because a health care professional is required for the administration of every intravenous dose (60).

Selting *et. al.* stated that inhaled cisplatin is a promising method of treatment for both primary and secondary lung tumours with minimal serum concentration of cisplatin detected compared to intravenous cisplatin (62). This was demonstrated in the *in vitro* release study of cisplatin-loaded albumin nanoparticles by Das *et. al.* and from a study investigating the extended cytotoxic activity of core-surface-cross-linked nanoparticles loaded with cisplatin by Xu *et. al.* (60, 63). When nano- or micro-carrier molecules are used to deliver cisplatin, the ability to deliver drugs preferentially to cancer tissues allowed for enhanced therapeutic efficacy and reduced side effects (63). Additionally, cisplatin is released over a longer period of time, leading to enhanced cytotoxic effects (60, 63).

In 2007, cisplatin encapsulated in aerosolised sustained release lipid vesicles were developed and a phase I clinical study was conducted to investigate the safety and pharmacokinetics in

humans (64). This study recruited 17 patients with primary cancer of the lung or metastatic cancer to the lungs with a life expectancy of at least 12 weeks who had no other standard treatment available for them due to unresponsiveness (64). Around 40 to 50% of the encapsulated cisplatin was released immediately and the remaining 50 to 60% of total cisplatin was found to be delivered in a sustained release manner. The study concluded that this treatment was feasible and safe as the adverse effects experienced by the patients were the general adverse effects of chemotherapy such as nausea and vomiting. Also, most other adverse effects experienced by the patients – dyspnoea, productive and irritative cough, and hoarseness – were not specific to the direct effects of cisplatin delivered by inhalation, but instead were due to an inhaled compound to the respiratory tract (64).

5. Summary

Silk proteins are widely established as drug delivery platforms; however, to our knowledge there are no inhalable formulations of silk proteins. A drug carrier is required in order to deliver drugs to the lungs in order to optimise delivery to the site of action and silk proteins are good candidates due to the properties described above.

The silk-based carriers were designed for potential application in delivery of various drugs, however with the given time frame, two types of drugs were investigated in this project – antibiotic and anticancer drugs.

Targeted delivery of antibiotics via inhalation using silk carriers would be beneficial for many patients with regular or frequent uses of oral or intravenous antibiotics for infections in the respiratory tract, especially with some evidence that sericin naturally possesses antibacterial actions (20).

It is clear that there is a need of better treatment regimens for lung cancer. Targeted delivery of cisplatin to the lungs may improve the side effect profile of currently injected cisplatin. When silk fibroin is cross-linked in order to deliver cisplatin at a modified release, the cytotoxicity of cisplatin may be also improved.

II. Research Proposal

1. Significance and aims of the project

This project is focused on the development of new silk-based particles for localised delivery of anticancer drugs to the lungs. Apart from the instance where sericin was formulated into inhalable particles via spray drying by Genc *et. al,* silk has not been developed into drug carriers for pulmonary delivery (20, 51). This project aims to optimise the formulation of inhalable silk-based particles to act as carriers for cisplatin, an anticancer drug, for potential treatment of lung cancer through pulmonary delivery. Also, cytocompatibility studies were conducted to investigate the effects of silk on lung cells, and to observe differences between the cytotoxic effects of cisplatin when formulated with various silk-based particles.

Cisplatin was the chosen anticancer drug to be delivered using the silk-based carrier particles for two main reasons:

- The systemic adverse effects such as nephrotoxicity, ototoxicity, mucositis and mylosuppression, can be minimised through targeted local delivery (60).
- Currently marketed formulations of cisplatin are short lasting and require frequent dosing, therefore the controlled release formulations of cisplatin are considered to be valuable (60).

Currently, there is no commercially available product for the controlled release medications through inhalation. Often inhalation medications need to be administered two to four times daily leading to poor patient compliance (54).

For the case of silk fibroin, a crosslinking agent was required to achieve controlled release properties. Genipin was the ultimate choice for the purpose of this project as the cytocompatibility studies of genipin conducted previously confirmed the safety of genipin to

use as biomaterials (65, 66). Therefore, no additional experiments were required to prove the cytocompatibility of genipin for this project. Genipin is described as a non-toxic crosslinking agent for silk fibroin in biomedical applications that could "maintain the biocompatibility, bioactivity as well as improving the water resistance and mechanical properties of silk fibroin materials" (65).

Fabrication of the silk-based particles was conducted using two methods – spray drying and spray-freeze-drying. Spray drying is a relatively simple, one-step process to convert silk-based aqueous solutions into dried particles with narrow particle size distributions (54). However, a shortcoming of the spray drying method is that varying yields are produced. Spray-freeze-drying is an efficient method with high yields of up to almost 100%. Despite the requirements of longer time, more caution with handling cryogenic fluids and higher costs, spray-freeze-drying produced particles with favourable characterisation and aerosolisation performance (54).

Spray-freeze-drying protein formulations require the use of a lyoprotectant – a sugar or sugar alcohol – to protect the protein structure in the low temperatures during the drying process. However, the inclusion of sugar in the formulations has additional benefits as it improves stability and acts as a matrix-former to prevent agglomeration upon drying (67). Sucrose, trehalose and mannitol, all of which are sugars, were used as lyoprotectants in the formulation of silk-based particles. Mannitol is an approved excipient for dry powder inhaler formulations while trehalose is listed as one of the promising alternatives (54). The differences between the formulations arising from the choice of lyoprotectant were also identified in this project.

2. Specific aims

- To demonstrate that the novel silk-based formulations are inhalable and could be developed into controlled release delivery systems.
- To show that silk proteins naturally exhibit antimicrobial actions and that the silk formulations can synergistically enhance the efficacy of antibiotics.
- To demonstrate the cytocompatibility of the silk-based formulations.
- To compare the cytotoxicity of the normal or cross-linked silk-based cisplatin formulations.

3. Research plan

The following is a flow chart for the process of the formulation and optimisation of silk-based particles for lung delivery. At each step of the formulation, the particles were characterised to develop an optimised formulation for silk-based cisplatin particles.

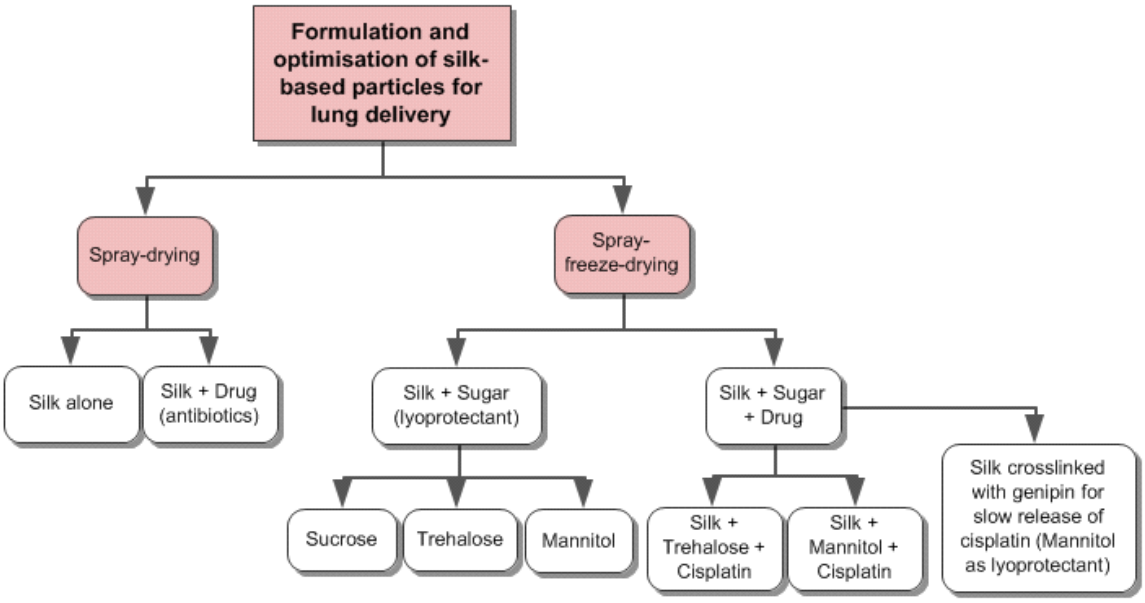

Figure 8. The process for formulation of silk-based particles for optimised formulation of silk-based cisplatin particles for pulmonary delivery

III. Materials and methods

1. Formulation of silk-based particles

1.1. Source of materials

Silk proteins (fibroin and sericin) extracted from both *A.mylitta* (AM) and *B.mori* (BM) species of silkworm were kindly supplied by Professor Kundu, the Department of Biotechnology, Indian Institute of Technology Kharagpur, prepared in scaffolds (fibroin) or powder (sericin) form. All other chemicals were purchased from Sigma-Aldrich (Castle Hill, Australia).

1.2. Silk protein solution preparation

The silk scaffolds or powder were weighed and cut into appropriate sizes to be dissolved in deionised water at concentrations ranging from 0.1% to 2% (w/v) with heating at 45°C and sonication for 10 minutes. Undissolved silk fibroin parts were removed by filtering through 0.22 µm syringe filters (Millipore, Millex® GP Filter Unit, Millipore Express PES Membrane, Darmstadt, Germany). For spray-freeze-drying silk solutions, a lyoprotectant (sucrose, trehalose or mannitol) was incorporated at concentrations of 0.5% or 1% (w/v). All solutions were prepared fresh on the day of experiment and were stored at 2 – 8 °C before use.

1.3. Incorporation of drug to silk solutions

The antibiotics used were ciprofloxacin and gentamicin, incorporated to silk solutions prepared for spray drying, at concentrations of 0.07% or 1% (w/v). Cisplatin was the chosen anticancer drug, incorporated to silk solutions prepared for spray-freeze-drying, at

concentrations of 0.05% or 0.1% (w/v). Drugs were weighed and dissolved in deionised water prior to mixing with the silk solutions.

1.4. Crosslinking of silk fibroin for controlled release of drug

Prior to adding drug to the silk solutions, genipin was added to the silk solutions at a concentration of 0.05% (w/v) in order to produce formulations of silk cross-linked with genipin. The solution was mixed using a magnetic stirrer for 15 hours at room temperature.

1.5. Fabrication of particles from spray-drying

Silk solutions with or without drug were prepared for spray drying using a lab scale spray-dryer (Büchi Mini Spray-Dryer B-290, Büchi Labortechnik, Flawil, Switzerland). The spray dryer was used in an open loop, with Büchi Dehumidifier B-296 in blowing mode. The operation condition used were as follows: liquid feed rate at 1.7, 3.5, 4.2 and 4.8 ml/min, aspiration at 100%, airflow with gas supply pressure 50-60 mbar, and inlet and outlet temperatures at 120 ºC and 61-87 ºC, respectively.

1.6. Fabrication of particles from spray-freeze-drying

The solution prepared for spray-freeze-drying was placed into a syringe fitted onto a PHD 2000 syringe pump (Harvard Apparatus, Holliston, MA, USA), used to feed solution at a rate of 0.5 ml/min through an ultrasonic nozzle (Sonozap 130K50ST), powered by an ultrasonic generator (Sonaer Inc, New York, USA). Particles were collected in a beaker containing liquid nitrogen, in an insulated tub containing liquid nitrogen surrounding the beaker to keep

stable temperature. Samples were transferred into the freeze dryer (Christ Alpha 1-4, B.Braun Biotech International, Melsungen, Germany) for drying under vacuum. The temperature was set to -20ºC, for 24 hours for primary drying, followed by secondary drying at increasing temperatures of 10ºC per hour until final temperature of 20ºC was reached. The vacuum was set to 0.1 mbar, however actual vacuum measured was between 0.07 - 0.12 mbar.

Table 2. A list of silk-based particles formulated for the purpose of this project

Method of production	**Formulation**	**Concentration ratio**
Spray dried silk alone	BM fibroin only	N/A
	AM fibroin only	
	BM sericin	
	AM sericin	
Spray dried silk + antibiotics	BM fibroin + ciprofloxacin	10:1
	AM fibroin + ciprofloxacin	5:1
	AM fibroin + gentamicin	5:1
Spray-freeze-dried silk alone	BM fibroin + sucrose	2:1
	BM fibroin + trehalose	1:1, 2:1, 1:2
	BM fibroin + mannitol	1:1
	AM fibroin + trehalose	1:1
Spray-freeze-dried silk + cisplatin	BM fibroin + trehalose + cisplatin	1:1:1, 5:5:1, 10:5:1
	AM fibroin + trehalose + cisplatin	5:5:1
	BM fibroin + mannitol + cisplatin	5:10:1, 10:20:1, 10:8:1
Spray-freeze-dried cross-linked silk + cisplatin	BM fibroin + mannitol + cisplatin + genipin	10:20:1:1

2. Characterisation of silk-based particles for pulmonary delivery

2.1. Assessment of particle size and morphology

2.1.1. Particle size distribution by dynamic light scattering

Geometric particle size and the size distribution of the particles were measured by laser diffraction using Mastersizer (Malvern Instruments, Worcestershire, UK). Dry dispersion with refractive index of 1.0 was used. Triplicate samples were analysed for reliability. Mass median diameter (D(0.5)), which represents the diameter at which 50% of the particles had by mass are larger and 50% are smaller, was identified, and this was considered as the average particle diameter by mass.

2.1.2. Particle size and morphology

Scanning electron microscopy (SEM) was used to observe the morphology and size of the particles after producing each batch of particles. Samples were dispersed onto carbon tape, mounted on SEM stubs, and sputter coated with approximately 20 nm thick gold using a K550X sputter coater (Quorum Emitech, Kent, UK). Images were obtained using Hitachi S-4500 field emission scanning electron microscope (Hitachinaka-shi, Ibaragi, Japan). The approximate particle sizes observed in the SEM micrographs were used to alter the parameters for the formulation of fibroin particles.

2.1.3. Three-dimensional analysis of surface topography

Atomic force microscopy (AFM) was used for observing particle size and imaging 3D surface topography. The particles were dispersed onto Tempfix® (Plano GMBH, Wetzlar,

Germany) prepared on a glass slide. MFP-3D-BIO^{TM} AFM (Asylum Research, Santa Barbara, USA) was used in AC mode and images were produced in 256 x 512 sample points at a scan rate of 0.30 – 0.40 Hz and scan size 600 nm – 1.5 μm. The images were processed into colour, 3D images and were analysed using the Igor Pro software program (Version 6.22A, Asylum Research, Santa Barbara, USA).

2.2. Determination of amorphous or crystalline structures

To determine whether the particles are amorphous or crystalline, an X-ray diffractometer (XRD-6000, Shimadzu Scientific Instruments, Tokyo, Japan) was used to measure samples under ambient conditions with angular increments of 0.02˚ covering a 2θ range of 2 to 80˚.

2.3. Stability of particles upon exposure to humidity

To monitor the stability of the formulated particles, moisture sorption profiles were determined using a dynamic vapour sorption (DVS) analyser (DVS Intrinsic, Surface Measurement Systems Ltd., London, UK). Samples were exposed to two sorption-desorption cycles, from 0 to 90% relative humidity, at 25 ˚C.

2.4. *In vitro* aerosolisation performance and lung deposition

In order to assess the *in vitro* aerosolisation performance, the aerodynamic diameters of the particles were calculated after dispersion of particles using a next generation impactor (NGI) (Copley Scientific Limited, Nottingham, United Kingdom). A 5 mg of sample was placed inside a gelatin capsule (size 3) to be dispersed using an Aeroliser® (Pharmaxis Ltd, Frenchs

Forest, Australia), at airflow of 60 L/min for a duration of 4 seconds. Particles were collected according to their aerodynamic diameter at 7 stages with cut-off points 8.06, 4.46, 2.82, 1.66, 0.94, 0.55 and 0.34 microns when dispersed at 60 L/min (68). Then 5 ml of calcium chloride ($CaCl_2$) 60% solution was used to dissolve the particles at each stages and 1 ml of each solution was used for quantification of fibroin using a UV-Vis spectrophotometer with λ_{max} at 274 nm (UV-1800, Shimadzu Corporation, Tokyo, Japan). A standard curve was generated in order to quantify the results. The fine particle fraction (FPF), the proportion of particles that are smaller than 5 µm in diameter from the emitted dose per actuation, was calculated using the proportion of the fine particle dose less than 5 µm in the total actuated dose in the impactor.

3. Investigation for antibacterial action naturally exhibited by silk proteins

3.1. Preparation of silk samples

Raw materials of silk were used for the disc diffusion assay, for fibroin and sericin from both AM and BM species. Silk stock solutions were each prepared at 1 mg/ml concentration and were diluted as required for each assay.

3.2. Antimicrobial susceptibility testing

3.2.1. Disc diffusion assay

A Mueller-Hinton agar, containing 22 g of Mueller-Hinton broth (Sigma-Aldrich, Castle Hill, Australia) and 15 g of Agar in deionised water, was prepared to be poured into petri dishes at a depth of approximately 5 mm and were left overnight. Mueller-Hinton agar was used

instead of nutrient agar as per recommendations for antimicrobial susceptibility testing from Clinical and Laboratory Standard Institute (69). The agar surface was inoculated by using a swab dipped in a cell suspension adjusted to the turbidity of a 0.5 McFarland standard (approximately 10^6 cells/ml). The three strains of bacteria were used were *P.aeruginosa*, *S.aureus* and *E.coli*. Sterilised paper discs filled with 25, 50 and 100 µg of silk sample were placed on top of the inoculated agar. This experiment was carried out in triplicates. The plates were incubated overnight in air at 36˚C and the zone of inhibition was measured using a ruler.

3.2.2. Broth dilution assay

Ten test tubes containing 5 ml of Mueller-Hinton broth were inoculated with *Pseudomonas aeruginosa* (*P.aeruginosa)*, *S.aureus* or *E.coli* adjusted to the turbidity of a 0.5 McFarland standard (approximately 10^6 cells/ml). AM and BM sericin and fibroin solutions were added to the test tubes each at ten different concentrations doubling from 0.098 µg/ml to 50 µg/ml. This experiment was carried out in duplicates. Incubation was done overnight in air at 36˚C and a visual inspection of turbidity was carried out for indication of bacteria growth, and minimum inhibitory concentration (MIC) was determined.

3.2.3. Determination of minimum bactericidal concentration

In order to determine the minimum bactericidal concentration (MBC), or whether the observed antibacterial activity was bacteriostatic or bactericidal, a 100 µl sample was taken out from each of the two tubes with no bacteria growth after treatment with silk protein solution from the broth dilution assay. The samples were each mixed with 5ml of sterile Mueller-Hinton broth in sterile test tubes. This experiment was carried out in duplicates. The

test tubes were incubated overnight in air at 36˚C and a visual inspection of turbidity was carried out for indication of bacteria growth.

4. *In vitro* cytocompatibility of silk proteins and cytotoxicity of silk-cisplatin particles

4.1. Cell culture and maintenance

Human lung carcinoma epithelial cell line A549 was purchased from ATCC®. A549 cells are responsible for the diffusion of substances across the alveoli of lungs and thus it was used to investigate the cytocompatibility of silk and to assess cytotoxicity of silk particles loaded with cisplatin. Cells were maintained using "normal media" consisting of Dulbecco's Modified Eagle's Medium (DMEM) with 4500mg/L D-glucose, L-glutamine, with 10% foetal bovine serum (FBS), were used with 1% Penstrep® or 1% antibiotic-antimycotic, as available (All from Gibco by Life Technologies, USA, except FBS from Sera Laboratories, UK). Cells were maintained at 37˚C in 95% air and 5% CO_2 atmosphere. Medium was renewed every 2 to 3 days and passaged as needed when monolayer was 80-85% confluent. When passaging cells, the monolayer cells were washed with phosphate buffered saline (PBS), and were treated with TrypLE™ Express (Gibco by Life Technologies, USA) or Trypsin/EDTA (Sigma-Aldrich, USA), as available, to detach the adherent cells. For trypsinisation process, enough trypsin was added to cover the cells (4 ml for T-75 flask), incubated for 2-3 minutes and visually checked for cell detachment by tapping the side of the flask and looking under the microscope. A small amount of media (2-3 ml) was added to stop the trypsinisation process and the cells were transferred to a 15 ml tube to be centrifuged at 1500 rpm for 2 minutes. The supernatant was discarded and cells were resuspended in a desired volume of media to be transferred into a new flask. Mycoplasma testing was conducted twice for two separate batches of cells and results were negative at both times. All

polystyrene plastic flasks and plates used were of tissue culture grade. Each experiment was carried out in triplicates.

4.2. Preparation of samples for cell viability assays

4.2.1. Formulation of two dimensional (2D) silk scaffolds using silk solutions

2D silk scaffolds were formulated with the purpose to seed cells and culture on top of the scaffolds in order to test the cytocompatibility of silk proteins. AM and BM silk fibroin scaffolds and raw silk sericin powders were each dissolved in deionised water at desired concentrations, then were sterilised by filtering through 0.22 µm syringe filters (Millipore, Millex® GP Filter Unit, Millipore Express PES Membrane). The silk solutions were used to cast 2D films on the 96-well plates, to be dried to form 2D silk scaffolds. These 2D silk fibroin scaffolds were treated with ethanol to induce insolubility by altering the structure of fibroin, as well as for sterilisation purposes. The scaffolds were washed three times with PBS and were sterilised with ultra-violet (UV) light for 30 minutes inside the biosafety cabinet, prior to seeding cells for cell viability assays.

4.2.2. Preparation of silk conditioned media using formulated particles

Samples were prepared using silk alone, silk + sugar (ratio 2:1), silk + mannitol + cisplatin (10:20:1), or silk + mannitol + cisplatin + genipin (10:20:1:1) formulations, dissolved at 1mg/ml and 10mg/ml concentrations in normal media for 24 hours at 37˚C in the water bath. Sterilisation was done by filtering the sample dissolved in media through a syringe connected

to a 0.22 µm syringe filter (Millex® GP Filter Unit, Millipore Express PES Membrane, Millipore, USA).

4.3. Cell viability and proliferation assays

For methyl thiazolyl tetrazolium (MTT; 3-(4,5-Dimethylthiazol-2yl)-2, 5-diphenyl tetrazolium bromide) and alamarBlue® assays, cells were seeded on top of the 2D silk scaffolds (prepared as described in section 4.2.1), whereas Cell Counting Kit-8 (CCK-8) assay had cells seeded directly onto the tissue culture well plates then treated with silk-based particles dissolved in media (prepared as described in section 4.2.2).

For each assay, A549 cells were seeded at a density of 2000 cells/well on 96-well plates, prepared in triplicates for each sample. Each well contained 100 µl media which was not renewed until the end of each experiment. For experiments with duration of seven days, small amounts of media (50 µl) were added to each well on the fourth day.

4.3.1. AlamarBlue® cell viability assay

Cells were seeded onto the 2D silk scaffolds and were monitored daily using a light microscope (Olympus CK40, Tokyo, Japan). Cells were maintained in normal maintenance conditions. At each predetermined time point, (days 1, 3, and 7), 10 µl of alamarBlue® dye was added to each well and were incubated for 3 hours at 37ºC in the dark inside the incubator. Fluostar Optima plate reader (BMG Labtech, Ortenberg, Germany) was used at excitation 544 nm / emission 590 nm to measure fluorescence intensity.

4.3.2. MTT cell viability assay

On the day of experiment, a stock solution of yellow tetrazole dye, MTT (Sigma-Aldrich, Castle Hill, Australia), was prepared by dissolving in deionised water to achieve 5 mg/ml concentration. This was stored in the dark at 4ºC. Cells were seeded onto the 2D silk scaffolds and were maintained in normal maintenance conditions. At each predetermined time point (days 0, 1, and 3), MTT solution was added (10 µl/well) and incubated for 3 hours at 37ºC in the dark, inside the incubator. After incubation, the formazon crystals were dissolved by adding 100 µl of isopropanol to each well, pipetting up and down, and using the plate shaker for 20 minutes. Optical density was measured spectrophotometrically at 570-690 nm using an ELISA plate reader.

4.3.3. CCK-8 cell viability assay

Cells were seeded and were allowed to attach to the bottom of the wells (3-4 hours after seeding) before replacing normal media with conditioned media containing the particles (prepared as described in section 4.2.2). Cells were maintained in normal maintenance conditions. At each predetermined time point (days 1, 3 and 7), media was removed and cells were washed twice using sterile PBS. Fresh normal media (100 µl) was added to each well and placed back into the incubator. After one hour, 10 µl of CCK-8 reagent (Dojindo Molecular Technologies, Inc, Tokyo, Japan) was added to each well and was incubated for 2 hours at 37ºC in the dark inside the incubator. The optical density (OD) of each well was measured using a microplate reader at 450 nm (Tecan Safire^2, Switzerland).

4.4. Picogreen® DNA quantification assay

The DNA content in cells treated with various formulations was measured using a Picogreen® double-stranded DNA (dsDNA) Quantitation Kit (Invitrogen Molecular Probes, USA), according to the manufacturer's protocol. Briefly, cells were seeded at 2000 cells/well in 96-well plates and were allowed to attach with incubation in normal media. Cells were washed with sterile PBS and were incubated with filter-sterilised, conditioned media containing 1 mg/ml of silk-alone, silk + sucrose (2:1), silk + mannitol + cisplatin (10:20:1), or silk + mannitol + cisplatin + genipin (10:20:1:1) (prepared as described previously in section 4.2.2).

Picogreen® assay was done after 24 and 72 hours of incubation. At each time point, cells were washed with PBS, detached using trypsin, and were resuspended in sterile water for cell lysis and release of DNA through freeze-thaw cycles repeated three times. Tris-ethylenediamine-tetraacetic acid (TE) buffer was used to dilute the solution containing cells to a total volume of 500 µl, then Quant-iT™ Picogreen® reagent (Invitrogen Molecular Probes, USA) 0.5% in TE buffer was added to each sample. After incubation at room temperature in the dark for 5 minutes, 100 µl of each sample was transferred onto a black 96-well plate in order to measure the fluorescence using Fluostar Optima plate reader (BMG Labtech, Ortenberg, Germany) at excitation 450 nm / emission 544 nm. Each experiment was carried out in triplicates.

4.5. Changes in cell morphology

Cells were seeded at a density of 2.5 x 10^5 cells/well on a 24-well plate and were cultured for 24 hours with normal media, and then normal media was replaced with filter-sterilised, conditioned media containing 1 mg/ml of silk-alone, silk + sugar (2:1), silk + mannitol + cisplatin (10:20:1), or silk + mannitol + cisplatin + genipin (10:20:1:1) (prepared as described

in section 4.2.2). Changes in cell morphology due to different treatment conditions were examined using light microscopy and immunofluorescence imaging.

4.5.1. Phase images

Changes in cell morphology were observed using Olympus CK40 light microscope (Olympus, Tokyo, Japan) and phase images were taken using a transmitted light microscope (EVOS xl, Advanced Microscopy Group, Life Technologies, USA) with 10x and 20x magnifications at 24 and 48 hours.

4.5.2. Immunocytochemistry

Immunocytochemistry was used to monitor changes in morphology and in the expression of gap junction protein (beta-catenin) in response to silk-based formulations.

After 30 hours of incubation with conditioned media, media was removed and cells were washed twice using sterile PBS. Immunocytochemistry protocol from Abcam® was used with some modifications (70). Briefly, cells were fixed in paraformaldehyde 4% in PBS (prepared from powder purchased from Sigma-Aldrich, USA) with 20 minutes incubation at room temperature, followed by washing twice with cold PBS. Cells were permeabilised in PBS containing 0.1% Triton X (BDH Laboratory Supplies, England) for 20 minutes, washed three times with PBS, 5 minutes per wash. Blocking agents used were bovine serum albumin (BSA) 1% (Sigma-Aldrich, USA) or goat serum 5% (Invitrogen, Camarillo, CA, USA) in PBS, as available, for 30 minutes prior to incubation with primary antibody. Although BSA was known to be the most widely used blocking agent, the serum from the same animal species of

the secondary antibody was recommended to be used (82). Therefore, 5% goat serum was used as the blocking agent when available.

Primary antibody anti-beta catenin, clone 7F7.2; IgG (Millipore, USA) was diluted at ratios of 1:100, 1:250, 1:500 or 1:1000 in PBS, incubated overnight at 4˚C covered with foil to prevent exposure to light. After incubation, the cells were washed with PBS. The 1:250 dilution ratio was found to be appropriate for optimum staining, and this dilution ratio was used in all subsequent experiments.

Secondary antibody Alexa Fluor® 555 containing 5 mM sodium azide (Life Technologies, USA) was diluted at 1:200 in PBS and incubated for one hour at room temperature in the dark. The cells were washed with PBS. Counter staining with conjugated F-actin (ActinGreen™ 488, Life Technologies, USA) diluted at 2 drops/ml in PBS was incubated in the dark for 30 minutes at room temperature. Cells were washed with PBS. DAPI (4',6-Diamidino-2-Phenylindole, Dilactate) nucleus staining (Invitrogen Molecular Probes, USA) (diluted 1:2000 in PBS) followed with 5 minutes incubation, and then cells were washed and were imaged using a fluorescent microscope (Nikon Eclipse TE2000-U inverted microscope) at 20x magnification.

All washes after each staining were done in the dark, three times in PBS, 5 minutes per wash. Secondary antibody and DAPI were purchased from Invitrogen Molecular Probes, USA. Fluorescent images were merged using ImageJ software program downloaded from http://imagej.nih.gov/ij/download.html accessed on 16/01/2014.

4.6. Cell Metabolism

Cell metabolism was evaluated by biochemistry analysis using the YSI 2700 Select Biochemistry Analyser (YSI Incorporated, Yellow Springs, USA). Samples of media were collected after 1, 3 and 7 days of incubation with A549 cells cultured with media containing silk alone, silk + sugar (2:1), silk + mannitol + cisplatin (10:20:1), or silk + mannitol + cisplatin + genipin (10:20:1:1) formulations. L-lactate and D-glucose levels in media were measured in g/L and were expressed in a single graph.

4.7. Cell Migration and Invasion

Cell migration and invasion were analysed using transwell cell culture chambers (8 µm pore size, BD Biosciences, Australia). A549 cells were kept in low serum media (containing 1% FBS) for 24 hours then were trypsinised and resuspended in low serum medium and placed in the upper chamber of the transwell insert (50,000 cells/well). Conditioned media containing silk with or without cisplatin and genipin, were placed in the upper chamber for "accelerated escape" and in the lower chamber for "suppressed attraction" (as seen in Figure 9). Incubation was for 3 or 8 hours in a humidified atmosphere with 95% air and 5% CO_2 at 37˚C. Then cells were fixed with 4% paraformaldehyde, and were stained for 30 minutes using 2% crystal violet in 10% ethanol. The non-invasive cells in the upper chamber were removed by wiping with a cotton swab. Cells in the lower surface of the transwell insert which migrated through the pores were imaged using a transmitted light microscope (EVOS xl, Advanced Microscopy Group, Life Technologies, USA) at 10x magnification and the number of migrated cells were counted using ImageJ software. Average number of migrated cells per image were graphed and analysed.

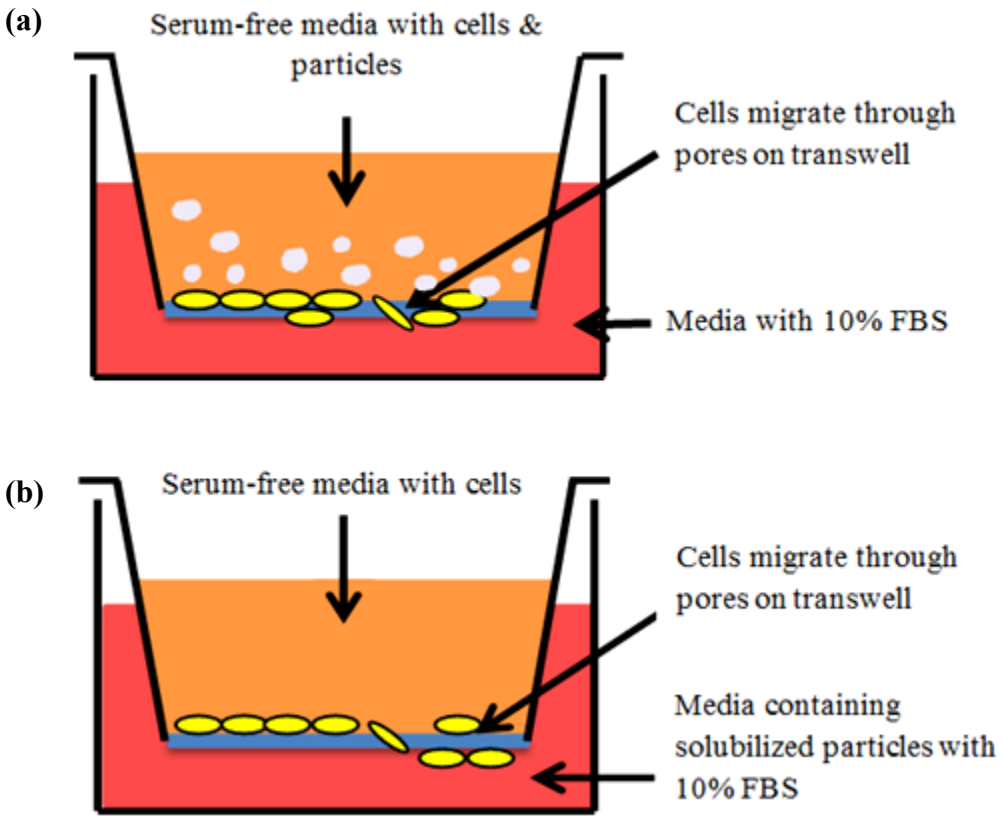

Figure 9. A schematic diagram of the experiment design for cell migration assays per transwell; (a) "accelerated escape" assay and (b) "suppressed attraction" assay

4.7.1. "Accelerated escape"

For each transwell, 50,000 cells were seeded, incubated for one hour and then conditioned media containing silk alone, silk + mannitol + cisplatin (10:20:1) or silk + mannitol + cisplatin + genipin (10:20:1:1) at the concentration of 1 mg/ml in low serum media was added to the upper chamber and incubated for 8 hours.

4.7.2. "Suppressed attraction"

For each transwell, 50,000 cells were seeded, incubated for one hour and then conditioned media containing silk alone, silk + mannitol + cisplatin (10:20:1) or silk + mannitol +

cisplatin + genipin (10:20:1:1) at 1 mg/ml in normal media with 10% FBS was added to the lower chamber and incubated for 8 hours.

4.8. Cell wound repopulation assay

Cells were seeded at a density of 2.5 x 10^5 cells/well and cultured in normal media until 90% confluent. Then cells were incubated in low serum media (containing 1% FBS) for 24 hours prior to this assay. Silk-conditioned media were also prepared 24 hours prior to this assay (as described in section 4.2.2) and filter-sterilised immediately before adding to wells. A pipette tip (200 µl) was used to scratch a wound on the midline of the culture well. Wound repopulation was documented using a transmitted light microscope (EVOS xl, Advanced Microscopy Group) with 10x magnification at 0, 24, and 48 hours. ImageJ software program was used for quantitative analysis, to measure and compare the area of wound at each time points.

4.9. Statistical analysis

All data were produced in triplicates (n = 3) for reproducibility. Data were analysed and presented as means ± standard deviation of samples, except when indicated as standard error of means. The differences between the experimental and control groups were analysed using one-way analysis of variance (ANOVA) test. A p-value less than 0.05 were indicated as having a statistically significant difference.

IV. Results and discussion

1. Characterisation of silk-based particles

1.1. Assessment of particle size and morphology

1.1.1. Particle size analysis of spray dried silk-based particles

Laser diffraction for geometrical size analysis for spray dried particles consisting of AM fibroin and BM fibroin showed that mass median diameter (D(0.5)), otherwise known as the average particle diameter by mass, were 7.03 µm and 5.20 µm respectively (Table 2). These formulations were suitable sizes for deposition in the lungs, as the particles 1 to 5 µm in diameter are capable of being deposited in the small airways and alveoli, while the particles 5 to 10 µm in diameter are mainly deposited in the large airways (71).

Table 3. Mean particle size (µm) of spray dried particles, as determined by laser diffraction analysis; shows mass median diameter (D(0.5)) for each formulation. Both AM and BM fibroin particles were produced at flow rate of 4.2 ml/min, atomiser 55 mbar, aspiration 100%, and inlet temperature 120 °C; the table shows average of three experimental repeats ± standard deviation.

	D(0.1)	D(0.5)	D(0.9)
AM fibroin	2.89 ± 0.60	7.03 ± 0.19	15.28 ± 19.87
BM fibroin	1.71 ± 0.09	5.20 ± 0.69	16.73 ± 5.73

Spray dried silk fibroin particles observed from the SEM micrographs were between 0.5 µm and 10 µm in size, with most particles in the range of 2 µm to 4 µm (Figure 10).

Particle sizes varied according to different parameters used on the spray dryer, and the optimisation of inlet temperature, aspiration, atomisation flow and the feed rate of solution led to inhalable sizes of silk particles. An obvious reduction in size was observed when lower feed rates were used. Figures 10 (a) and (b) show the same batch of BM fibroin produced at a feed rate of 4.2 ml/min which resulted in similar in particle sizes, while (c) and (d) show two different batches of AM fibroin produced at feed rates of 1.7 ml/min and 4.2 ml/min respectively. Overall, particles were smaller when lower feed rates were used, especially for AM fibroin where the liquid feed rate of 1.7 ml/min was used (Figure 10 (c) & (d)). This demonstrated that the lower feed rates of silk solutions into the spray dryer produced smaller particles sizes.

Also, higher atomisation flow and thus, the smaller droplets of silk solution led to smaller particles. This was explained by more energy being supplied to break up the liquid droplet into smaller droplets during the atomisation step (72).

The AM and BM sericin solutions, which were spray dried using lower feed rates of 1.0 ml/min, produced smaller particles (Figure 11). From the SEM micrographs, it can be seen that the particle sizes are smaller compared to fibroin particles observed previously and the majority of those particle sizes were around 1 to 5 μm. Although it is known that higher feed rate produces better yields, lower feed rates were used in order to produce particle sizes less than 5 μm to be suitable for potential delivery to the lower airways (72).

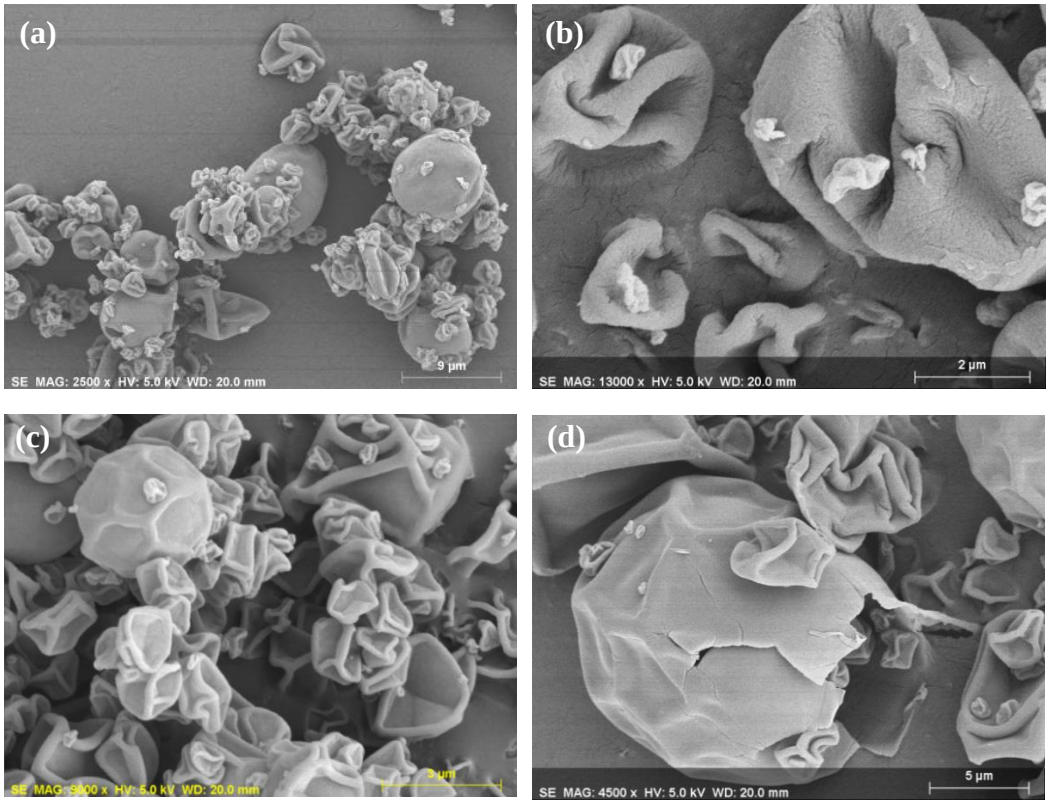

Figure 10. SEM micrographs of spray dried silk particles of: (a)(b) BM fibroin and (c)(d) AM fibroin produced using 2% (w/v) silk solutions; all batches were produced at a feed rate of 4.2 ml/min except (c) which was produced at 1.7 ml/min. All other parameters were consistent: atomiser 55 mbar, aspiration 100%, and inlet temperature 120 °C.

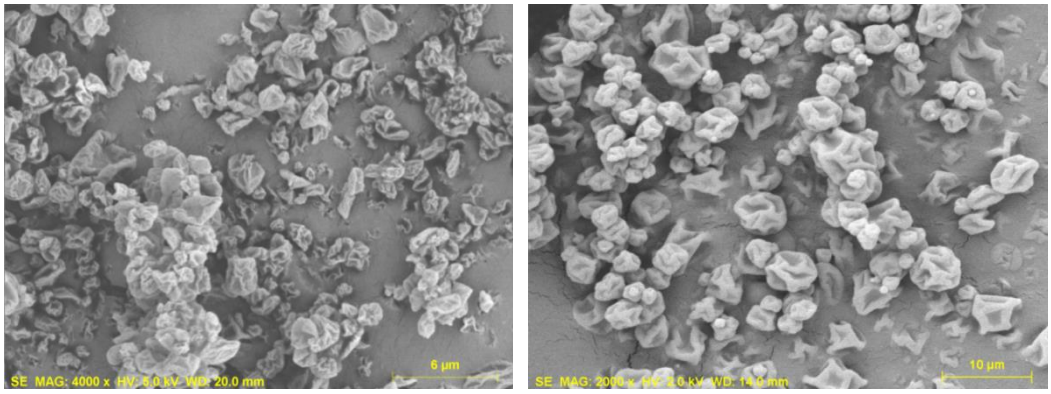

Figure 11. SEM micrographs of spray dried BM sericin *(left)* and AM sericin *(right)* produced using the following parameters: feed rate of 1.0 ml/min, atomiser 55 mbar, aspiration 100%, and inlet temperature 120 °C

1.1.2. Particle size analysis of spray-freeze-dried particles

Particle sizes assessed by observing the SEM micrographs highlighted that the spray-freeze-dried particles were larger than the spray dried silk-based particles. The size distributions of spray-freeze-dried formulations containing trehalose and mannitol as lyoprotectants, measured using dynamic light scattering, revealed significantly larger geometrical particle sizes compared to spray dried particles. The average particle diameter by mass (D(0.5)) of triplicated samples averaged 22.75 μm and 10.08 μm for spray-freeze-dried silk + mannitol + cisplatin and silk + mannitol + cisplatin + genipin formulations respectively (Figure 12 (a) and (b)). It can be seen that the crosslinking of fibroin lowered the average particle size and broadened the particle size distribution. Porous polymeric microparticles for inhalation are required to have diameters between 5 and 30 μm and are able to achieve high aerosolisation efficiency as a consequence of reduced particle density (73). Therefore these cisplatin-containing silk-based particles showed potential for aerosolisation and lung deposition.

The spray-freeze-dried fibroin particles containing sucrose could not be measured using dynamic light scattering due to agglomeration and the inability to be dispersed. The formulation containing trehalose as a lyoprotectant was able to be dispersed. However, the result showed a bimodal distribution of particle size with most particles in the range of 10 to 30 μm or around 1 mm. The peak showing the larger particles on Figure 12 (c) is likely to represent the agglomerated particles and not single particles, therefore, trehalose was an inferior lyoprotectant compared to mannitol in achieving suitable particle sizes for pulmonary delivery (Figure 12 (c)).

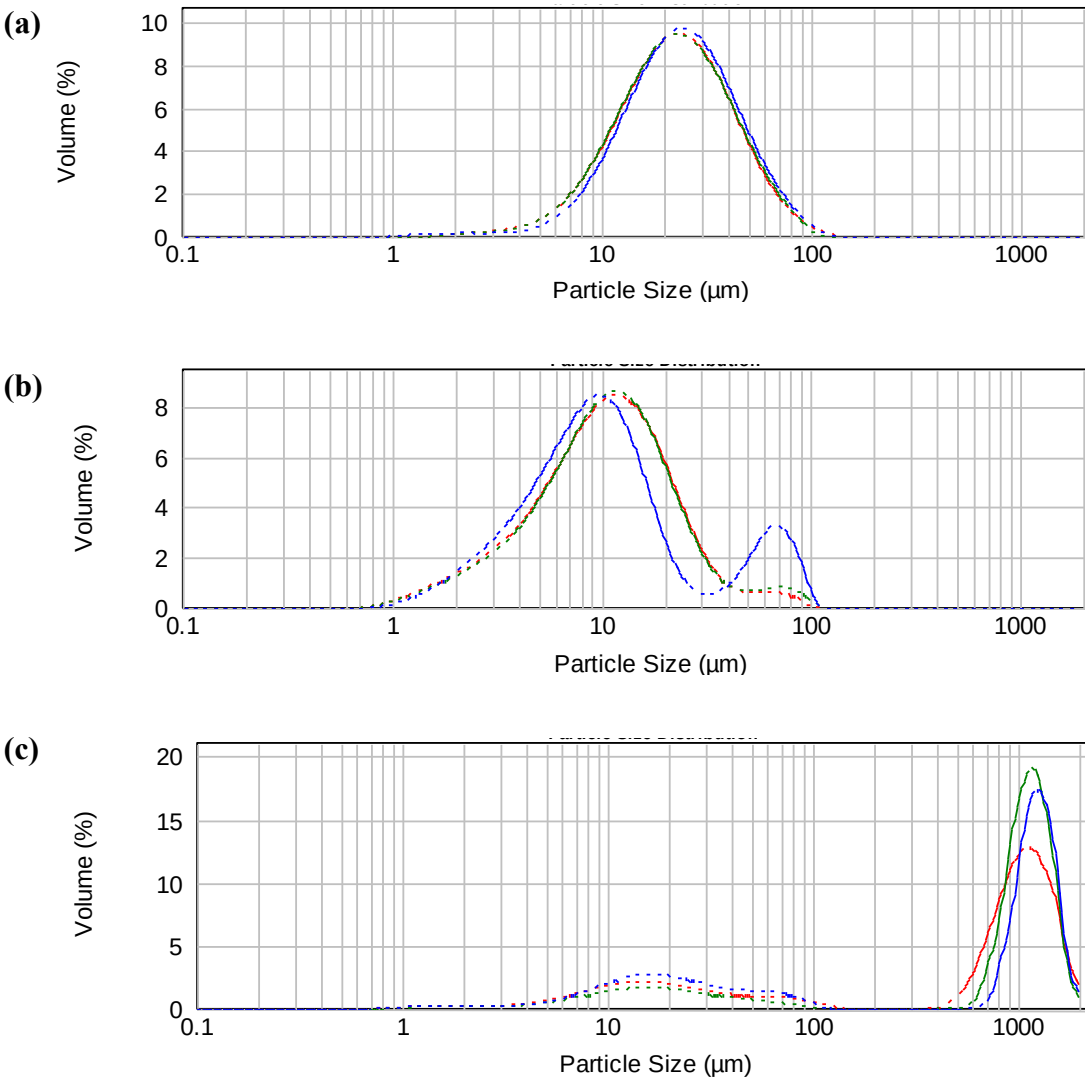

Figure 12. Particle size distributions for spray-freeze-dried: (a) silk + mannitol + cisplatin, (b) silk + mannitol + cisplatin + genipin and (c) silk + trehalose formulations; the samples were triplicated, as represented by the three colours in each panel.

1.2. Morphology

1.2.1. The morphology of spray dried particles

(a) Silk fibroin formulations, with no drug incorporated

From the particles that had burst open, it was demonstrated that spray-dried particles were spherical and hollow (Figure 10 (d)). The ruptured or collapsed particles observed on the SEM micrographs were the result of the spherical and hollow particles being unable to maintain their shape in the high vacuum used during the process of imaging. This confirmed that there were empty spaces inside the spray dried particles.

The surfaces of these particles were rough, rugged and irregular as seen in the height retraced AFM images in Figure 13. Since the roughness or corrugation of the particles play an important role in aerosolisation performance, these particles showed potential for successful lung deposition.

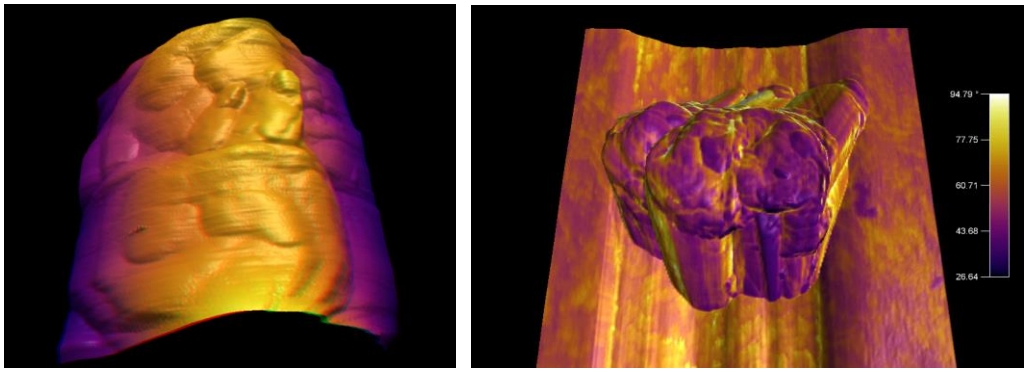

Figure 13. AFM images showing topography of spray-dried BM *(left)* and AM *(right)* silk fibroin particles; used scan rate 0.30 Hz and 0.4 Hz and scan size 600 nm and 1.5 µm, respectively

(b) Silk fibroin formulations, containing antibiotics

The silk particles containing antibiotics, regardless of ciprofloxacin and gentamicin, were agglomerated overall as can be seen from the SEM micrographs in Figure 14. The surface of the particles containing antibiotics were more wrinkled compared to particles spray dried with silk alone as presented previously in Figure 10. The AM fibroin formulation containing ciprofloxacin as seen in Figure 14 (a), consisted of small amounts of larger particles with smooth surfaces and appeared to have a more wide particle size distribution. The formulation containing gentamicin and BM fibroin with ciprofloxacin had more uniform sizes overall and wrinkled surfaces on majority of the particles as can be seen in Figure 14 (b) and (c).

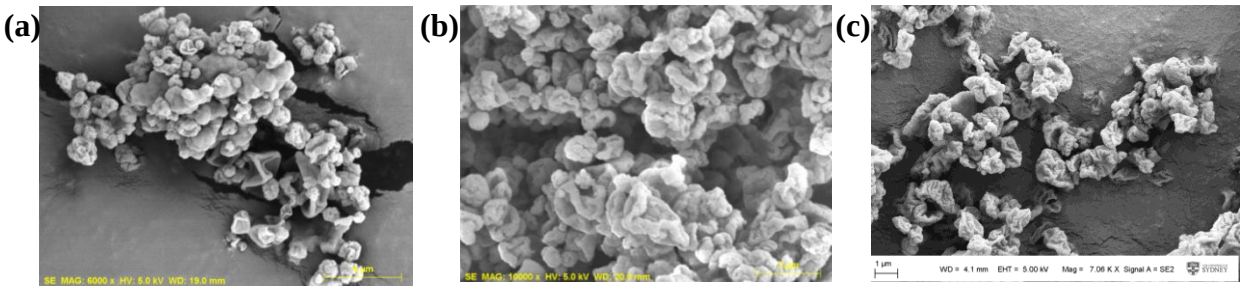

Figure 14. SEM micrographs portraying silk as carriers of drugs; (a) spray dried AM fibroin 0.5% + ciprofloxacin 0.1%, (b) spray dried AM fibroin 0.5% + gentamicin 0.1%, (c) spray dried BM fibroin 0.7% + ciprofloxacin 0.07%

1.2.2. The morphology of spray-freeze-dried particles

(a) Silk fibroin formulations, with no drug incorporated

The SEM micrographs of spray-freeze-dried particles of BM fibroin, with sucrose as lyoprotectant, showed that the particles were spherical and porous (Figure 15). The particles were "fluffy", agglomerated and could neither be dispersed for laser diffraction particle size analysis nor for testing lung deposition using the next generation impactor. These qualities

made the BM fibroin formulation difficult to handle and therefore an alternative lyoprotectant (trehloase or mannitol) needed to be chosen.

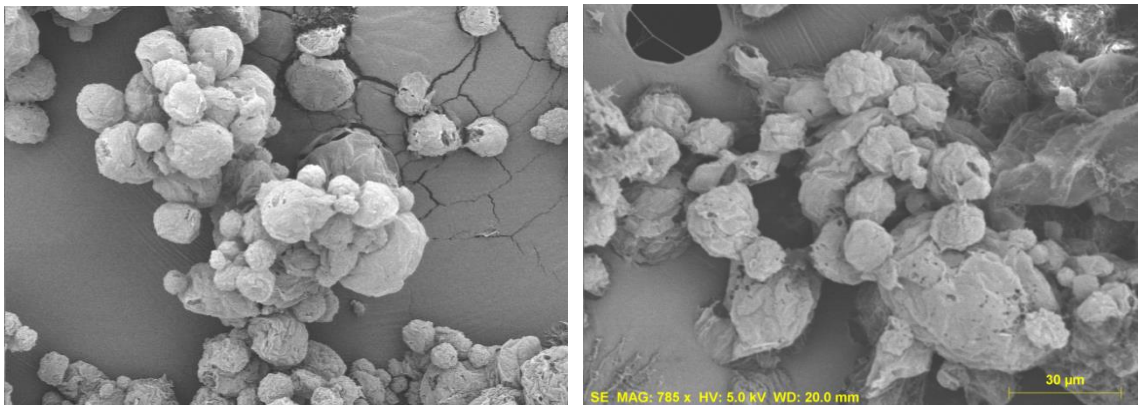

Figure 15. Spray-freeze-dried BM fibroin with sucrose as a lyoprotectant; silk:sucrose ratio was 2:1 *(the scale for both images are as indicated on the right)*

The morphology observed from the above SEM micrographs correlated well with the AFM images in Figure 16, showing the topography of the same batch of spray-freeze-dried BM fibroin particles formulated with sucrose. The topography of particles was more uniform between the particles within the same batch, compared to the spray dried particles. The spray-freeze-dried particles were larger and porous bearing characteristics which were favourable to achieving good aerosolisation performance. The aerodynamic size (d_a) for spherical particles was varied according to the particle density as well as the geometric diameter (d_g), as shown in the following equation:

$$d_a = d_g \sqrt{\frac{\rho}{\rho_0}}$$

where p is the mass density of the particle and p_0 is the unit standard particle density (1 g/cm^3) (49). Therefore, despite the particles having larger diameters in spray-freeze-dried formulations due to their porosity and low densities, they can also have suitable aerodynamic sizes for potential successful deposition in the lower airways (74).

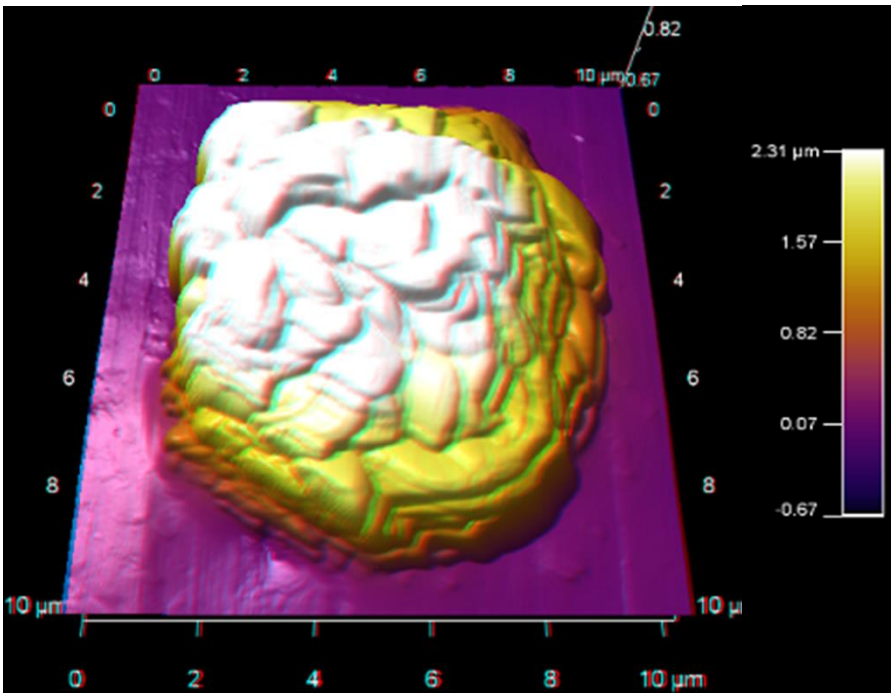

Figure 16. A three-dimensional AFM image of spray-freeze-dried BM fibroin formulated with sucrose as a lyoprotectant with silk to sucrose ratio 2:1, scan rate 0.4 Hz and scan size 10.24 µm

(b) Silk fibroin formulations containing cisplatin

The SEM micrographs of silk fibroin with trehalose together with cisplatin can be seen in Figure 17. Most particles appeared to be uniformly mixed, although backscattering SEM micrographs may show better compositional differences between the batches of particles.

The SEM micrographs in Figure 18 show silk fibroin and cisplatin at different concentration ratios. BM fibroin and trehalose concentrations were kept constant both at 0.5% and the concentration of cisplatin was varied (0.5%, 0.1%, 0.05%). However, the morphological differences between the formulations observed from the SEM micrographs were minimal.

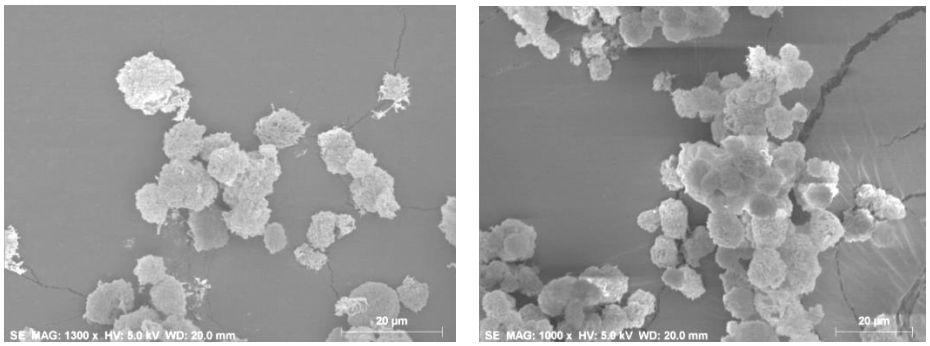

Figure 17. SEM micrographs of BM fibroin 1% mannitol 0.75% cisplatin 0.2%

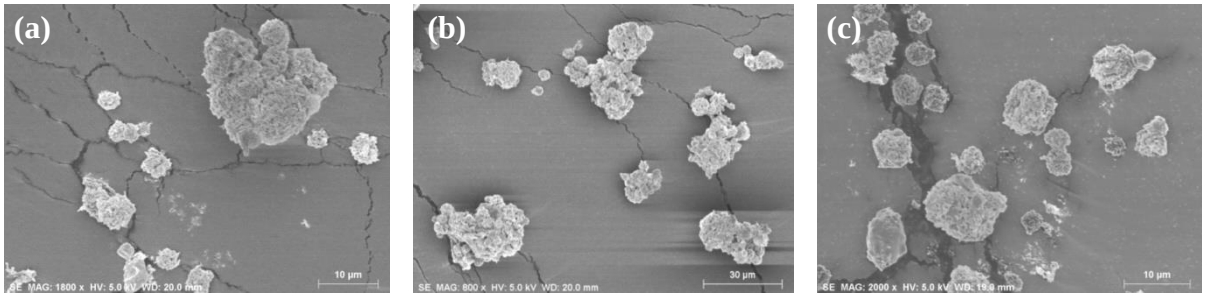

Figure 18. Spray freeze-dried silk-cisplatin particles with trehalose used as a lyoprotectant. Ratio of silk fibroin to cisplatin were (a) 1:1, (b) 5:1 and (c) 10:1

(c) Silk fibroin cross-linked with genipin loaded with cisplatin

The formulations with fibroin cross-linked with genipin prior to loading cisplatin are shown in SEM images in Figure 19. Some minor changes in the morphology were observed as a result of crosslinking with genipin. There were some obvious changes such as particles appearing to be more porous, however, the spherical shape was maintained in most particles and the level of agglomeration between the particles was similar to the non-crosslinked silk-based particles.

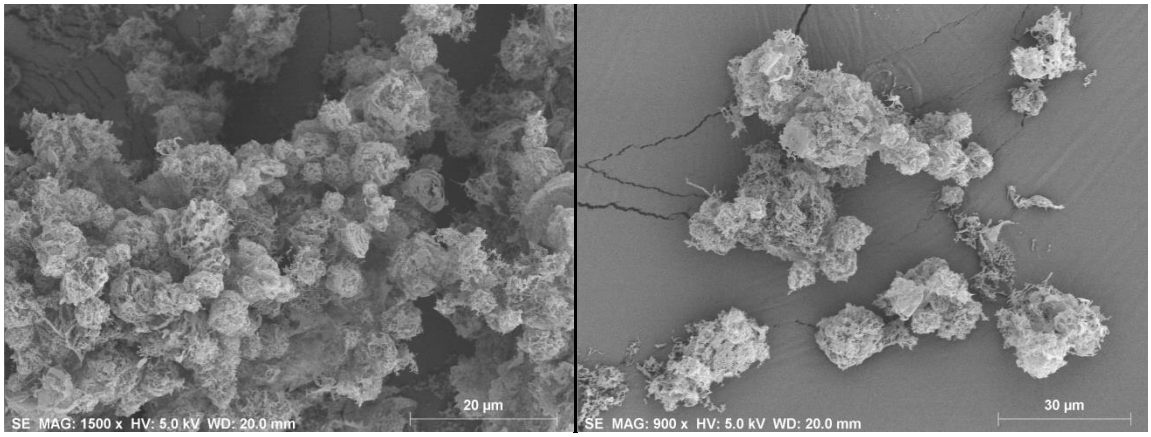

Figure 19. SEM micrographs of formulations of silk cross-linked with genipin; BM fibroin 0.5% + mannitol 1% + cisplatin 0.05% + genipin 0.05%

1.3. The effect of lyoprotectant on formulation of particles

Trehalose was the chosen lyoprotectant to be used in place of sucrose in order to achieve better dispersion and aerosolisation efficiency. In order to determine the optimum ratio of silk fibroin to trehalose, ratios of 1:1, 2:1 or 1:2 at various concentrations of BM fibroin to trehalose were used. The best combination for ideal morphology, as seen on the SEM micrographs, was found to be BM fibroin 0.5% with trehalose 0.5% (Figure 20 (d) and (e)). The particles in this particular formulation were porous yet spherical, and had approximate diameters between 5 and 20 µm.

However, when AM fibroin was spray-freeze-dried with trehalose as a lyoprotectant, the particles produced were hygroscopic and absorbed moisture immediately upon contact with water. Some of the particles "melted" upon contact with air as they absorbed water and disappeared. The remaining trehalose-containing particles were characterised using SEM to reveal the disappearance of single particles in Figure 21. Clumps of particles were formed as the single particles were connected to each other, which also explain the reason for much larger particle sizes observed in Figure 12 (c). The exact stage of the formulation process

where there was morphological change cannot be identified. However, it was assumed that the breakdown of the single particle structures may have occurred during the drying process in the freeze dryer. As both batches of AM fibroin were affected appeared to "melt", when spray-freeze-dried with trehalose as a lyoprotectant, this is likely to demonstrate an incompatibility between the AM fibroin and trehalose. For the subsequent formulations, only BM fibroin was used for this project, and trehalose was considered an unsuitable lyoprotectant for silk-based particles in this project.

As such, mannitol was used as an alternative lyoprotectant in this project. Formulations using various concentration ratios of BM fibroin and mannitol were used, and the optimum ratio of BM fibroin to mannitol was found to be 1:2 respectively, which required more sugar (mannitol) in order to maintain the shape and morphology of the particles (Figure 22). For the case of the 1:1 ratio, the morphology of the particles was not uniform, with only a distinct number of particles having spherical shape. The particle sizes in the 1:2 ratio of the above formulation were larger with average particle diameters between 10 and 30 μm, and showed potential aerosolisation due to the porous nature of the particles.

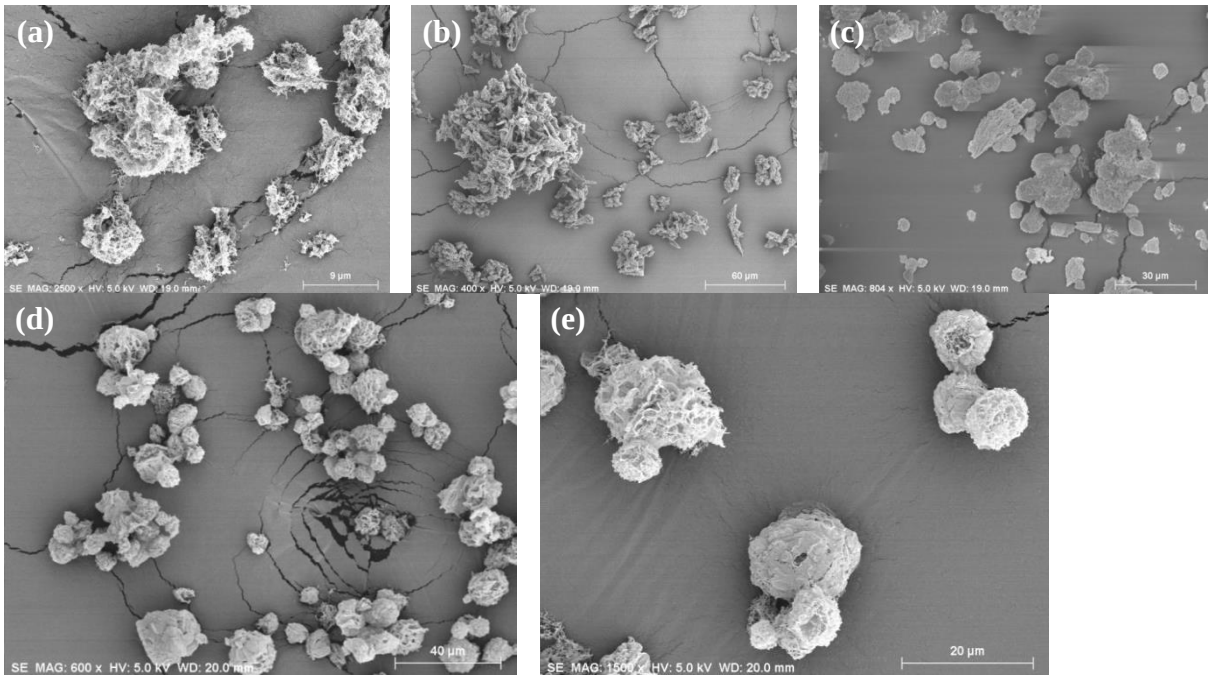

Figure 20. The effect of trehalose concentration on morphology of BM fibroin / trehalose particles compared at concentrations of: (a) 0.1% / 0.1%, (b) 0.5% / 0.25%, (c) 0.5%/1%, (d)(e) 0.5% / 0.5%

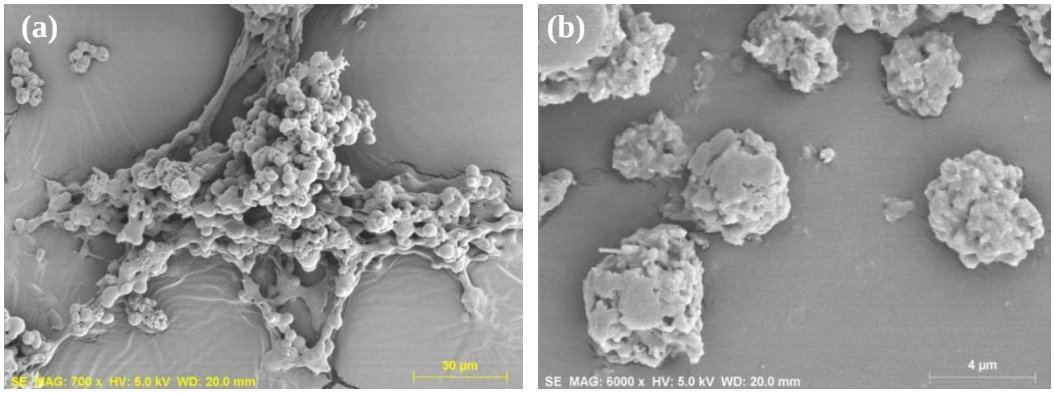

Figure 21. Spray-freeze-dried AM fibroin particles with trehalose as a lyoprotectant; (a) AM fibroin 1% trehalose 1% and (b) AM fibroin 0.5% trehalose 0.5% cisplatin 0.1%

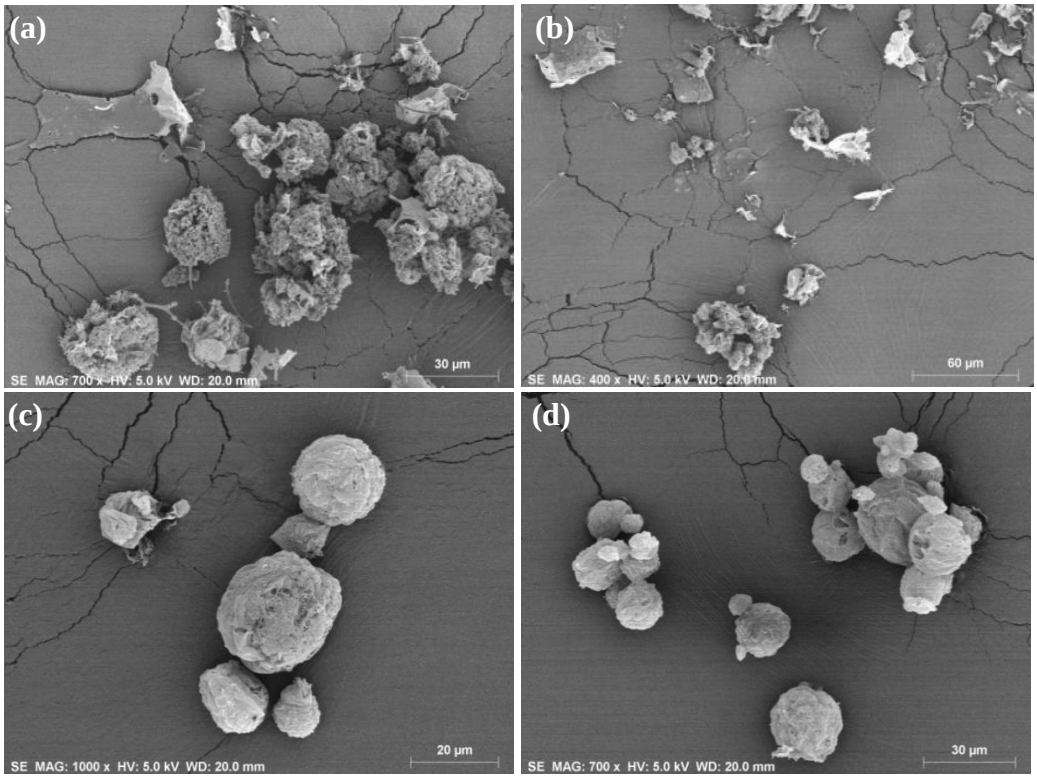

Figure 22. Spray-freeze-dried BM fibroin containing mannitol as lyoprotectant, loaded with cisplatin: (a)(b) BM fibroin 0.5% mannitol 0.5% cisplatin 0.1%, (c)(d) BM fibroin 0.5% mannitol 1% cisplatin 0.1%

1.4. Structure of particles and determination of crystallinity

The spray-freeze-dried BM fibroin 1% + sucrose 0.5% and BM fibroin 0.5% + trehalose 0.5% were analysed for crystallinity and both formulations were found to be amorphous (Figure 23). When mannitol was used as the lyoprotectant, the x-ray diffractogram of the formulations revealed sharp peaks that represented crystalline structures, regardless of the presence of cisplatin and genipin (Figure 24). The x-ray diffractograms for spray-freeze-dried formulations of silk + mannitol + cisplatin with or without genipin were observed to be the same as that of spray-freeze-dried silk + mannitol. Therefore, the same x-ray diffractogram was obtained for the above formulations, which have been presented as one graph in Figure 24.

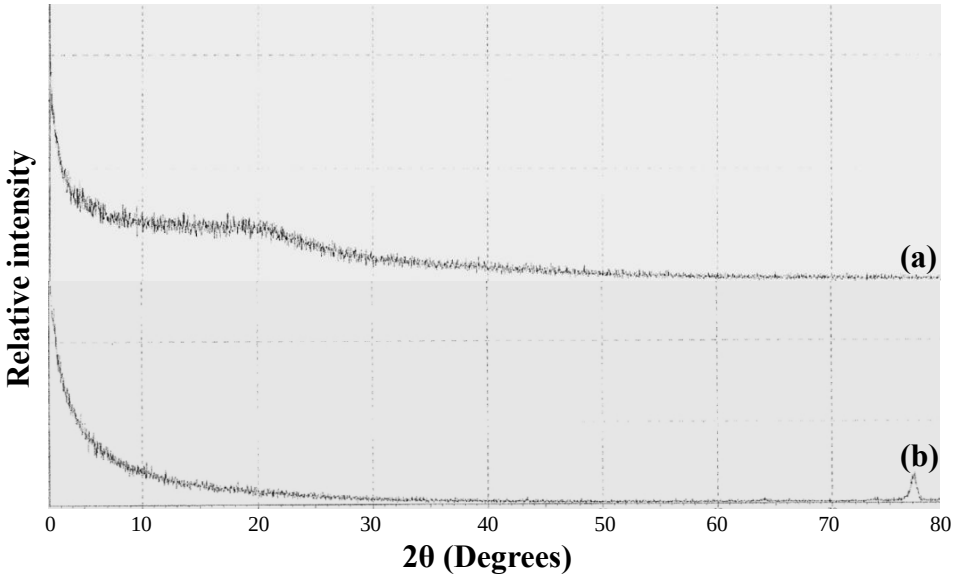

Figure 23. X-ray diffractograms showing amorphous structures for spray-freeze-dried particles: (a) BM fibroin 1% + sucrose 0.5% and (b) BM fibroin 0.5% + trehalose 0.5%; with angular increments of 0.02˚ covering a 2θ range of 2 to 80˚

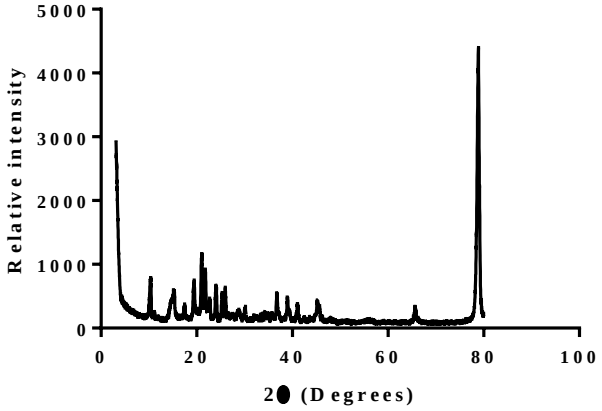

Figure 24. X-ray diffractogram showing crystalline structures for spray-freeze-dried BM fibroin 0.5% + mannitol 1%; with angular increments of 0.02˚ covering a 2θ range of 2 to 80˚

1.5. Stability of particles upon exposure to humidity

Due to the possible instability in the spray-freeze-dried BM fibroin formulation containing trehalose as a lyoprotectant, it was necessary to determine its moisture sorption profile using a DVS analyser (Figure 25). The change in the mass isotherm plot shows evidence of particles being unstable, indicating that the particles retain moisture when exposed to humidity especially in the second cycle. The moisture uptake reached a maximum of 50.98% at a relative humidity of 90%. Another peak in the change in mass was observed towards the end of the second cycle, which represented particles being unstable to moisture. However, the reasons or mechanisms behind this phenomenon remain subject to further investigation.

In contrast, the spray-freeze-dried BM fibroin formulation containing mannitol as a lyoprotectant was shown to be more stable compared to the formulation containing trehalose. The mass isotherm plot in Figure 25 shows that the second desorption cycle does not have a sudden change in mass, and the change in mass is more regulated, which demonstrated better stability in response to humidity compared to the formulation containing trehalose.

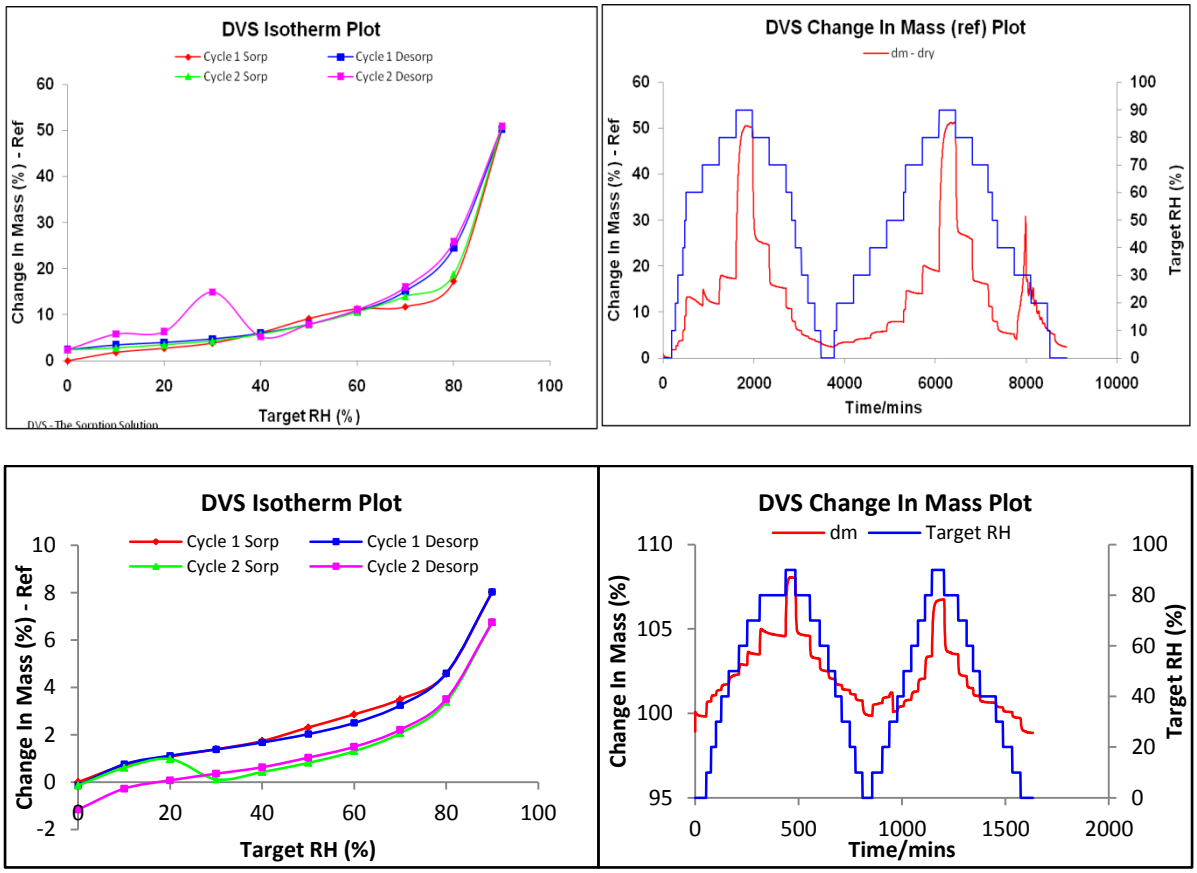

Figure 25. Moisture sorption isotherms for spray-freeze-dried BM fibroin with trehalose *(top)* and spray-freeze-dried BM fibroin with mannitol *(bottom)*

2. Investigation for antibacterial effects exhibited in natural silk proteins

2.1. Screening for presence of antibacterial activities

This assay qualitatively showed that one sample, BM sericin, had an antibacterial action against *S.aureus* as demonstrated by the clear zones around the discs treated with BM sericin solution that represented no growth of bacteria. The average zones of inhibition were measured to be 14 mm, 17 mm and 22 mm for 25 µg, 50 µg and 100 µg of BM sericin respectively, as shown in Figure 26.

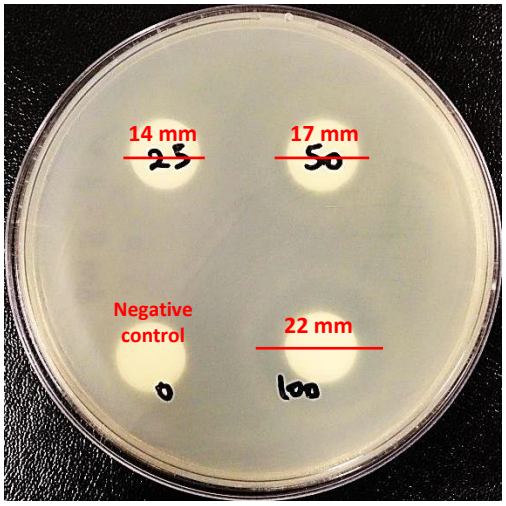

Figure 26. A *S.aureus*-inoculated Mueller-Hinton agar plate showing the zones of inhibition of BM sericin from the disc diffusion assay *(the same zones were measured for the triplicated samples)*

2.2. Determination of minimum inhibitory concentration

From the broth dilution assay, all test tubes excluding two test tubes containing Mueller-Hinton broth inoculated with *S.aureus* and treated with BM sericin were turbid, which indicated bacteria growth overnight. The concentrations of BM sericin in the two test tubes were 25 and 50 µg/ml. Therefore, the MIC of BM sericin against *S.aureus* was determined to be 25 µg/ml.

2.3. Assessment of the antibacterial activity

All samples tested for MBC were turbid, which indicated growth of bacteria overnight. This demonstrated that the antibacterial activity previously observed with BM sericin against *S.aureus* was bacteriostatic, instead of being bactericidal.

2.4. Conclusion and future studies

It was desired that silk drug delivery systems work synergistically with the incorporated anti-infective drug to combat infections. There were triplicated results that demonstrated positive antimicrobial action naturally exhibited by BM sericin, as presented above from the first disc diffusion assay and the broth dilution assay. However, the same results were unable to be replicated in subsequent experiments. Therefore, from these experiments, silk proteins cannot be concluded as exhibiting natural antibacterial actions.

Some hypothesis for the inability to reproduce the results were that there may be contamination in the samples that led to components other than silk protein, for example, the pesticides used while culturing the silk cocoons, to be responsible for the antimicrobial effect observed. Another hypothesis was that there was variability between the batches of processed silk proteins that led to only some batches having antimicrobial activity. In order to test these hypotheses in future studies, a gel electrophoresis could be conducted for every batch of samples received. However, it was not done for the purpose of this thesis, since the focus was on the formulation of silk proteins for use as a drug delivery vehicle.

3. Particle dispersibility and *in vitro* testing for deposition in the lungs

3.1. Dispersion of spray dried particles for *in vitro* lung deposition

The spray dried particles were found to be dispersed with almost no particles retained in the capsule inside an Aeroliser® inhaler device, after it was subject to airflow of 60 L/min for the duration of 4 seconds. The fine particle fraction (FPF), the proportion of particles with aerodynamic diameter less than 5 µm, was calculated to be 61.67% (Figure 27).

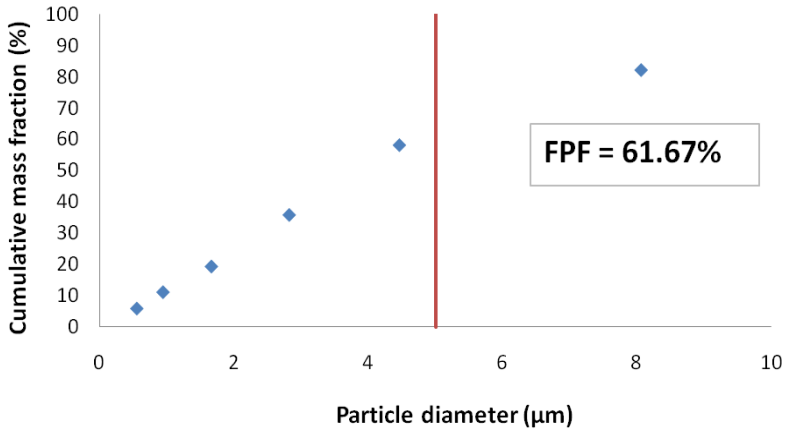

Figure 27. Cumulative mass fraction for spray dried BM fibroin particles, showing the fine particle fraction (FPF) of particles less than 5 µm in diameter; tested *in vitro* at airflow 60L/min for 4 seconds using a next generation impactor

3.2. Dispersion of spray-freeze-dried particles for *in vitro* lung deposition

The FPF of spray-freeze-dried BM fibroin with trehalose used as a lyoprotectant was calculated to be 62.25% (Figure 28). This was similar to spray dried BM fibroin particles that had FPF of 61.67%. These results showed that silk-based particles had high efficiency of aerosolisation, comparable or higher than those dry powder inhaler formulations currently on the market, including Seretide™ and Symbicort™ (75-77).

The above formulations were regarded as having successful *in vitro* lung deposition, compared to spray-freeze-dried fibroin with sucrose used as lyoprotectant. The FPF for spray-freeze-dried BM fibroin with sucrose was unable to be determined, as the majority of the particles were retained inside the capsule and could not be dispersed for *in vitro* testing. This was obvious from the difficulty in handling the powder as they were "sticky" and agglomerated (the SEM micrograph for this formulation is presented in Figure 15).

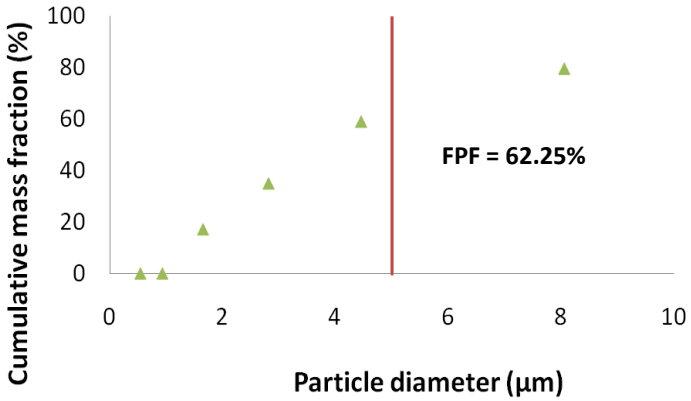

Figure 28. Cumulative mass fraction for spray-freeze-dried particles of BM fibroin 0.5% with trehalose 0.5%, showing the fine particle fraction (FPF) of particles less than 5 µm in diameter; tested *in vitro* at airflow 60L/min for 4 seconds using a next generation impactor

Due to the similarities in particle size and morphology between the drug-loaded and non-loaded spray-freeze-dried silk particles, aerosolisation performance was not investigated for the silk particles loaded with cisplatin. The conditions used in the production of particles in spray-freeze-drying were the same for both the drug-loaded and silk alone particles, and similar particle size and morphology were observed. Consequently, it is anticipated that the dispersion and aerosolisation performance would be comparable to the above presented data.

4. *In vitro* cytotoxicity assays of silk-based particles

4.1. Introduction

Cytocompatibility and toxicity for formulations containing silk alone, silk with lyoprotectant, and silk carrier loaded with cisplatin, were evaluated using various *in vitro* assays.

MTT, CCK-8 and alamarBlue® assays were used to compare cell viability and proliferation in the presence of silk protein with or without cisplatin to control group (no treatment). All assays were quantitative colorimetric assays and varied slightly in their mechanism of action; however each assay had their unique advantages, which are outlined below.

The MTT assay measured the cellular viability and mitochondrial activity of viable cells, by the formation of formazan dye generated by the activities of dehydrogenases in viable cells upon incubation with the MTT reagent. The CCK-8 assay was also based on the amount of formazan dye, but was more convenient and accurate as the CCK-8 reagent contains a highly water-soluble tetrazolium salt that automatically solubilises in the media, which eliminated the need to solubilise the formazan crystals, which was necessary for the MTT assay (78). The alamarBlue® is a highly sensitive assay that measures the metabolic activity as the oxidation-reduction indicator inside the reagent fluoresces and changes colour in response to cellular metabolic reduction (79, 80). A distinct advantage of the alamarBlue® assay was that the reagent is minimally toxic to living cells, therefore the same well plate could be carried on to do subsequent readings at different time points. Thus alamarBlue® assay allows for the least seeding error or plate-to-plate variability.

Both MTT and alamarBlue® assays were used to evaluate lung cell viability in the presence of raw silk proteins in this project. The CCK-8 assay was used to evaluate cell viability in the

presence of silk-based particles in media or pre-conditioned media containing silk-based particles with or without cisplatin delivered via normal or cross-linked silk formulations.

Other assays to support the data for cell viability assay results included in this thesis were measurements for cell metabolism and DNA quantification, along with cell migration and invasion, and wound repopulation assays. Phase and fluorescent microscopy were used to analyse changes in morphology of cells growing in the presence of the silk-based formulations, and are presented in this chapter.

4.2. Cell Viability Assays

Cells were exposed to treatments by having silk-based particles dissolved inside the media maintaining the cells, or cells were seeded on top of 2D silk scaffolds. The patterns of cell growths in these two methods were comparable. The purpose of the 2D scaffolds of silk proteins in both alamarBlue® and MTT assays was to investigate the cytocompatibility of silk proteins, solely from the contact between the cell and silk proteins, without the influence of the size, shape, surface energy or other properties of the particles. CCK-8 assay was used to determine the cytocompatibility of silk-based carriers and cytotoxicity of the formulations with silk-based carriers delivering cisplatin.

Similarities in cell proliferation were demonstrated for most 2D silk scaffold samples – across all fibroin and sericin from both AM and BM species (Figure 29 & 30). The cells proliferated in a normal manner in the presence of silk proteins and all types of silk proteins were cytocompatible, especially until day 3, where there were no statistical differences observed for both alamarBlue® and MTT assays (Figure 29 & 30). There were more variances in cell proliferation when alamarBlue® assay was carried on until day 7 (Figure 29).

This was an expected result, as the media combined with AM and BM silk fibroin showed increased viscosity and formed a gel structure upon culturing for this extended period. Results of the one-way ANOVA statistical analysis and Bonferroni's multiple comparisons test for the data from alamarBlue® assay proved that the differences in cell growth for AM and BM fibroins compared to control were statistically significant. Both AM and BM sericin at both 0.1% and 1% concentrations showed no significant difference in cell growth over the seven days of experiment, except AM sericin had significantly higher proliferation on day 7 compared to control.

Since the formation of gel structure in media was observed for the alamarBlue® assay, MTT assay was carried out for a duration of three days, using three separate well plates. There were significant differences in cell proliferation between control and most samples on day 1, however no significant differences were observed on day 3 (Figure 30). The reason for this could be that the cells seeded on the 2D silk films were proliferating at a slower rate and later at a similar rate to cells growing on tissue culture plate (control). Other reasons for this result could due to seeding error or plate-to-plate variability, taking into account that there were separate well plates set up for each time point (due to the design of the experiment, since MTT reagent is toxic and could not carry on multiple time points using one well plate as alamarBlue® assay).

Overall, the proliferation of cells on 2D silk scaffolds closely mimicked that of control, and thus both silk fibroin and sericin were considered to be cytocompatible with A549 cells.

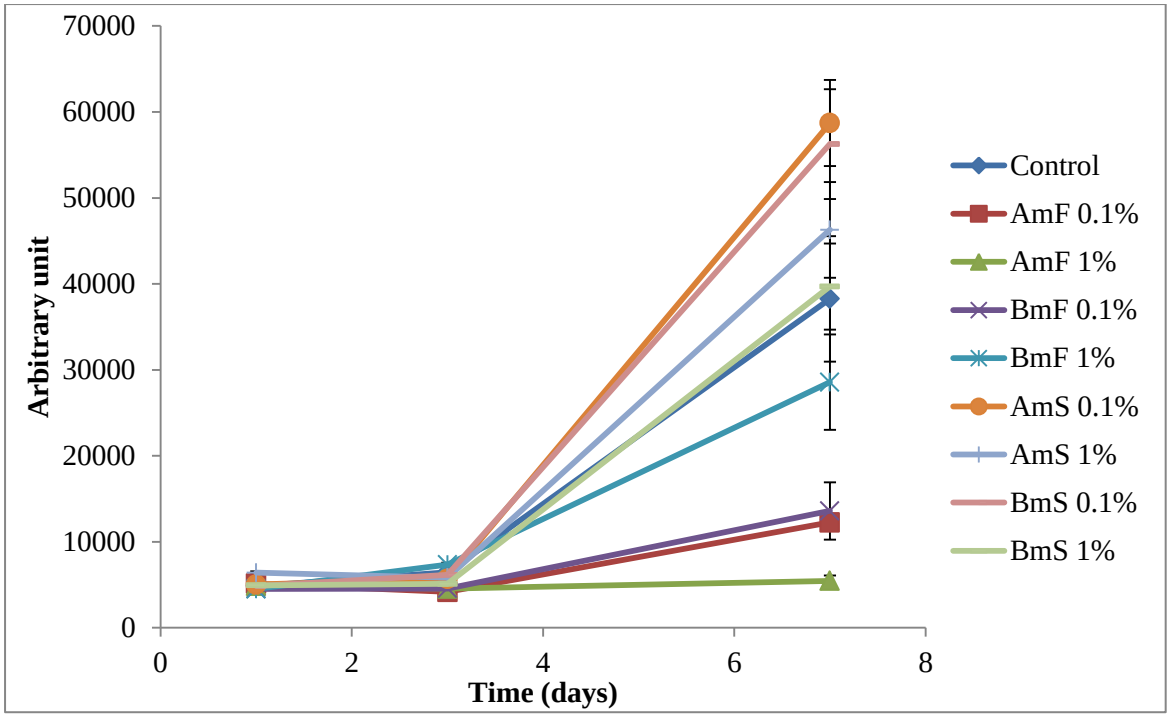

Figure 29. Results of alamarBlue® assay showing cell growth on two-dimensional silk scaffolds of two concentrations 0.1% and 1%. Seeding density was 2000 cells/well. Data are expressed as mean ± standard deviation and one-way ANOVA statistical analysis was used. AmF = AM fibroin, BmF = BM fibroin, AmS = AM sericin, BmS = BM sericin

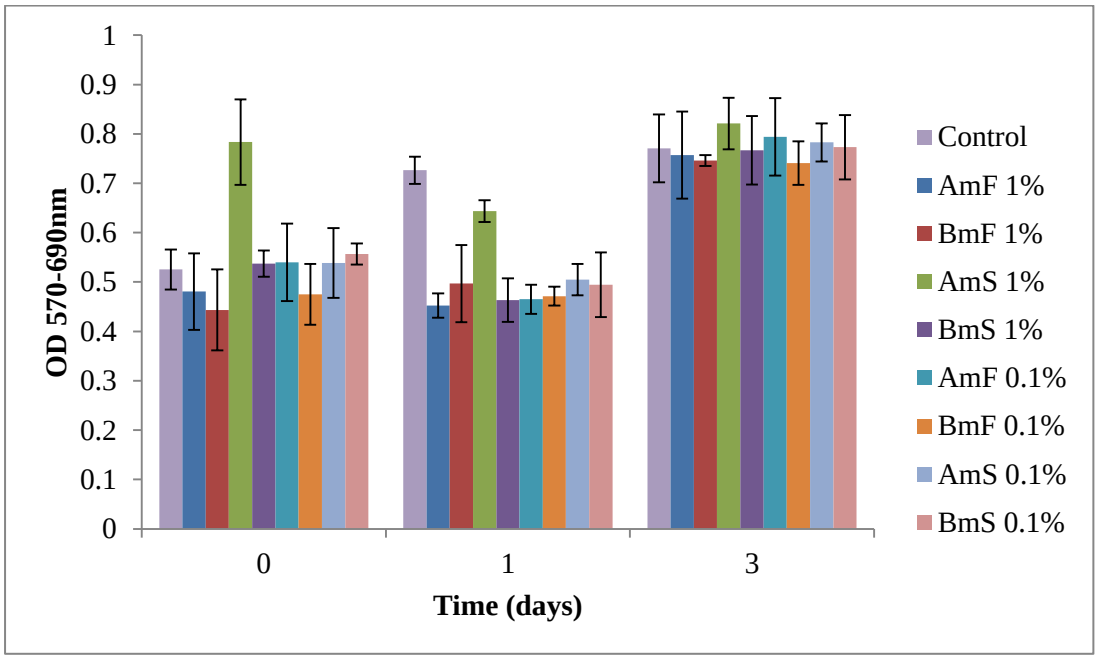

Figure 30. Results of MTT assay showing cell growth on 2D silk scaffolds of two concentrations 0.1% and 1%. Seeding density was 2000 cells/well. Data are expressed as mean ± standard deviation and one-way ANOVA statistical analysis was used. AmF = AM fibroin, BmF = BM fibroin, AmS = AM sericin, BmS = BM sericin

The cytocompatibility of silk fibroin alone was also proved from the CCK-8 assay, with silk alone and silk + sucrose proliferating in a similar manner to control, as shown in Figure 31. One-way ANOVA statistical analysis at each time point showed that differences in cell proliferation existed between the control and silk alone on days 3 and 7, while the cells treated with the formulation containing sucrose as lyoprotectant showed significant difference only on day 3 and no difference in proliferation on day 7 compared to control. The other two samples in CCK-8 assays, cisplatin-containing formulations with or without crosslinking of silk using genipin showed statistically significant suppression of growth of cells from day 1 and more cells were dead by day 3 as can be seen in Figure 31. The cytotoxic effect was maintained until day 7 and was considered that the cisplatin was effectively carried and delivered to the cancer cells by the silk-based particles formulated in this project.

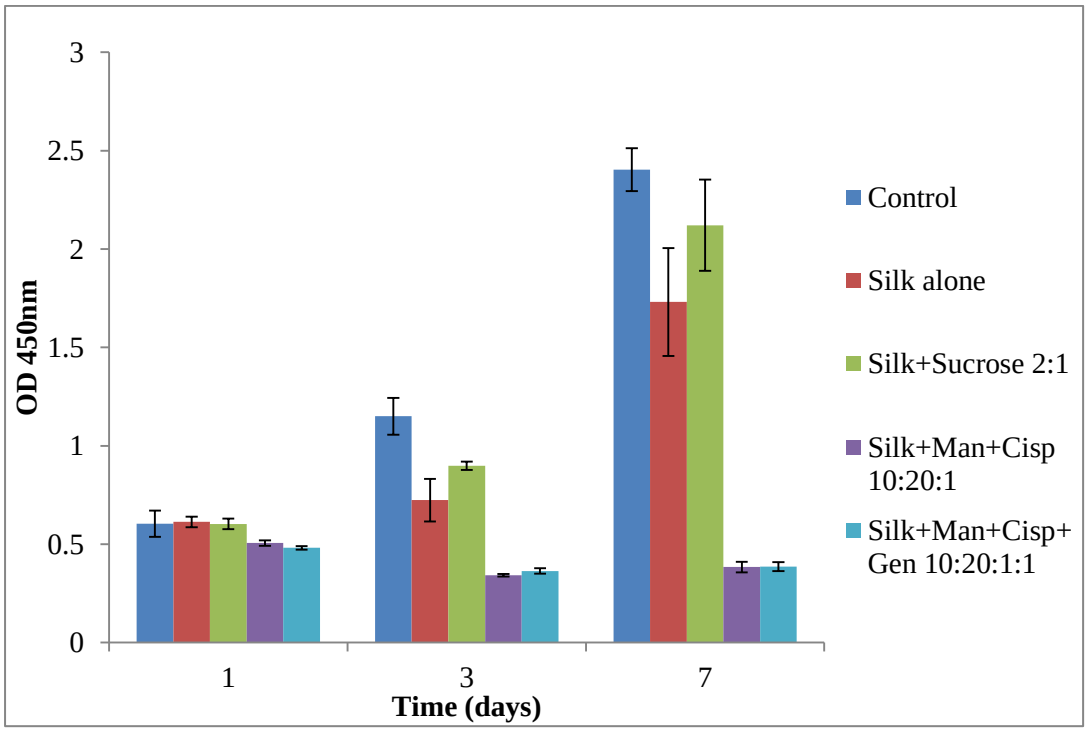

Figure 31. Results of CCK-8 assay: Cell proliferation with media containing silk fibroin ± sugar (Man = mannitol) ± cisplatin (Cisp) ± genipin (Gen) measured on days 1, 3 and 7. Concentration of particles used was 1mg/ml (w/v) for all samples; data are expressed as mean ± standard deviation and one-way ANOVA statistical analysis was used.

Due to the higher proliferation of cancer cells observed in response to the silk-sucrose formulations compared to the formulation containing silk alone, the effect of concentration of sugar used as lyoprotectant in the cisplatin-containing formulations were tested. The cytotoxicity of cisplatin in "high sugar" formulation (silk + mannitol + cisplatin ratio 10:20:1) and "low sugar" formulation (silk + mannitol + cisplatin ratio 10:8:1) were compared at overall particle concentrations of 1 mg/ml and 10 mg/ml and results are presented in Figure 32. There were no significant differences in day 1 across all formulations, however one-way ANOVA statistical differences were observed in all formulations compared to control from the second day. The cytotoxicity of cisplatin did not differ significantly according to sugar content in 10 mg/ml overall concentration however the effect of high concentration of mannitol superseded the cytotoxicity of cisplatin in 1 mg/ml and reached a statistically significant difference on days 2 and 7. Therefore the cytotoxic effect of cisplatin was analysed to be affected by sugar content only when the concentration of cisplatin itself was low. Nevertheless, it is recommended that future studies have alternative method of formulating these particles, in order to eliminate or reduce the sugar content in order to evaluate the cytotoxicity of cisplatin carried by silk particles.

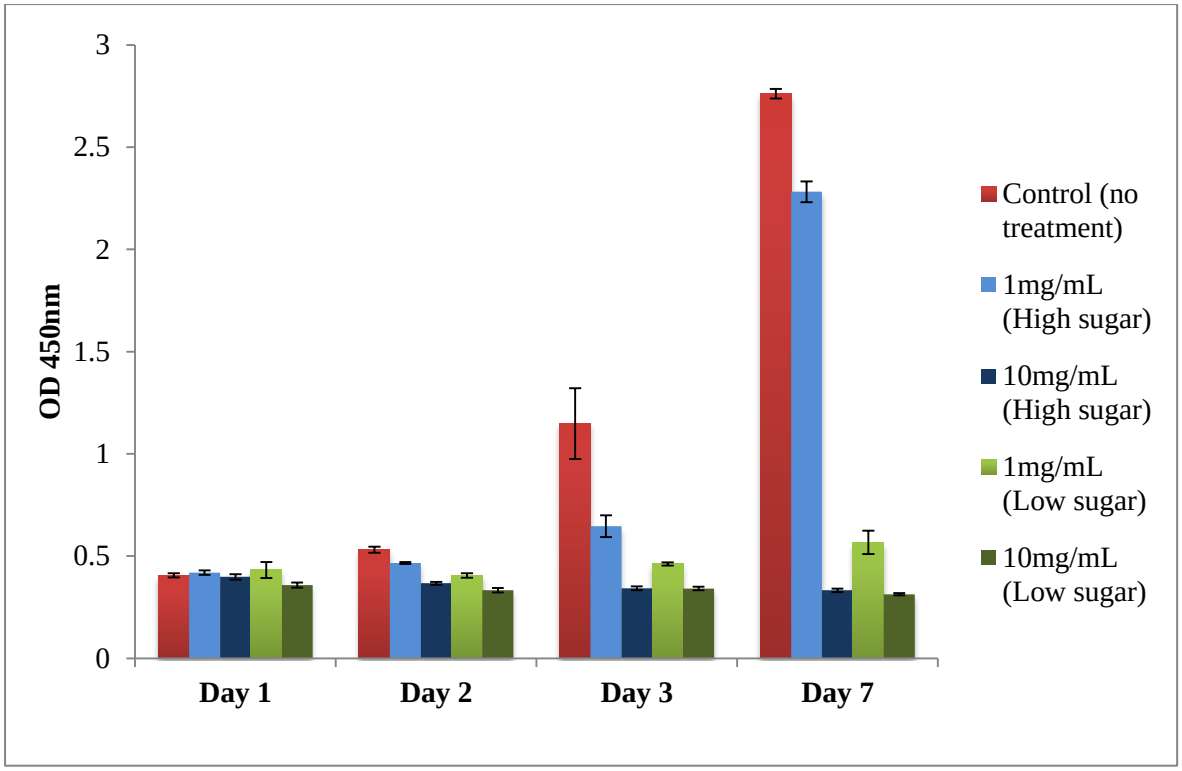

Figure 32. Comparison between formulations of silk fibroin + cisplatin 1mg/ml or 10mg/ml with high or low mannitol concentrations; data are expressed as mean ± standard error of mean and one-way ANOVA statistical analysis was used.

The comparison of cell viabilities between normal silk + cisplatin and cross-linked silk + cisplatin formulations for both 1 mg/ml and 10 mg/ml concentrations are shown in Figure 33. The differences observed were more obvious and statistically significant in the 1 mg/ml formulations. The cross-linked silk + cisplatin formulation had significantly higher cytotoxic effect than the normal silk + cisplatin formulation at 1 mg/ml concentrations. The differences between the cytotoxicity of normal silk + cisplatin 10 mg/ml and cross-linked silk + cisplatin 1mg/ml were not significant across the seven days according to one-way ANOVA statistical analysis at each time point. This demonstrated that a similar level of cytotoxicity is achieved even at one-tenth concentration of cisplatin, when it is delivered via cross-linked silk carrier. This result highlighted the benefits of using cross-linked fibroin over normal fibroin as carriers for cisplatin.

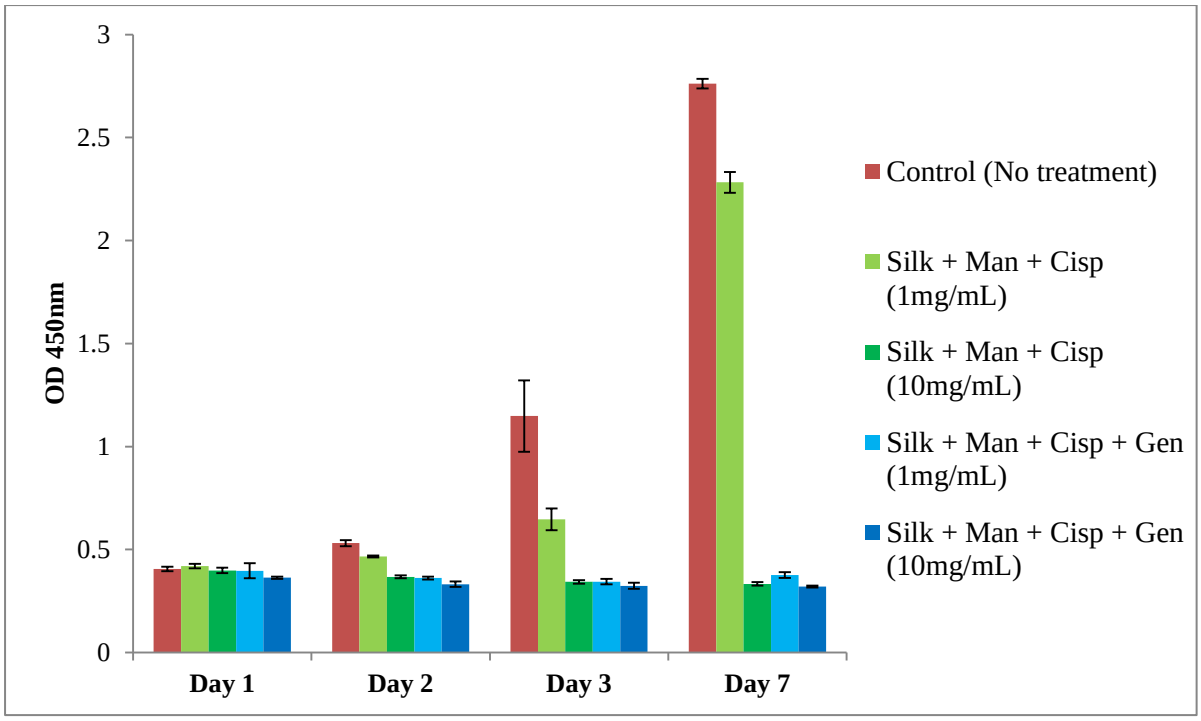

Figure 33. Comparison between formulations of Silk + Cisp (silk + mannitol + cisplatin; 10:20:1) or Silk (cross-linked) + Cisp (silk + mannitol + cisplatin + genipin; 10:20:1:1) at 1mg/ml or 10 mg/ml concentrations; data are expressed as mean ± standard error of mean and one-way ANOVA statistical analysis was used.

4.3. Double strand DNA content (Picogreen® assay)

The results from cell viability assays were confirmed by DNA content assay using the Picogreen® assay. As seen in Figure 34, the DNA content was comparable across all conditions on the first day after the treatment, and then clear differences were observed after 3 days of incubation. It was obvious that silk alone or silk + sugar has similar number of cells to the control group, and that cells treated with cisplatin had minimal changes in DNA content from day 1 to day 3. These results were consistent with the results from the cell viability assays.

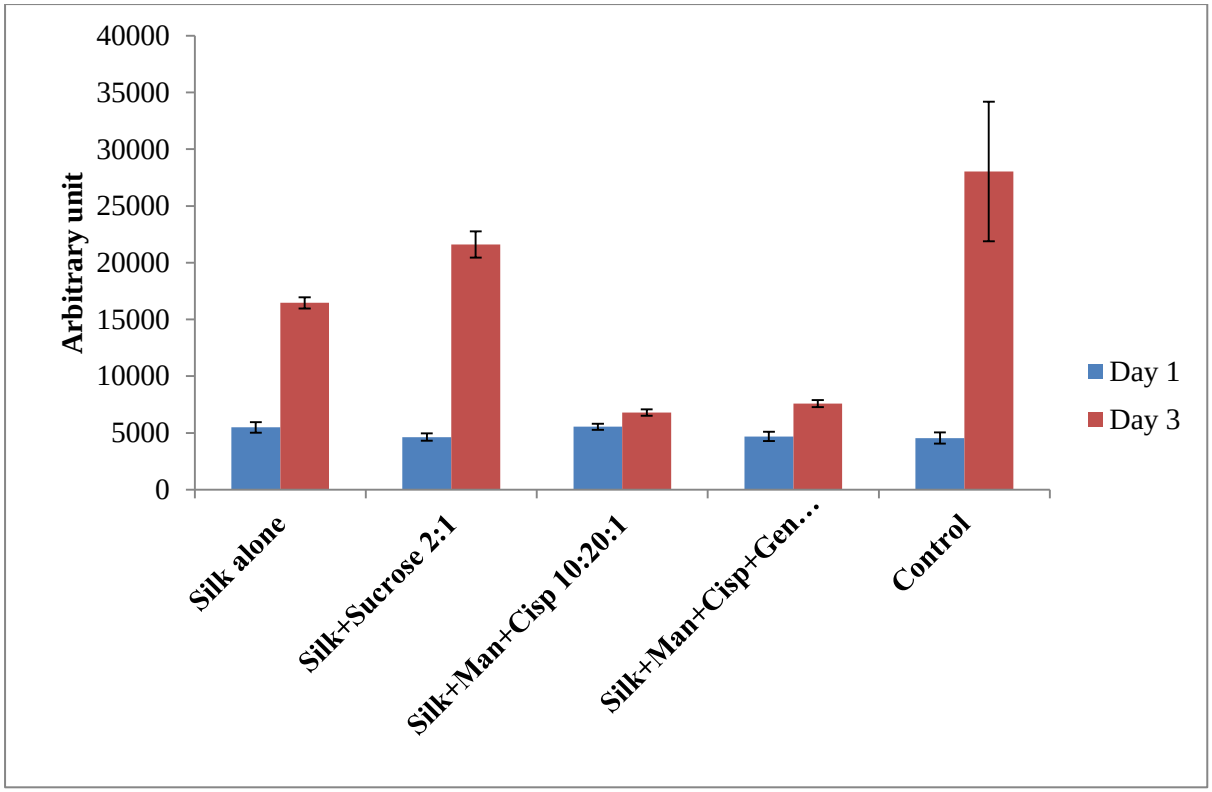

Figure 34. Quantification of DNA contents purified from A549 cells cultured in the presence of 1mg/ml of silk alone, silk + sucrose (2:1), silk + mannitol + cisplatin (10:20:1), silk + mannitol + cisplatin (10:20:1:1) formulations, or control (no treatment); data are expressed as mean ± standard deviation and one-way ANOVA statistical analysis was used.

4.4. Changes in cell morphology with silk-based treatment

The morphology of A549 cells treated with silk and silk + sugar particles were very similar to cells in normal media with no treatment, and supported the data obtained from the cell viability assays (Figure 35). In Figure 36, the similarities were observed on the images obtained from fluorescent microscopy, and this clearly demonstrated that the silk was compatible to A549 cells, and that cells grown in the presence of silk-based particles proliferated in a similar way to the cells grown in normal media. When sugar was added to the spray-freeze-dried formulations as a lyoprotectant, it enhanced the growth of cells as the sugar was an energy source for the cells to grow (81). This was observed from the phase

images in Figure 35, where cells proliferated and had grown on top of each other in a similar way to control group, as they became over-confluent in the presence of silk and sugar.

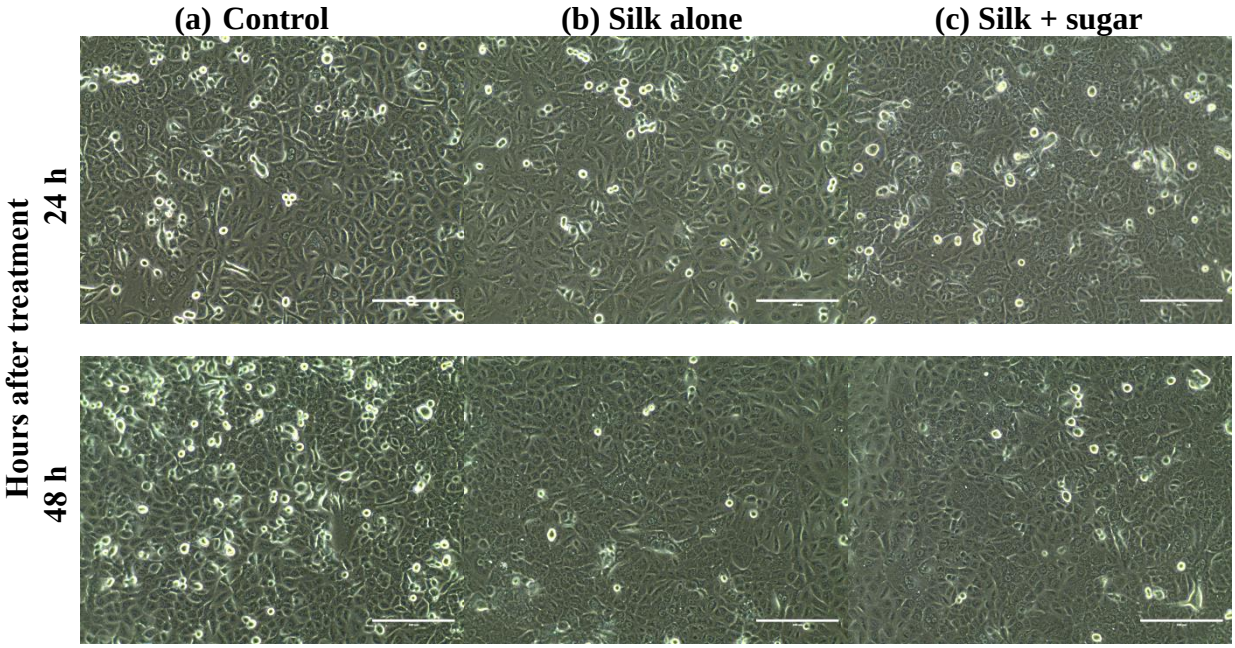

Figure 35. Similar morphology can be observed for (a) Control (b) Silk alone (c) Silk + sugar, at 24 hours and 48 hours of treatment

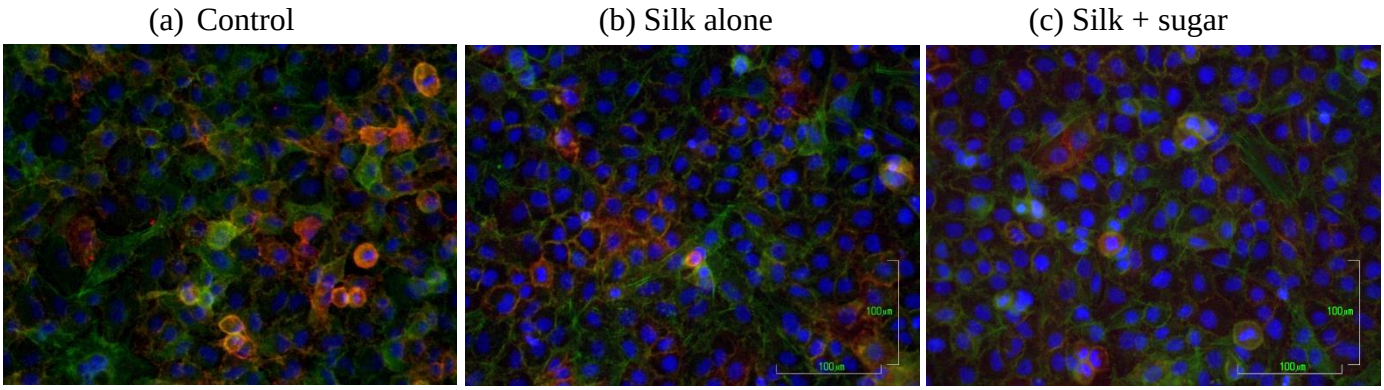

Figure 36. Similarities in morphology of control and silk-treated cells, stained F-actin (green), beta-catenin (red) and DAPI (blue)

For the cells treated with cisplatin, obvious reductions in the number of living and attached cells were observed, and also distinct morphological differences for those surviving cells were observed in contrast to control group (Figure 37). There was a significantly less number of living cells in the formulation that had silk cross-linked with genipin. Despite the same concentrations of cisplatin incorporated in the normal and cross-linked silk formulations, it was observed that the cross-linked silk formulations had stronger cytotoxicity (Figure 37 (c)). The sizes of the surviving cells were also different; the cells that received no treatment (control) had average perimeters of 106.68 μm whereas the cisplatin-containing normal and cross-linked silk-based particles led to cells having average perimeters of 175.24 μm and 205.15 μm respectively, after 48 hours of treatment with conditioned media (Figure 38). One-way ANOVA statistical analysis showed statistically significant differences in the cell sizes compared to control for the cells treated with silk + mannitol + cisplatin formulation at both 24 and 48 hours. However the cross-linked silk had significant effect in cell size only at 48 hours and not 24 hours. The enlargement of cells were indicative of senescence-like cells, where they are metabolically active but has lost the function to divide, as a result of being treated with cisplatin. The delayed significant enlargement of cells treated with cisplatin delivered via cross-linked silk was interpreted as the delay in the cytotoxicity of cisplatin delivered using cross-linked silk.

The effect of this silk + mannitol + cisplatin + genipin formulation was remarkably evident in the reduced number of cells, change in the shape of surviving cells and presence of senescence-like cells as observed in the enlarged actin in Figure 39 (e). Figure 39 (d) and (e) showed significantly less number of nuclei (shown in blue; stained with DAPI) after 48 hours of treatment with cisplatin compared to control and silk-treated cells in (a), (b) and (c), which indicated that there were less number of living cells.

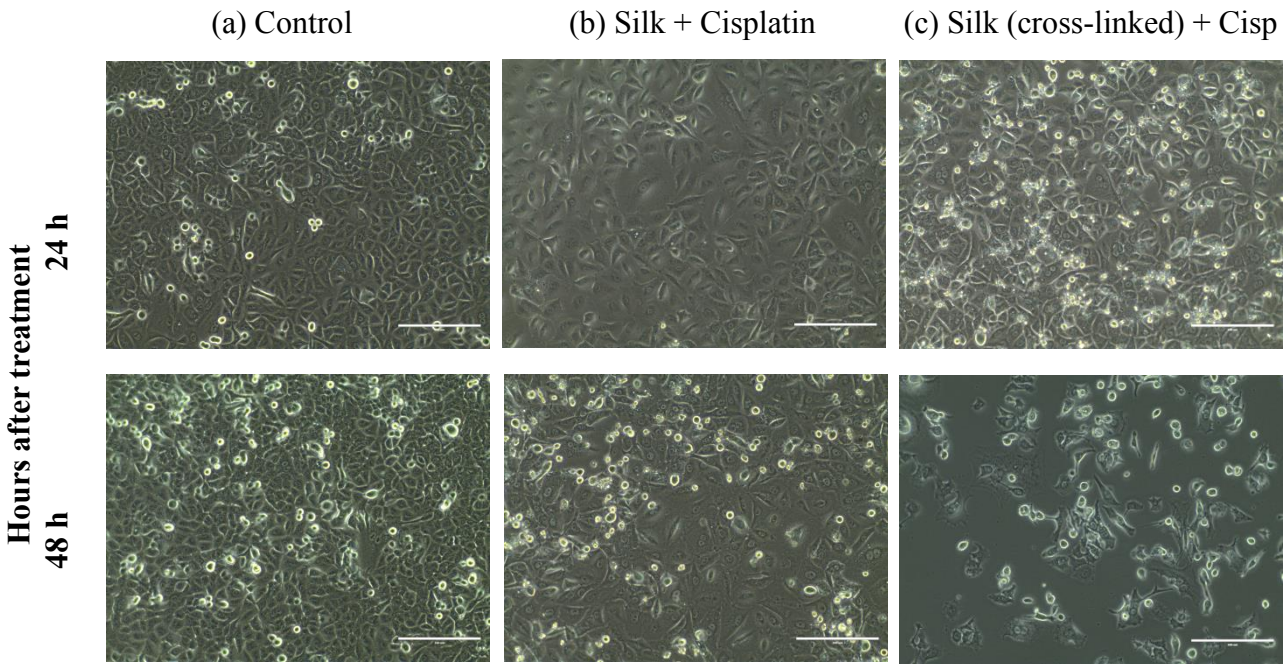

Figure 37. Morphological differences of A549 cells after 24 and 48 hours of treatment with silk-based cisplatin particles, with different impacts for normal and cross-linked silk formulations. Formulations used were Control (normal media), Silk + Cisplatin (silk + mannitol + cisplatin 10:20:1), or Silk (cross-linked) + Cisp (silk + mannitol + cisplatin + genipin 10:20:1:1), each at 1mg/ml concentration

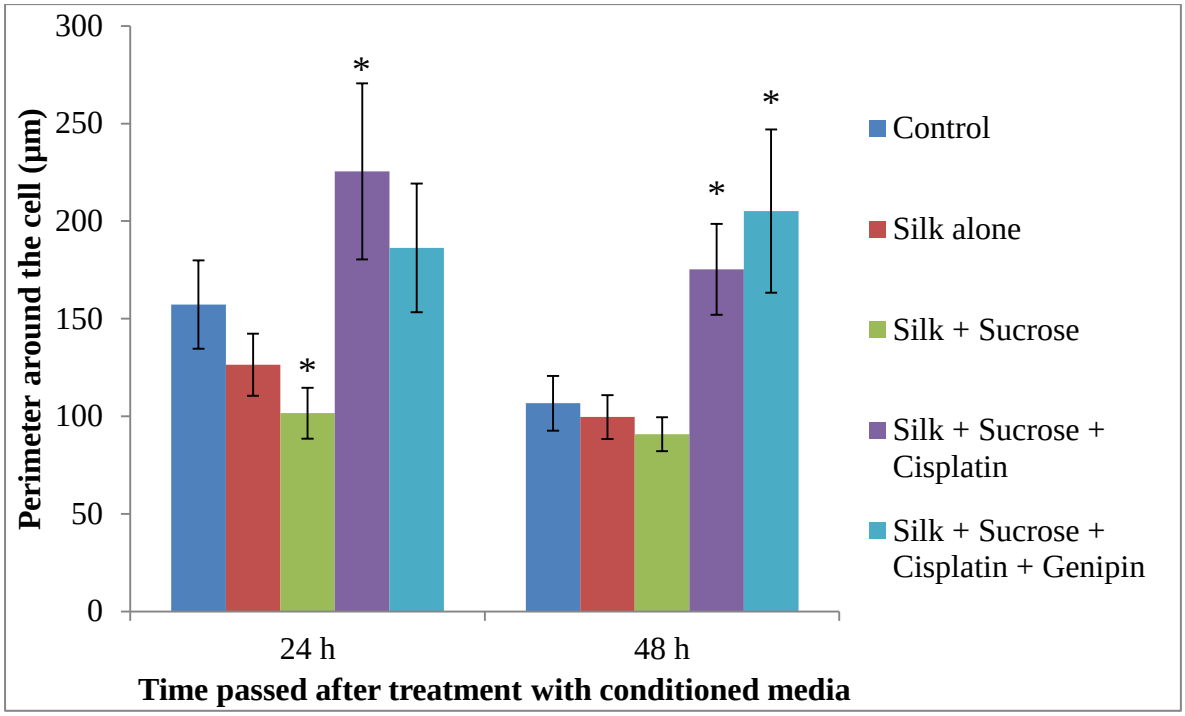

Figure 38. The conditioned media with different formulations have varying effects on the average size of the cells. * indicates significant difference in cell size to control group; data are expressed as mean ± standard deviation and one-way ANOVA statistical analysis was used for statistical significance.

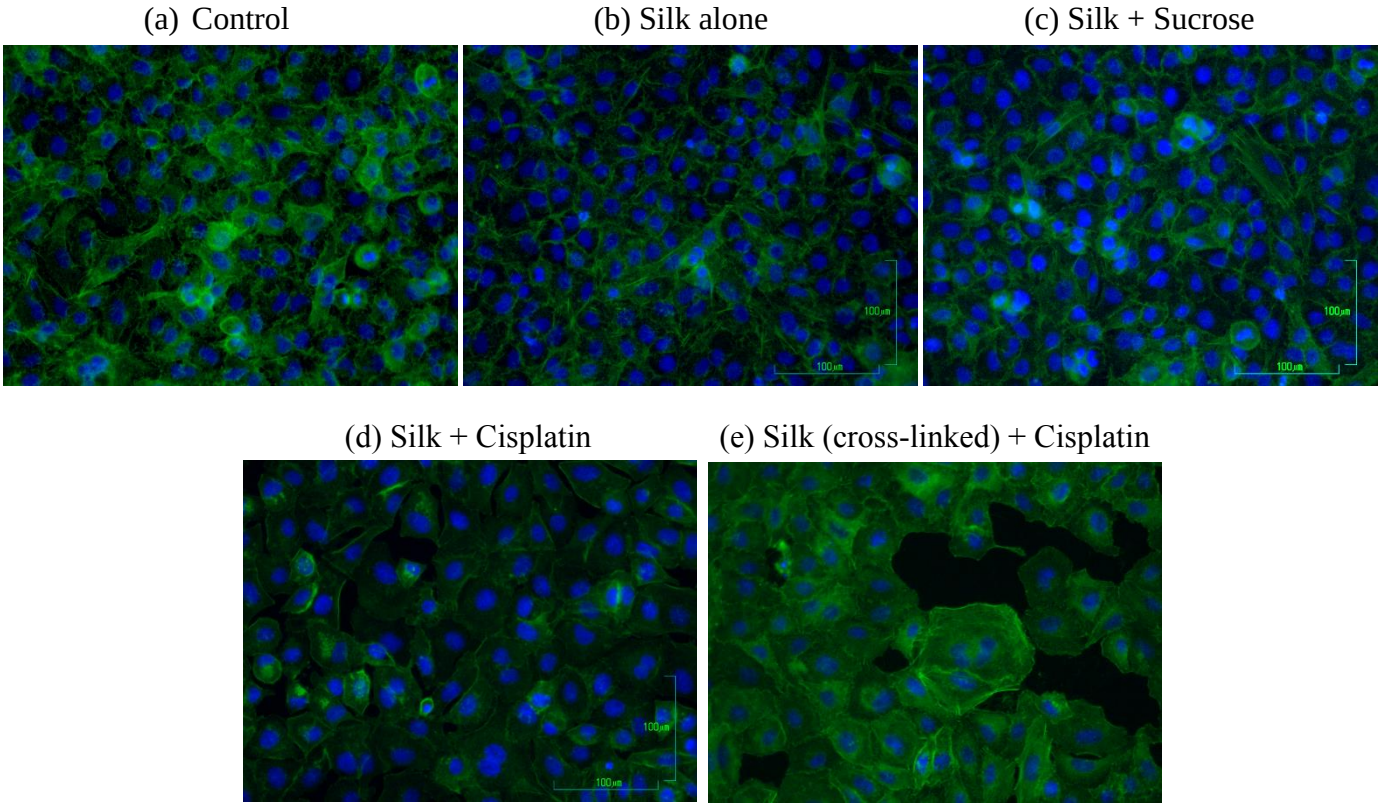

Figure 39. Immunofluorescence images after 48 hours of treatment with (a) normal media (control) (b) silk alone, (c) silk + sugar, (d) silk + mannitol + cisplatin 10:20:1 and (e) silk + mannitol + cisplatin + genipin 10:20:1:1. Stained with F-actin (green) and DAPI (green)

4.5. Cell Metabolism (YSI)

The glucose concentration decreased by 1.5 g/L in the culture medium for control (no treatment), from 4.17 ± 0.09 g/L to 2.67 ± 0.19 g/L after seven days (Figure 40). The treatment with silk alone showed similar results with glucose concentration changed by 1.45 g/L from 5.16 ± 0.51 g/L to 3.71 ± 0.35 g/L after seven days of experiment.

In contrast, there were minor changes in the glucose concentration for the medium with cells treated with cisplatin delivered via normal or cross-linked silk, decreasing only by 0.76 g/L and 0.39 g/L respectively, after seven days. This reflected that there were certainly less number of cells that are metabolically active and thus had subsequently reduced glucose uptake from the media, which supported the results from the CCK-8 cell viability assay.

Similarly, there was no significant lactate release over the seven days for cells treated with both normal and cross-linked silk based formulations (Figure 40). This finding also supported the data from cell viability assays, as lactate is produced by mammalian cells as a metabolite by-product during the process while glucose is utilised for energy production (81). The increases in lactate concentration in media for silk alone and silk + sugar treated cells were similar to the increase observed in the control group, which represented cell proliferation over time.

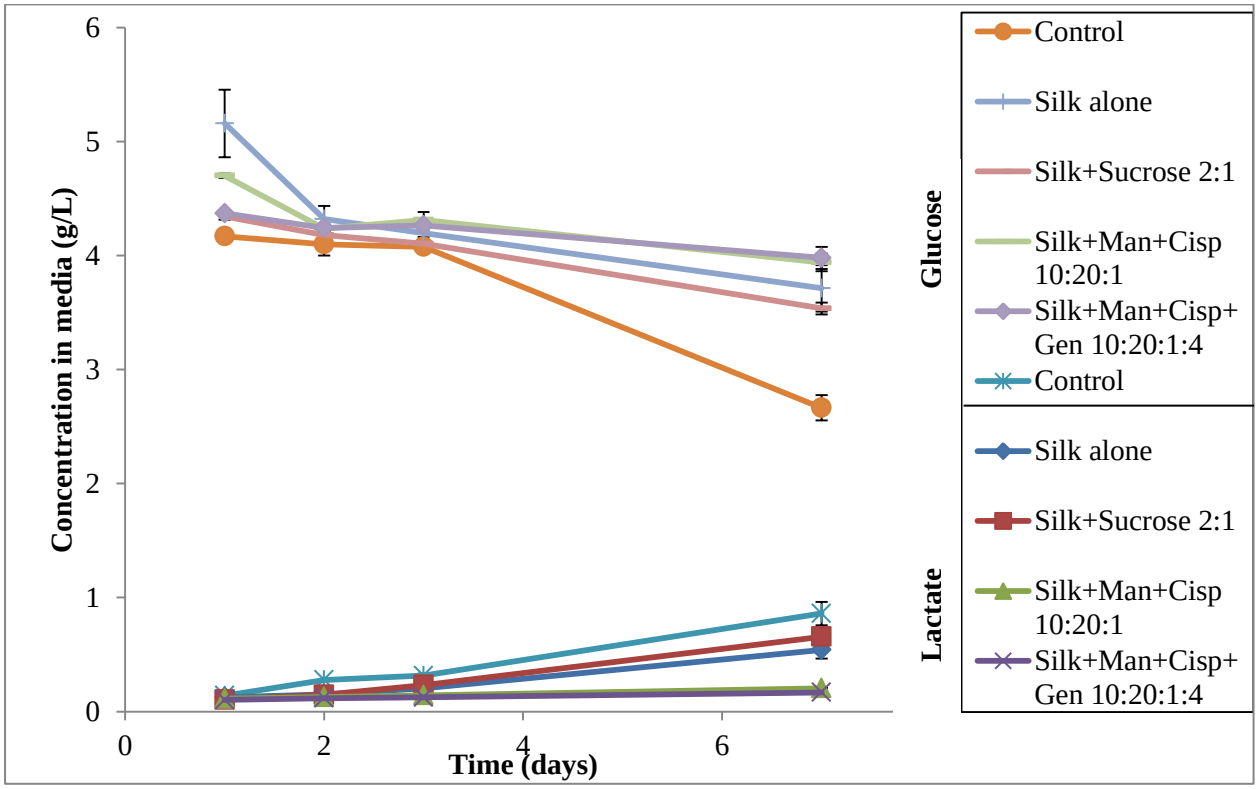

Figure 40. Cell metabolism: Increasing lactate levels and decreasing glucose levels detected in media as cells proliferate during incubation with silk ± cisplatin formulations. Data are expressed as mean ± standard error of mean.

4.6. Cell Migration and Invasion

In “Accelerated escape”, differences in cell migration were not distinguished, except between control group and other treatment groups (Figure 41). It was desired for the cells treated with silk alone to stay in the upper chamber rather than migrating away from silk-containing media to the lower chamber containing high serum, to mimic the control group. However, it was observed that the cells treated with silk only migrated in a similar manner to silk + mannitol + cisplatin formulations. The cisplatin delivered via cross-linked silk did not have a significant difference in cell migration compared to cisplatin delivered via normal silk, when analysed by one-way ANOVA statistical analysis.

When the particles were placed in the lower chamber to measure the suppressed movement of the cells from the upper chamber to the lower chamber (“suppressed attraction”), the results were more closer to the hypothesis compared to the results of the first design of this experiment (“accelerated migration”). The cells moved from upper chamber to the lower chamber containing silk favourably, while less number of cells migrated when cisplatin was present in the lower chamber (Figure 42). However, there were no significant differences observed in the cisplatin delivered via cross-linked or normal silk. The differences in cell responses may be greater if the formulation is modified, possibly by using a higher concentration of genipin for cross-linking or by altering the cross-linking time.

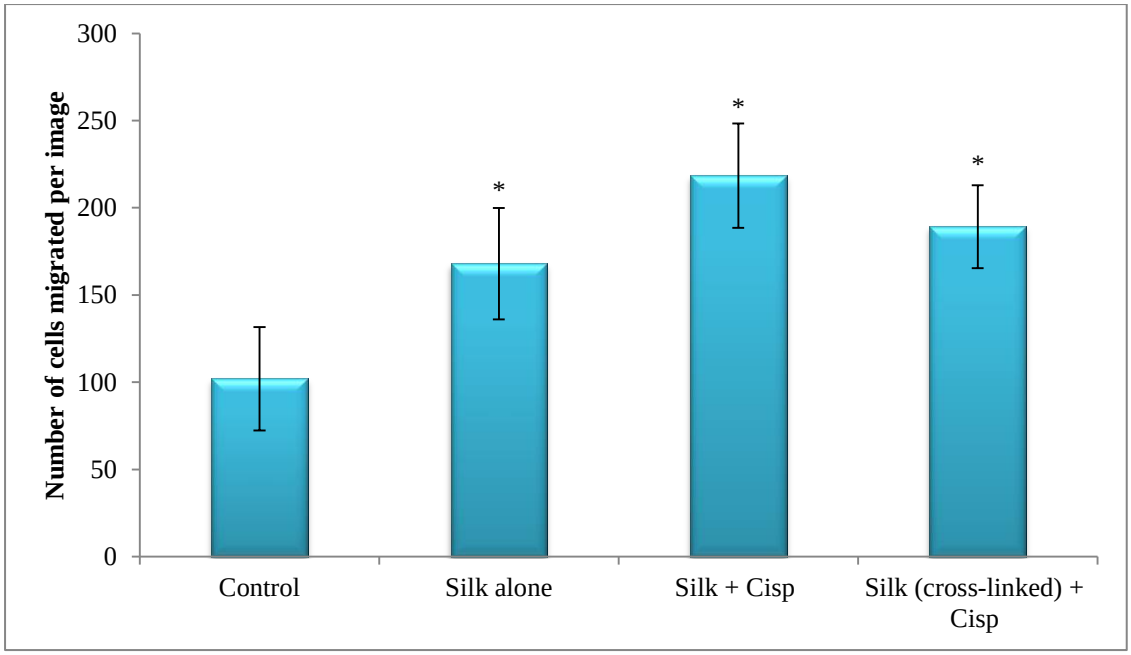

Figure 41. Average number of cells migrated over 8 hours from low serum media containing silk alone, silk + mannitol + cisplatin (Silk + Cisp) or silk+ mannitol + cisplatin + genipin (Silk (cross-linked) + Cisp) particles to high serum media ("Accelerated escape") * indicates significant difference compared to control ($p<0.05$), as analysed using one-way ANOVA; data are expressed as mean ± standard deviation.

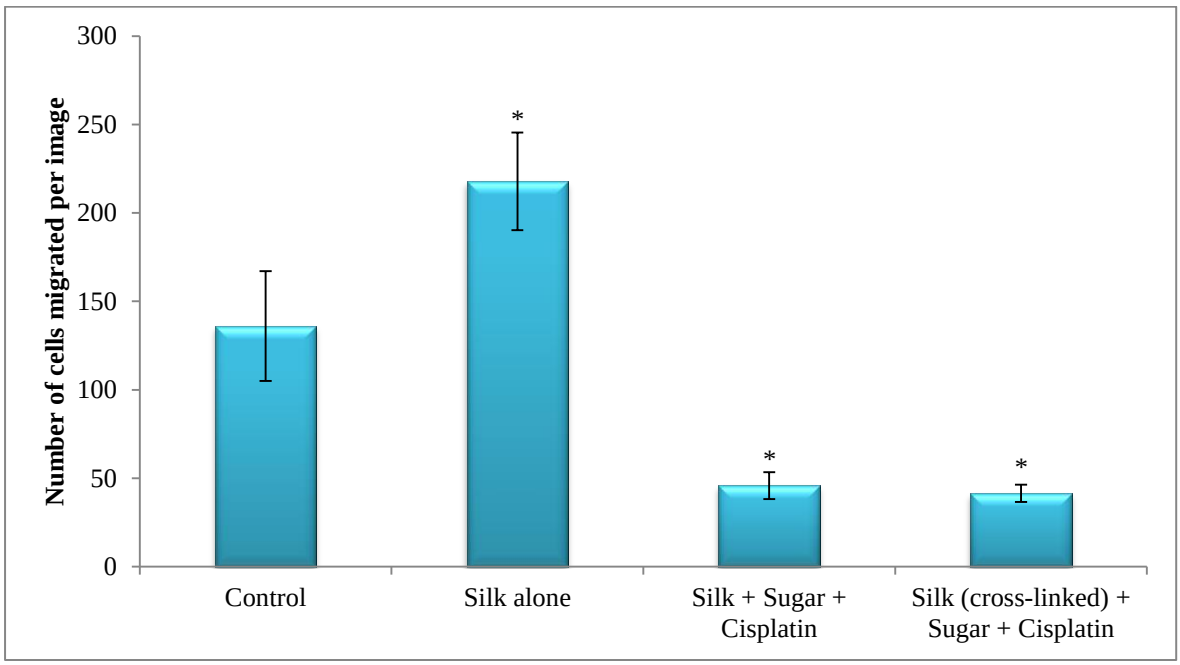

Figure 42. Average number of cells migrated over 8 hours from low serum media to high serum media containing particles ("Suppressed Attraction") Particles were added to the bottom chamber, each at concentrations of 1mg/ml. * indicates significant difference compared to control ($p<0.05$), as analysed using one-way ANOVA; data are expressed as mean ± standard deviation.

4.7. Wound repopulation assay

At 48 hours after replacing media, the area of the wounds were almost completely closed by the cells treated with normal media and media containing silk regardless of the presence of sugar. In contrast, the wounds remained unclosed for those treated with cisplatin. As seen in Figure 43, the cells treated with formulations with silk alone or silk with sugar had repopulated and closed the wound in a similar manner to control. The cells treated with cisplatin-containing normal or cross-linked silk formulations did not repopulate and instead, the cytotoxic treatment had detached and killed the cells that were attached on the tissue culture plate (Figure 44).

The extent of repopulation was quantified by measuring the area of the unclosed wound at 24 hours. Figure 45 demonstrates that the percentage of wound area repopulated for cross-linked silk + cisplatin formulation was much lower than the other groups. Both the silk alone and silk with sugar had approximately 80% of wound area repopulated after 24 hours of treatment. One-way ANOVA statistical analysis revealed that the statistically significant differences in wound closure occurred only between control and the formulation with cross-linked silk (silk + mannitol + cisplatin + genipin). The results from this assay again highlighted that the cytotoxic effect of cisplatin is more potent when it is delivered to the cells via cross-linked silk particles.

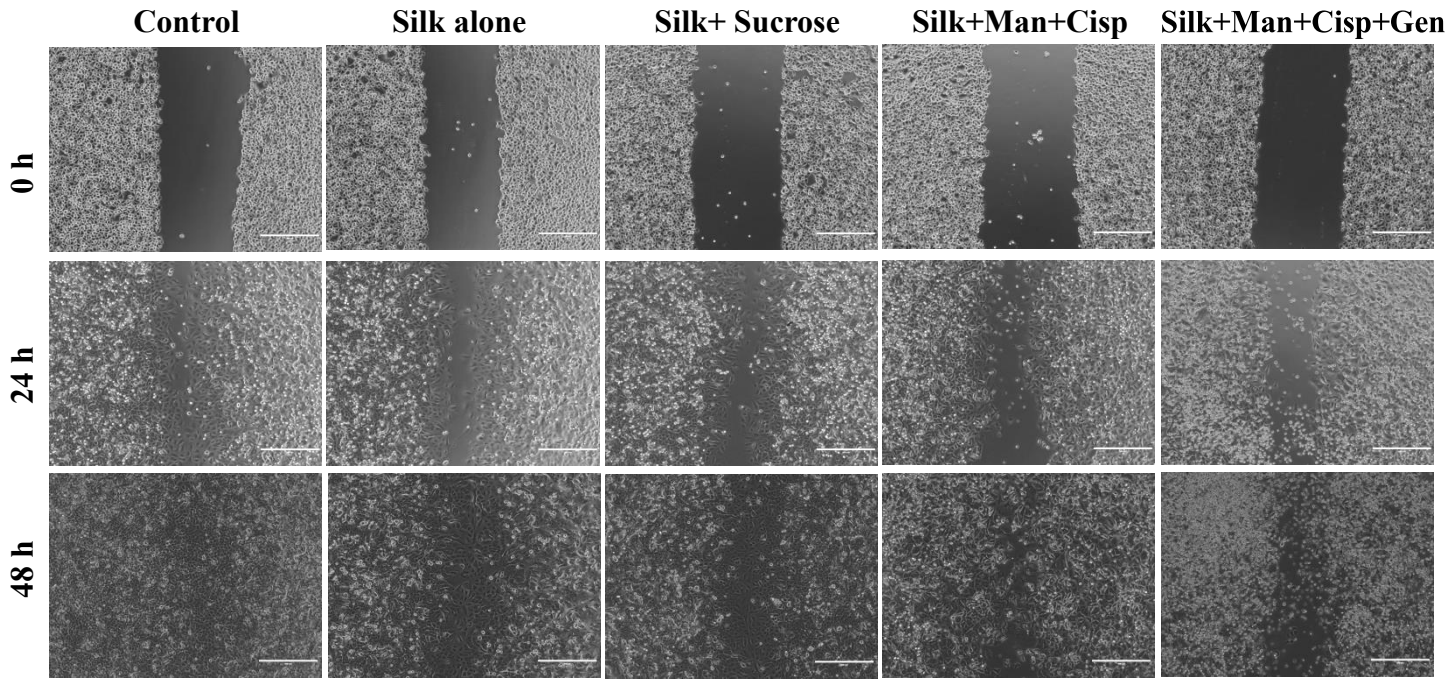

Figure 43. Wound repopulation assay. The "wound" created using a pipette tip in the middle of a confluent monolayer of cells, was repopulated and the gap is closed for cells treated with silk alone and silk + sucrose (2:1) formulation, whereas the gap remained unclosed for cells treated with silk + mannitol (Man) + cisplatin (Cisp) (10:20:1) and silk + mannitol (Man) + cisplatin (Cisp) + genipin (Gen) (10:20:1:1) formulation.

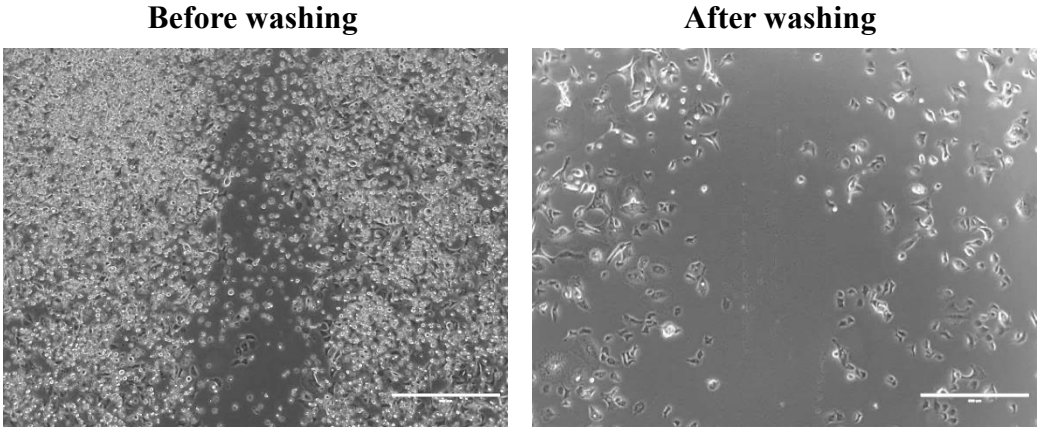

Figure 44. Phase images of cells treated with silk + mannitol + cisplatin + genipin (10:20:1:1) formulation after 48 hours of incubation, before *(left)* and after *(right)* washing with PBS to wash away detached or dead cells

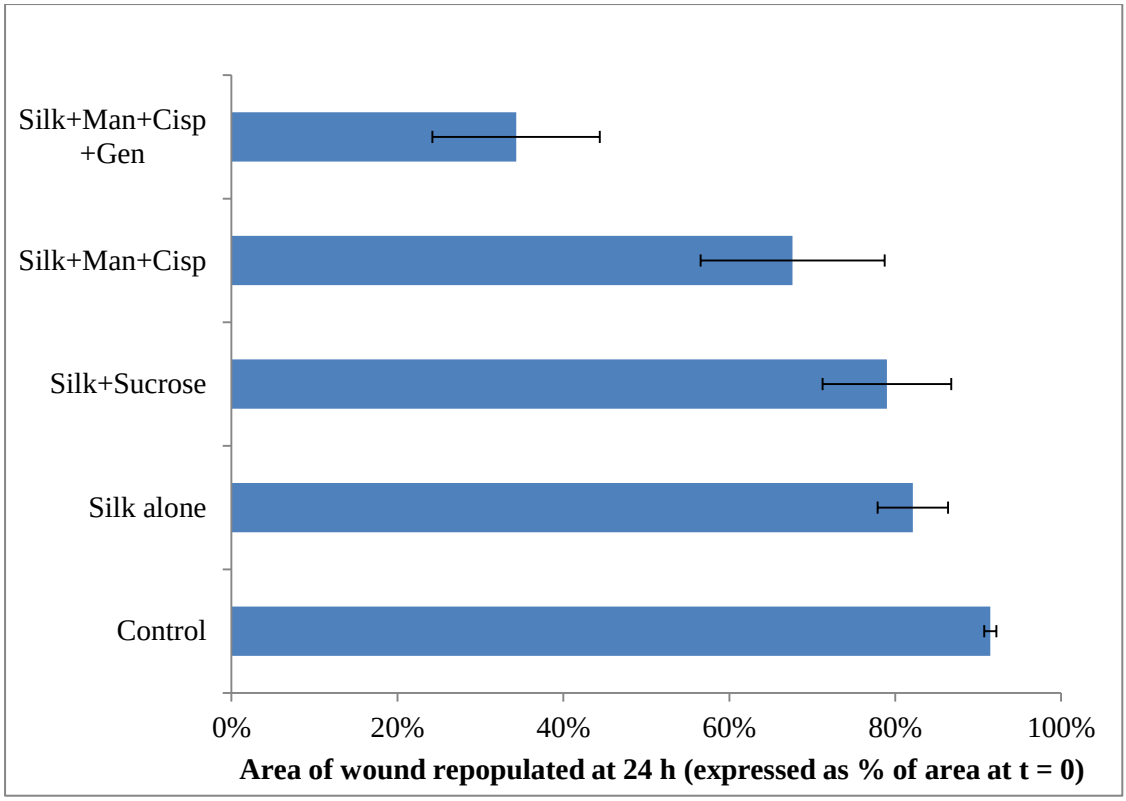

Figure 45. Percentage of wound closed after 24 hours incubation with silk alone, silk + sucrose (2:1) formulation, silk + mannitol (Man) + cisplatin (Cisp) (10:20:1) and silk + mannitol (Man) + cisplatin (Cisp) + genipin (Gen) (10:20:1:1) formulations. Data are expressed as mean ± standard deviation and one-way ANOVA statistical analysis was used.

4.8. Conclusion and need for further studies

From the above results and discussions, it can be concluded that silk fibroin alone is cytocompatible, and that A549 lung cells can grow and proliferate on top of the 2D silk scaffolds as well as in the presence of silk particles dispersed in media.

The presence of mannitol or other sugars used as lyoprotectants that were included during the spray-freeze-drying process may have diminished the cytotoxic effects of cisplatin in some formulations. It would be of benefit if particles were formulated using an alternative method in the future, without the need of sugar, so that the effects of silk and cisplatin could be distinguished and more specific conclusions could be drawn.

The above cell viability assays using A549 cell monolayers were sufficient to draw conclusions for the purpose of this thesis; however it is imperative that new lung models are designed in future studies to advance the experiments for cytotoxicity studies. Growing three dimensional (3D) lung cancer cells, in contrast to growing in 2D monolayers, would mimic the biology of the human lung cancer development more closely and may contribute to the advances in treatment for lung cancer (41).

V. Conclusions and Future Work

Silk particles have been formulated to act as efficient carriers of drugs with a focus on delivering drugs targeted for lung delivery. Cisplatin was successfully incorporated into silk drug carriers and this project demonstrated potential to deliver cisplatin directly to the lungs via dry powder inhalers instead of the conventional injection method. The aerosolisation performance of the particles demonstrated the ability for adequate dispersion and reaching down to the lower airways. These inhalable silk fibroin particles were found to be cytocompatible with lung cells. These lung cells showed normal growth and proliferation in the presence of silk proteins in the media.

The hypothesis that silk proteins naturally exhibit antibacterial activity was not confirmed or rejected in this thesis due to an inability to generate reproducible data, possibly related to variability of silk materials supplied for this project.

However, the silk carriers were loaded with an anticancer drug, cisplatin, to be formulated for targeted delivery to the lungs. The formulation was optimised for particle size, morphology and stability to be suitable for pulmonary delivery. Silk fibroin was cross-linked with genipin for a modified release of cisplatin, and the formulation was shown to have more cytotoxic effect compared to immediate release of cisplatin. This demonstrated that the cross-linked silk formulations delivered cisplatin in such a way that had more potent cytotoxic effects.

Cisplatin on its own was not tested as a treatment group due to the focus of this project being on silk being used as a drug carrier. The given time frame of this project did not allow the extra time to design sterilisation methods for cisplatin or for optimisation of dosage of cisplatin tested. Many previous studies have demonstrated the cytotoxic responses of A549 cells to cisplatin alone, for example a study by Zhang et al (2003) tested the cytotoxicity of cisplatin alone and compared with the combination with another anticancer drug Gleevec

using MTT assay (82). More recent examples are studies by Kim et al (2006) and Zhang et al (2014), in search for ways to enhance chemosensitivity of A549 cells toward cisplatin (83, 84). Nevertheless, future studies may include a positive control, cisplatin alone, in order to compare the cytotoxicity of cisplatin alone and cisplatin released from the silk-based particles.

It is recommended also that future studies have alternative method of formulating these silk-based particles, in order to eliminate or reduce the presence of sugar used as lyoprotectants in the spray-freeze-dried formulations. Although it was demonstrated that the sugar content did not alter the cytotoxicity of the cisplatin according to sugar content in 10 mg/ml overall concentration, the sugar may have contributed to proliferation of cells generally.

Further studies may include a drug release study and investigation of rate of release with the resultant cytotoxic effects. Different levels of crosslinking of silk fibroin may be achieved by using various concentrations of genipin and altering the time of crosslinking. The differences in cytotoxicity between cisplatin released from cross-linked silk or normal silk microparticles were not as significant as expected in this project. The differences in cell responses may be greater if the formulation is modified, possibly by using a higher concentration of genipin for cross-linking or by altering the cross-linking time.

Degradation studies of silk fibroin, especially in an environment that mimics the lungs can be conducted to use results to estimate suitable doses of silk fibroin that could be administered for subjects in future animal studies, if feasible.

Overall, optimised formulations of silk-based drug carriers have been demonstrated to be cytocompatible and had efficient aerosolisation for potential application in controlled release cisplatin treatment in lung cancer.

References

1. Wenk E, Merkle HP, Meinel L. Silk fibroin as a vehicle for drug delivery applications. Journal of Controlled Release. 2011;150(2):128-41.
2. Römer L, Scheibel T. The elaborate structure of spider silk: Structure and function of a natural high performance fiber. Prion. 2008;2(4):154-61.
3. Cao Y, Wang B. Biodegradation of Silk Biomaterials. International Journal of Molecular Sciences. 2009;10(4):1514-24.
4. Wenk E, Wandrey AJ, Merkle HP, Meinel L. Silk fibroin spheres as a platform for controlled drug delivery. Journal of Controlled Release. 2008;132(1):26-34.
5. Cheema SK, Gobin AS, Rhea R, Lopez-Berestein G, Newman RA, Mathur AB. Silk fibroin mediated delivery of liposomal emodin to breast cancer cells. International Journal of Pharmaceutics. 2007;341(1–2):221-9.
6. Kasoju N, Bora U. Silk Fibroin in Tissue Engineering. Advanced Healthcare Materials. 2012;1(4):393-412.
7. Numata K, Kaplan DL. Silk-based delivery systems of bioactive molecules. Advanced Drug Delivery Reviews. 2010;62(15):1497-508.
8. Kundu B, Rajkhowa R, Kundu SC, Wang X. Silk fibroin biomaterials for tissue regenerations. Advanced Drug Delivery Reviews. 2013;65(4):457-70.
9. Widhe M, Johansson J, Hedhammar M, Rising A. Invited review current progress and limitations of spider silk for biomedical applications. Biopolymers. 2012;97(6):468-78.
10. Hofer M, Winter G, Myschik J. Recombinant spider silk particles for controlled delivery of protein drugs. Biomaterials. 2012;33(5):1554-62.
11. Omenetto FG, Kaplan DL. New Opportunities for an Ancient Material. Science. 2010;329(5991):528-31.
12. Moisenovich MM, Pustovalova O, Shackelford J, Vasiljeva TV, Druzhinina TV, Kamenchuk YA, et al. Tissue regeneration in vivo within recombinant spidroin 1 scaffolds. Biomaterials. 2012;33(15):3887-98.
13. Kundu SC, Dash BC, Dash R, Kaplan DL. Natural protective glue protein, sericin bioengineered by silkworms: Potential for biomedical and biotechnological applications. Progress in Polymer Science. 2008;33(10):998-1012.
14. Kundu SC, Kundu B, Talukdar S, Bano S, Nayak S, Kundu J, et al. Invited review nonmulberry silk biopolymers. Biopolymers. 2012;97(6):455-67.
15. Zhang J, Kaur J, Rajkhowa R, Li JL, Liu XY, Wang XG. Mechanical properties and structure of silkworm cocoons: A comparative study of Bombyx mori, Antheraea assamensis, Antheraea pernyi and Antheraea mylitta silkworm cocoons. Materials Science and Engineering: C. 2013;33(6):3206-13.
16. Patra C, Talukdar S, Novoyatleva T, Velagala SR, Muhlfeld C, Kundu B, et al. Silk protein fibroin from Antheraea mylitta for cardiac tissue engineering. Biomaterials. 2012;33(9):2673-80.
17. Tao H, Kaplan DL, Omenetto FG. Silk Materials – A Road to Sustainable High Technology. Advanced Materials. 2012;24(21):2824-37.
18. Kim U-J, Park J, Joo Kim H, Wada M, Kaplan DL. Three-dimensional aqueous-derived biomaterial scaffolds from silk fibroin. Biomaterials. 2005;26(15):2775-85.
19. Kundu J, Chung Y-I, Kim YH, Tae G, Kundu SC. Silk fibroin nanoparticles for cellular uptake and control release. International Journal of Pharmaceutics. 2010;388(1–2):242-50.
20. Senakoon W, Nuchadomrong S, Sirimungkararat S, Senawong T, Kitikoon P. Antibacterial action of eri (samia ricini) sericin against escherichia coli and staphylococcus aureus. Asian Journal of Food and Agro-Industry. 2009;2(Special Issue):S222-8.
21. Zhang J, Pritchard E, Hu X, Valentin T, Panilaitis B, Omenetto FG, et al. Stabilization of vaccines and antibiotics in silk and eliminating the cold chain. Proceedings of the National Academy of Sciences. 2012;109(30):11981-6.
22. Hu X, Kaplan DL. 2.212 - Silk Biomaterials. In: Editor-in-Chief: Paul D, editor. Comprehensive Biomaterials. Oxford: Elsevier; 2011. p. 207-19.

23. Okazaki Y, Tomotake H, Tsujimoto K, Sasaki M, Kato N. Consumption of a Resistant Protein, Sericin, Elevates Fecal Immunoglobulin A, Mucins, and Cecal Organic Acids in Rats Fed a High-Fat Diet. The Journal of Nutrition. 2011;141(11):1975-81.
24. Pritchard EM, Kaplan DL. Silk fibroin biomaterials for controlled release drug delivery. Expert Opinion on Drug Delivery. 2011;8(6):797-811.
25. Hazeri N, Tavanai H, Moradi AR. Production and properties of electrosprayed sericin nanopowder. Science and Technology of Advanced Materials. 2012;13(3):035010.
26. Nayak S, Talukdar S, Kundu SC. Potential of 2D crosslinked sericin membranes with improved biostability for skin tissue engineering. Cell & Tissue Research. 2012;347(3):783-94.
27. Wang X, Wenk E, Hu X, Castro GR, Meinel L, Wang X, et al. Silk coatings on PLGA and alginate microspheres for protein delivery. Biomaterials. 2007;28(28):4161-9.
28. Qu J, Wang L, Hu Y, Wang L, You R, Li M. Preparation of Silk Fibroin Microspheres and Its Cytocompatibility. Journal of Biomaterials and Nanobiotechnology. 2013;4(1):84-90.
29. Rajkhowa R, Hu X, Tsuzuki T, Kaplan DL, Wang X. Structure and Biodegradation Mechanism of Milled Bombyx mori Silk Particles. Biomacromolecules. 2012 2012/08/13;13(8):2503-12.
30. Pritchard EM, Dennis PB, Omenetto F, Naik RR, Kaplan DL. Physical and chemical aspects of stabilization of compounds in silk. Biopolymers. 2012;97(6):479-98.
31. Chen M, Shao Z, Chen X. Paclitaxel-loaded silk fibroin nanospheres. Journal of Biomedical Materials Research Part A. 2012;100A(1):203-10.
32. Hofer M, Winter G, Myschik J. Recombinant spider silk particles for controlled delivery of protein drugs. Biomaterials. 2012;33(5):1554-62.
33. Sobajo C, Behzad F, Yuan X-F. Silk: A potential medium for tissue engineering. Eplasty. 2008;8(e47):438-46.
34. Seib FP, Kaplan DL. Doxorubicin-loaded silk films: Drug-silk interactions and in vivo performance in human orthotopic breast cancer. Biomaterials. 2012;33(33):8442-50.
35. Mandal BB, Kundu SC. Self-assembled silk sericin/poloxamer nanoparticles as nanocarriers of hydrophobic and hydrophilic drugs for targeted delivery. Nanotechnology. 2009;20(35):355101.
36. Shi P, Goh JCH. Release and cellular acceptance of multiple drugs loaded silk fibroin particles. International Journal of Pharmaceutics. 2011;420(2):282-9.
37. Lammel AS, Hu X, Park S-H, Kaplan DL, Scheibel TR. Controlling silk fibroin particle features for drug delivery. Biomaterials. 2010;31(16):4583-91.
38. Blüm C, Scheibel T. Control of Drug Loading and Release Properties of Spider Silk Sub-Microparticles. BioNanoScience. 2012;2(2):67-74.
39. Subia B, Kundu SC. Drug loading and release on tumor cells using silk fibroin–albumin nanoparticles as carriers. Nanotechnology. 2013;24(3):035103.
40. Imsombut T, Srisa-ard M, Srihanam P, Baimark Y. Preparation of silk fibroin microspheres by emulsificationdiffusion method for controlled release drug delivery applications. e-Polymers. 2011;11(1):936.
41. Mishra DK, Sakamoto JH, Thrall MJ, Baird BN, Blackmon SH, Ferrari M, et al. Human Lung Cancer Cells Grown in an Ex Vivo 3D Lung Model Produce Matrix Metalloproteinases Not Produced in 2D Culture. PLoS ONE. 2012;7(9):e45308.
42. Stallings-Mann ML, Waldmann J, Zhang Y, Miller E, Gauthier ML, Visscher DW, et al. Matrix metalloproteinase induction of Rac1b, a key effector of lung cancer progression. Science translational medicine. 2012;4(142):142ra95.
43. Spiro SG, Tanner NT, Silvestri GA, Janes SM, Lim E, Vansteenkiste JF, et al. Lung cancer: Progress in diagnosis, staging and therapy. Respirology. 2010;15(1):44-50.
44. American Cancer Society, Inc. Cancer death rates by site of cancer, age-adjusted per 100,000 population in the US, 1930-2008. Surveillance Research, 2012.
45. Institute NC. Surveillance, Epidemiology, and End Results Program. SEER Stat Fact Sheets: Lung and Bronchus Cancer: National Cancer Institute [Accessed February 2014]. Available from: http://seer.cancer.gov/statfacts/html/lungb.html

46. National Cancer Research Institute (NCRI). The percentage of site-specific research funding for cancers in 2002 and 2010. Accessed via http://scienceblog.cancerresearchuk.org/2011/06/29/near-doubling-of-uk-cancer-research-funding-in-less-than-10-years/ on 08/04/2014.
47. Pancreatic Cancer Action, UK. Research funding spent on specific cancers by NCRI, related to the percentage of total cancer deaths in the UK by tumour site. Accessed via http://pancreaticcanceraction.org/pancreatic-cancer/about/research-funding/ on 08/04/2014.
48. Yang W, Peters JI, Williams RO, 3rd. Inhaled nanoparticles--a current review. International Journal of Pharmaceutics. 2008;356(1-2):239-47.
49. Sung JC, Pulliam BL, Edwards DA. Nanoparticles for drug delivery to the lungs. Trends in Biotechnology. 2007;25(12):563-70.
50. Wang Y-B, Watts AB, Peters JI, Williams Iii RO. The impact of pulmonary diseases on the fate of inhaled medicines—A review. International Journal of Pharmaceutics. 2014;461(1–2):112-28.
51. Genc G, Narin G, Bayraktar O. Spray drying as a method of producing silk sericin powders. Journal of Achievements in Materials and Manufacturing Engineering. 2009;37(1):78-86.
52. Mansour HM, Rhee Y-S, Wu X. Nanomedicine in pulmonary delivery. International Journal of Nanomedicine. 2009;4:299-319.
53. El-Sherbiny IM, Smyth HDC. Biodegradable nano-micro carrier systems for sustained pulmonary drug delivery: (I) self-assembled nanoparticles encapsulated in respirable/swellable semi-IPN microspheres. International Journal of Pharmaceutics. 2010;395(1-2):132-41.
54. Pilcer G, Amighi K. Formulation strategy and use of excipients in pulmonary drug delivery. International Journal of Pharmaceutics. 2010;392(1–2):1-19.
55. Hu C-MJ, Aryal S, Zhang L. Nanoparticle-assisted combination therapies for effective cancer treatment. Therapeutic Delivery. 2010;1(2):323-34.
56. Babu A, Templeton AK, Munshi A, Ramesh R. Nanoparticle-based drug delivery for therapy of lung cancer: Progress and challenges. Journal of Nanomaterials. 2013;(1):1-11.
57. Zhang F, Tian J, Wang L, He P, Chen Y. Correlation between cell growth rate and glucose consumption determined by electrochemical monitoring. Sensors and Actuators B: Chemical. 2011;156(1):416-22.
58. Roa WH, Azarmi S, Al-Hallak MHDK, Finlay WH, Magliocco AM, Lobenberg R. Inhalable nanoparticles, a non-invasive approach to treat lung cancer in a mouse model. Journal of Controlled Release. 2011;150(1):49-55.
59. Zarogoulidis P, Darwiche K, Krauss L, Huang H, Zachariadis GA, Katsavou A, et al. Inhaled cisplatin deposition and distribution in lymph nodes in stage II lung cancer patients. Future Oncology. 2013;9(9):1307-13.
60. Das S, Jagan L, Isiah R, Rajesh B, Backianathan S, Subhashini J. Nanotechnology in oncology: Characterization and in vitro release kinetics of cisplatin-loaded albumin nanoparticles: Implications in anticancer drug delivery. Indian Journal of Pharmacology. 2011;43(4):409.
61. MIMS. Mims Online. Full Product Information: Cisplatin Injection. Pfizer. 2014;March 2014.
62. Selting K, Waldrep JC, Reinero C, Branson K, Gustafson D, Kim DY, et al. Feasibility and Safety of Targeted Cisplatin Delivery to a Select Lung Lobe in Dogs via the AeroProbe® Intracorporeal Nebulization Catheter. Journal of Aerosol Medicine and Pulmonary Drug Delivery. 2008;21(3):255-68.
63. Xu P, Van Kirk EA, Li S, Murdoch WJ, Ren J, Hussain MD, et al. Highly stable core-surface-crosslinked nanoparticles as cisplatin carriers for cancer chemotherapy. Colloids and Surfaces B: Biointerfaces. 2006;48(1):50-7.
64. Wittgen BPH, Kunst PWA, Born Kvd, Wijk AWv, Perkins W, Pilkiewics FG, et al. Phase I study of aersolized SLIT cisplatin in the treatment of patients with carcinoma of the lung. Clinical Cancer Reseach. 2007;13(8):2014-21.
65. Wang L, Wang Y, Qu J, Hu Y, You R, Li M. The Cytocompatibility of Genipin-Crosslinked Silk Fibroin Films. Journal of Biomaterials and Nanobiotechnology. 2013;4(3):213-21.
66. Wang C, Lau TT, Loh WL, Su K, Wang D-A. Cytocompatibility study of a natural biomaterial crosslinker—Genipin with therapeutic model cells. Journal of Biomedical Materials Research Part B: Applied Biomaterials. 2011;97B(1):58-65.
67. Chan H-K, Kwok PCL. Production methods for nanodrug particles using the bottom-up approach. Advanced Drug Delivery Reviews. 2011;63(6):406-16.

68. Brochure:. Quality Solutions for Inhaler Testing. Copley Scientific Limited, Nottingham, United Kingdom. 2012:36.
69. Product Information Sheet: Mueller Hinton Agar (7101) via http://www.neogen.com/Acumedia/pdf/ProdInfo/7101_PI.pdf Clinical and Laboratory Standard Institute.Rev 3, June 2011; accessed on 26/02/2014.
70. Immunocytochemistry and Immunofluorescence Protocol: Guideline procedure for staining of cell cultures using immunofluorescence Abcam, accessed from www.abcam.com/technical in March 2014.
71. Labiris NR, Dolovich MB. Pulmonary drug delivery. Part I: Physiological factors affecting therapeutic effectiveness of aerosolized medications. British Journal of Clinical Pharmacology. 2003;56(6):588-99.
72. Tee LH, Luqman Chuah A, Pin KY, Abdull Rashih A, Yousof YA. Optimization of spray drying process parameters of Piper betle L. (Sirih) leaves extract coated with maltodextrin. Journal of Chemical and Pharmaceutical Research. 2012;4(3):1833-41.
73. Zhang X, Baughman CB, Kaplan DL. In vitro evaluation of electrospun silk fibroin scaffolds for vascular cell growth. Biomaterials. 2008;29(14):2217-27.
74. D'Addio S, Chan J, Kwok PCL, Prud-homme R, Chan H-K. Spray freeze dried large porous particles for nano drug delivery by inhalation. Respiratory Drug Delivery. 2012;3:695-8.
75. Aubier M, Pieters W, Scholosser N, Steinmetz K. Salmeterol/fluticasone propionate (50/500 mug) in combination in a Diskus inhaler (Seretide) is effective and safe in the treatment of steroid-dependent asthma. Respiratory Medicine. 1999;93(12):876-84.
76. Bateman E, Britton M, Carrillo J, Almeida J, Wixon C. Salmeterol/fluticasone combination inhaler. A new, effective and well tolerated treatment for asthma. Clinical Drug Investigation. 1998;16(3):193-201.
77. Taki M, Marriott C, Zeng X, Martin G. The aerodynamic deposition of drugs from combination DPI formulations: The influence of particle size and drug-drug and interactions. Drug Delivery to the Lungs. 2008;19
78. Technologies DM. Cell Counting Kit-8: Description Japan: Dojindo Molecular Technologies, INC; 2013 [cited 2014 14/03/2014]. Available from: http://www.dojindo.com/store/p/456-Cell-Counting-Kit-8.html.
79. Invitrogen Life Technologies. Inventor alamarBlue Assay. U.S. p.27
80. Hamid R, Rotshteyn Y, Rabadi L, Parikh R, Bullock P. Comparison of alamar blue and MTT assays for high through-put screening. Toxicology in Vitro. 2004;18(5):703-10.
81. Ozturk SS, Jorjani P, Taticek R, Lowe B, Shackleford S, Ladehoff-Guiles D, et al. Kinetics of Glucose Metabolism and Utilization of Lactate in Mammalian Cell Cultures. In: Carrondo MT, Griffiths B, Moreira JP, editors. Animal Cell Technology: Springer Netherlands; 1997;355-60.
82. Zhang P, Gao W, Turner S, Ducatman B. Gleevec (STI-571) inhibits lung cancer cell growth (A549) and potentiates the cisplatin effect in vitro. Molecular Cancer. 2003;2(2):1.
83. Kim HR, Kim S, Kim EJ, Park JH, Yang SH, Jeong ET, Park C, Youn MJ, So HS, Park R. Suppression of Nrf2-driven heme oxygenase-1 enhances the chemosensitivity of lung cancer A549 cells toward cisplatin. Lung Cancer. 2008;60(1):1-3.
84. Zhang B, Liu ZM, Hao FG, Wang M. siRNA-directed clusterin silencing promotes cisplatin antitumor activity in human non-small cell lung cancer xenografts in immunodeficient mice. European Review for Medical and Pharmacological Sciences. 2014;18(11):1595-601.